Alma Mater Studiorum – Università di Bologna

DOTTORATO DI RICERCA IN

Scienze Biomediche e Neuromotorie

Ciclo XXXI

Settore Concorsuale: 05/D1

Settore Scientifico Disciplinare: BIO/09

DAILY TORPOR IN LABORATORY MICE: PHYSIOLOGICAL PHENOTYPING AND ROLE OF OREXINS
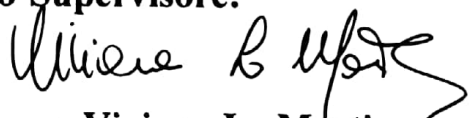
Presentata da: Alice Valli

Coordinatore Dottorato:

Prof. Pietro Cortelli

Supervisore:

Prof. Giovanna Zoccoli

Co-Supervisore:

Dr.ssa Viviana Lo Martire

Esame finale anno 2019

Index

Abbreviations' Index

A

Activity (*ACT*)

Slope of the ACT during cooling (*ACT-c*)

Slope of the ACT during rewarming (*ACT-R*)

Autonomic nervous system (*ANS*)

Arterial pressure (*AP*)

Agouti-related peptide (*AgRP*)

Ambient temperature (*Ta*)

B

brown adipose tissue (*BAT*)

The baseline (*B*)

Basal metabolic rate (*BMR*)

Body weight (*BW*)

C

Core body temperature (*CBT*)

Central nervous system (*CNS*)

Cutaneous vasoconstriction (*CVC*)

D

Mouse model missing a functional leptin receptor (*db/db mice*)

Dorsal raphe (*DR*)

Dorsomedial hypothalamus (*DMH*)

E

Electroencephalographic (*EEG)*

Electromyographic activity (*EMG*)

G

Blood glucose concentration or glycemia (*GLC*)

G-protein-coupled cell surface receptors (*GPCRs*)

H

Hypocretin 1 and 2 (*HCRT-1, HCRT-2*)

Slope of HP during cooling (*HP-c*)

Heart period (*HP*),

Slope of HP during rewarming (*HP-R*)

Heart rate (*HR*)

I

Intracerebroventricular (*ICV*)

Percentage of time spent in indeterminate state (*%IND*)

K

Knock-out mice for the pre-pro-orexin gene (*KO-HCRT*)

L

Lateral hypothalamic area (*LHA*)

the locus coeruleus (*LC*)

length of the cooling period (*L-c*)

Length rewarming period (*L-r*)

M

Median preoptic nucleus (*MnPO*)

N

Neuropeptide Y (*NPY*)

Non-rapid eye movement sleep
(*NREM*)

Percentage of time spent in NREM
sleep (*%NREM*)

O

Orexin A and B (*ORX A, ORX B*)

Mice carrier of a mutation in the leptin
gene (*Ob/ob mice*)

Orexins A and B (*ORXS*)

Orexin A receptor (*ORX-1R*)

 Orexin B receptor (*ORX-2R*)

P

Parabrachial nucleus (*PBN*)

Parasympathetic nervous system (*PNS*)

Preoptic area (*POA*)

Preoptic anterior hypothalamus
(*POAH*)

Thalamus para-ventricular-nucleus
(*PVNT*)

R

Rapid-eye movement sleep (*REM*)

Percentage of time spent in REM sleep
(*%REM*)

Resting metabolic rate (RMR)

Raphe pallidus (*RPa*)

S

Systolic blood pressure (*SBP*)

Slope of SBP during cooling (*SBP-c*)

Slope of SBP during rewarming (*SBP-r*)

Suprachiasmatic Nucleus (*SCN*)

Sympathetic nervous system (*SNS*)

Slow wave activity (*SWA*)

T

Deep torpor (T)

Body temperature (T_b)

Slope of T_b during cooling ($T_b\text{-}c$)

Slope of T_b during rewarming ($T_b\text{-}r$)

Torpor metabolic rate (TMR)

Tuberomammillary nucleus (TMN)

Thermoneutral zone (TNZ)

Transient receptor potential channels (TRP)

Hypothalamic temperature set point (T_{set})

U

Uncoupling protein-1 ($UCP1$)

V

Ventrolateral preoptic nucleus ($VLPO$)

Ventromedial hypothalamus (VMH)

Ventral tegmental area (VTA)

W

Wakefulness (W),

Control mice (WT)

Introduction to Torpor

Torpor general aspects

The large seasonal and daily environmental changes in temperature and food availability obligated organisms to develop adaptation during evolution (Geiser 2004). Endotherms, like mammals and birds, can maintain a constant body temperature of 37°C over a wide range of ambient temperatures. This is the result of their high metabolic rate that generates heat, even during rest, and maintains body temperature (Tb) often well above ambient temperature (Ta). Thus, endothermy allows maintaining internal temperatures at the level of maximum physical performance (Heldmaier, Ortmann et al. 2004; Ruf and Geiser 2015). For all endotherms living in temperate climates maintaining Tb has high energy costs (Geiser 2004). Therefore, the life of endotherms depends upon a continuous high supply of food (Heldmaier, Ortmann et al. 2004).

In case of an adverse environmental condition and scarce food availability, reducing thermoregulatory costs allows animals to redirect energy to different tasks and so optimize growth and reproduction (van der Vinne, Gorter et al. 2015). This is more crucial for small endotherms because the surface area/volume ratio increases as size decreases, so they must produce substantial amounts of endogenous heat to compensate for high heat loss during cold exposure (Geiser 2004).

Therefore, a widespread solution for endotherms, who cannot escape harsh environmental conditions by migration, is to suspend the maintenance of high Tb (torpid state) and then re-warm and return to a normal level of activity when the environment becomes favorable (Melvin and Andrews 2009).

Four conditions are required for a euthermic animal to undergo in a torpid state, and the mechanisms of none of them are currently clearly known (Sunagawa and Takahashi 2016). First, the animal has to turn off, or at least suppress, the thermoregulatory system, producing a marked decrease in temperature. In normal conditions, the

lowering of Tb would trigger a response by the thermoregulatory mechanism, but such a response is abolished during torpor (Sunagawa and Takahashi 2016).

Second, the animal must be able to endure low respiration levels or low oxygen supply. In torpid animals, the oxygen consumption is reduced to the 2–3% of that in an aroused state (Andrews 2007).

Third, the animal must be resistant to hypothermia because during torpor hibernators typically have a minimum Tb of 2–10 °C (Carey, Andrews et al. 2003).

Fourth, the animal must be able to return to a normal metabolic state by producing heat starting from a hypometabolic state and to tolerate this rise in heat (Sunagawa and Takahashi 2016).

Animals that can display torpor are a wide and uneven group of species and are present in most of the orders of mammals (Melvin and Andrews 2009), including primates (Dausmann, Glos et al. 2004). This suggests that the ability to suppress metabolic rate was probably a trait present in the ancestral mammal. The trait was later lost in many mammals but remain present in many small species with a high energy expenditure during normothermia. Particularly, many of these animals eat food that becomes seasonally unavailable (Geiser 1998; Cerri 2017).

Laboratory mouse and chipmunk represent two good examples to highlight that the expression of torpor is responsive to the availability of food. Laboratory mouse (Mus Musculus) shows daily torpor only when fasted in cold ambient temperature (Hudson and Scott 1979). During the hibernation season, Eastern chipmunk (Tamias Striatus) whose food hoard was greater had a higher frequency of normothermia and a higher mean Tb than the ones whose food hoard are smaller (Landry-Cuerrier, Munro et al. 2008) (Melvin and Andrews 2009).

Today, an unequivocal and agreed definition of torpor is still missing, even if this topic is deeply investigated in the physiological research field since the beginning of XX century.

Indeed, torpor is a physiological state of temporary inactivity characterized by a profound reductions of basal metabolic rate (BMR) and Tb (Melvin and Andrews 2009;

Bouma, Verhaag et al. 2012; Careau 2013; Ruf and Geiser 2015), it is also characterized by a lowering of heart rate (HR) and respiration (reduce current volume, respiration frequency and ventilation)(Carey, Andrews et al. 2003). Although metabolic rate during torpor may be a fraction in respect to normothermic individuals the regulation of Tb during torpor is not abandoned. Tb is regulated at or above a species- or population-specific minimum (Geiser 2004).

It is difficult to pinpoint accurately the absolute value reached by physiological variables involved in torpor because there is great variability intra and inter-species (Hudson and Scott 1979). For example, Tb during torpor bouts falls from normothermic values (35 to 38 °C) (Melvin and Andrews 2009) to an extreme value of -2.7°C in arctic ground squirrel, while in Ursus Americanus it decreases to 28-30°C (Ruf and Geiser 2015; Silvani, Cerri et al. 2018), commonly Tb decrease under 25°C and BMR is reduced by the 70 to 95% (Carey, Andrews et al. 2003; Geiser 2004; Storey and Storey 2010).

Laboratory mouse (Mus Musculus) is one of the most widely studied laboratory mammals, it can enter bouts of daily torpor upon caloric restriction or food deprivation. During torpor Tb in mice fall from 36.6°C (euthermic values) to a minimum of 20 °C (Silvani, Cerri et al. 2018), with a concomitant fall in heart rate from 600 beats per minute (bpm) to a minimum of 160 bpm; the blood pressure also significantly declines during torpor (Swoap and Gutilla 2009).

Circadian periods of slight hypometabolism are regularly observed during the 24 h. During the resting phase, the metabolic rate of mammals decreases by about 20% below the level of metabolic rate during the active phase. This shallow circadian hypometabolism is often associated with a 0.5 - 2 °C decrease in core body temperature (Heldmaier, Ortmann et al. 2004).

The multifactorial nature of the torpor mechanisms still not well characterized in literature; the environmental, physiological, metabolic, and molecular changes altogether can induce the animal to undergo torpor, but how they are connected still not clear (Melvin and Andrews 2009).

It would be important to discover the trigger to induce torpor because the drug-induced torpor (synthetic torpor) has a large number of applications. For example, in medicine, the outcome of this discovery would be great because, despite the dramatic decreases in Tb, metabolic rate, and, consequently, reduced blood flow, animals recovering from torpor bouts do not exhibit indications of tissue damage (Bouma, Verhaag et al. 2012) (Dave, Christian et al. 2012). The absence of injury upon rewarming and reperfusion makes torpor a good model to investigate protective mechanisms that could be employed as treatments for different trauma states as cardiac arrest, organ transplantation, major cardiac and brain surgery. Also, in transplantation medicine, reducing metabolism in donor organs may provide a better preservation method giving a greater time window for transplantation of organs to recipients (Bouma, Verhaag et al. 2012).

Like-wise Synthetic Torpor could be applied in long-duration space exploration because the reduction in metabolism would diminish the amount of food required for crew survival for long periods. Moreover, disuse atrophy of skeletal muscle and bones would be cut down (Cerri 2017).

For all the characteristics pointed above Torpor is the closest state to death which mammals can reach and at the same time allows animals to survive in arduous environmental conditions (Ruby, Barakat et al. 2004).

Principal torpor behaviours: Hibernation and Daily torpor

Torpor works as a basic element for more complex behaviors (Cerri 2017), depending on the timing, duration, and depth, it can be categorized as seasonal and non-seasonal. Seasonal torpor is represented by two behaviors: estivation and hibernation.

The former is characterized by food store caches and variable lengths/depths of torpor episodes, or sometimes no Torpor, depending on food availability and the severity of environmental conditions, a common example of estivating animal is the chipmunk (Storey and Storey 2010).

Hibernation usually lasts from autumn to early spring and is typified using body the fuel reserves, mainly represented by the fat, to survive the winter. Thereby, this species is called fat-store hibernators, they are the most common hibernator category, and, in this paragraph, when you will find the term Hibernator it will be referred to them.

Hibernators, which include many mammals but only a single bird species, are generally small, and most weigh between 10 and 1000 g, with a median mass of 85 g (Geiser and Ruf 1995). However, the entire mass range of hibernators, for which metabolic data are available includes black bears (Ursus americanus), and it is from 5 to 80,000 g (Geiser 2004). During the weeks leading up to the hibernating season, hibernators undergo hyperphagia and build up huge white adipose depots that can increase body mass by 50% (Storey and Storey 2010).

Most of these species exhibit extensive fattening prior to the season in which they display torpor, this behavior is not observed in most of the non-seasonal torpid animals that typically enter torpor at times in which body mass is low, accordingly large fat stores is proved to inhibit daily torpor (Geiser 1998).

Lipids provide to hibernators the primary fuel source for the whole winter although some amino-acid catabolism also occurs, often in support of gluconeogenesis since carbohydrate stores are minimal and reserved in just few tissue types (Dark 2005).

Even hibernator brain can switch to a lipid-based economy by oxidizing ketone bodies that are synthesized by the liver (Storey and Storey 2010).

Hibernators do not remain torpid throughout all the hibernation season, but they present a hibernation pattern characterized by bouts of torpor, which are characterized by four different states: 1) entrance into hibernation; 2) maintenance of deep hibernation for several days; 3) arousal that terminates each torpor bouts; 4) a euthermic resting periods of 1-2 days, with normal Tb and high energy turnover that conclude the torpor bout (Heldmaier, Ortmann et al. 2004). Thus, the entire hibernation season of 6–7 months consists out of a sequence of 15 through 20 hibernation bouts (Heldmaier, Ortmann et al. 2004).

This hibernation pattern is similar trough the different hibernating species.

Entrance into torpor is characterized by a rapid reduction of metabolic rate until the minimum is reached. The metabolic reduction is paralleled by a rapid decrease of Tb, which continues into deep hibernation, the second and longer phase. Deep hibernation is terminated with the arousal, when animals raise their Tb to euthermic level, in a time lapse of some hours, through a burst of heat production (Heldmaier, Ortmann et al. 2004). During arousal from torpor bout are used two main power source: non-shivering thermogenesis, mainly in brown adipose tissue, and shivering thermogenesis, produced by skeletal muscles, that is only a supplement to the former (Cannon and Nedergaard 2004). The percentage of time spent in arousal and interbout is short, because of its high energetic cost (Storey and Storey 2010).

In order to have a prolonged period of hypometabolism during hibernation season, the circadian system seems to be inactivated, so, torpid bouts can give a reliance on energy stores (Ruf and Geiser 2015).

The length of torpor season (e.g., up to 8.5 months in the Richardson's ground squirrel (Wang 2011)) and the significant decrease of Tb during torpor, allow a very high energy savings that could be as high as 88% in comparison with animals that remain euthermic in the same period (Wang and W. Wolowyk 2011). However, the repeated arousals and the euthermic periods are energetically very costly. For example, in marmots, 72% of all energy reserves required for the entire hibernation season are

consumed during arousals (17%) and the euthermic periods (57%) (Heldmaier, Ortmann et al. 2004).

An example of hibernator is ground squirrel, during torpor can drop his heartbeat from >200 beats/min in interbout to <10 beats/min in torpor (Milsom, Zimmer et al. 1999).

Daily torpor, is a widely used pattern of torpor in mammals and, in contrast to hibernation, also in birds (Geiser 2004). This form of torpor is usually not as deep as hibernation (Heldmaier, Ortmann et al. 2004), in fact, it lasts only for hours rather than days or weeks and it is usually interrupted by daily foraging and feeding (Geiser 2004). Daily heterotherms are unable to express multiday torpor bouts. Many daily heterotherms may employ torpor throughout the year, although torpor use often increases in winter (Geiser 2010). In order to facilitate foraging, mating, migrations etc. daily heterotherms employ the circadian system to control torpor timing to stay entrained with the light-dark cycle (Ruf and Geiser 2015). Daily torpor is usually restricted to the night, whereas, in nocturnal mammals and birds, it is common in the second part of the night and the early morning.

In daily torpor the extent of hypometabolism and hypothermia is usually less pronounced if compared to hypometabolism in hibernation; consequently, also less energy is saved (Heldmaier, Ortmann et al. 2004).

Recent evidence from the field, suggests that daily torpor may also be used to restrict foraging times to only few hours per day in the early evening, with torpor bouts lasting for most of the day. Together with passive rewarming in the sun, this reduces daily energy expenditure by up to 80% (Geiser 2010; Jastroch, Giroud et al. 2016).

A daily torpor bout follows the same events sequence observed in hibernation, i.e. entrance into torpor, maintenance of deep torpor, arousal, and return to the euthermic state (Heldmaier, Ortmann et al. 2004).

The minimum Tb reached in daily torpor strongly depends on species and ambient temperature (Bouma, Verhaag et al. 2012). The lowest tolerable range of Tb is from 10 to 22°C with a mean value of 17 °C (Geiser 1998); even though there is a large variation among species, it stays considerably higher than a hibernator's.

On average, daily heterotherms are smaller than hibernators weigh between 5 and 50 g, with a median of 19 g, in a complete range of from 2 to 9000 g (Geiser 2004).

The metabolic rate during daily torpor is on average reduced to about 30% of the BMR (Geiser 2010) although this percentage is strongly affected by body mass and other external factors.

The onset of daily torpor is typically facilitated by food deprivation, although spontaneous torpor in presence of an adequate food supply has also been observed in many species (Wang and W. Wolowyk 2011). Daily torpid species and hibernators have a different reaction to food deprivation: small daily heterotherms will perish if food is absent for several days (Kennedy and Macfarlane 1971), whereas hibernators can survive for months.

So, the main energy supply of daily heterotherms remains ingested food rather than stored body fat, and they appear to balance energy expenditure and uptake on a daily basis (Geiser 2004).

As proof of it, daily torpor can be induced in laboratory mouse with a caloric restriction protocol, which induce replicable torpor bouts, with a mean length of 2-4 hours (Vicent, Borre et al. 2017).

Therefore, daily torpor is not simply a breakdown of thermoregulation due to starvation, these small mammals maintain control of their Tb, so they remain endotherms because they can alternate between a euthermic tachy-metabolic state and a torpid brady-metabolic state with largely reduced body functions. They can even use endothermic thermoregulation when torpid (Hudson and Scott 1979; Jastroch, Giroud et al. 2016).

Another fundamental difference between Hibernating and daily torpid animals is the mechanisms of the metabolic rate reduction, that will be analyzed more specifically in the chapter titled "Interaction between metabolism and torpor". Also, the effect of torpor on subsequent sleep pattern is different. In hibernating animals who display deep torpor, regulation of temperature and sleep seems to be reduced to a level that currently cannot be measured reliably. In contrast, animals who display daily torpor appear to

make use of the same processes, although applied in an extreme way, which reduces body temperature at the onset of sleep in humans (Kräuchi 2011).

For all these reasons it has been discussed whether daily torpor, estivation and hibernation are based on different physiological mechanisms or are different branches of the same adaptation. At present no clear qualitative differentiation is known. The physiological properties of daily torpor, estivation, and hibernation are very similar. All are characterized by major reductions of metabolic rate, heart rate, ventilation, body temperature, and in the torpid state thermoregulatory control is maintained. This suggests that they are based on a common paradigm of physiological inhibition. The classifications of hibernation, daily torpor, or estivation simply represent gradual differences in the timing, the duration, and the amplitude of physiological inhibition (Heldmaier, Ortmann et al. 2004).

Advantage and disadvantage of torpor use in different species

Differences and similarities between daily torpor and hibernation has been extensively discussed in Ruf T. and F. Geiser's paper titled "Daily torpor and hibernation in birds and mammals" (Ruf and Geiser 2015).

Daily torpor allows to keep entrain the light-dark cycle using short (less than a day) torpor bouts; and daily heterotherms continue to remain active and forage above ground, as opposed to hibernators that show multiday torpor bouts. Species that employ multiday torpor, on the other hand, benefit from larger body mass facilitating higher body energy stores; moreover, they reach a lower metabolic rate during deep torpor bouts, to maximize energy savings.

Hibernation and daily torpor also differ in their primary source of energy: during hibernation, animals can use either body fat or food stores reserve, whereas in daily torpor animals need to continue foraging. This factor more likely explains the significant difference in body mass between daily heterotherms and hibernators.

Indeed, a small body mass holds down the size of body fat stores, not only in absolute storage amounts but also in terms of the percentage of body fat, so hibernators which seem to rely on endogenous energy stores benefit from an increased body size.

Daily heterotherms, on the other hand, which continue to forage, should benefit from a functional circadian system that keeps them entrained with the light-dark cycle and serves to optimize times of daily activity and rest.

Torpor state has a crucial role in hibernating and daily torpid animals, it facilitates migration in certain birds because it allows to balance the equilibrium between energy supply and energy demand (Doucette, Brigham et al. 2012). Torpor is an integral part of reproductive strategies that involve sperm storage in certain bats and other mammals, it can primarily serve as a water conservation mechanism, and it was found to lower the risk of extinction (Ruf and Geiser 2015). The latter finding is a consequence of hibernation behavior: typically, during torpor the animal retreats into secluded areas like underground burrows, and this reduces predation risk and results into higher survival rates than during active season (Geiser and Turbill 2009).

A recent experiment demonstrated that a single torpor bout in mice improves the memory process, and protect the memory against from the ambient stressors (e.g. cool ambient temperature and food shortage) (Nowakowski, Swoap et al. 2009).

Indeed, the animals try to reduce torpor when it is possible even though there are a lot of benefits derived from it. A clear example is fat-storing hibernators in with high body energy reserves reduce torpor and increase euthermic episodes during winter (Claudia, Karin et al. 2014; Zervanos, Maher et al. 2014).

The reasons why animals reduce entrance into torpor is still not clear but there are many hypotheses.

The sleep deprivation hypothesis claims that torpor could be an evolution of sleep but during torpor the time spent in a sleep state is deeply reduced or absent, as will be discussed in chapter "Sleep and Torpor". Actually, the relationship between sleep and torpor is complex, and it appears to be species specific (Kräuchi 2011).

The immune-suppression state is induced in torpor by low Tb, and it is reversed during periodic arousals (Bouma, Carey et al. 2010). As a matter of principle, immune-

suppression could be benefic because it saves energy, protects from inflammatory processes, and typically involves little risks since microbes proliferate very slow at low temperatures (Bouma, Carey et al. 2010). However, impaired immune function during torpor may increase the risk of contracting viral or fungal diseases that can be lethal (Prendergast, Freeman et al. 2002; Bouma, Carey et al. 2010).

A new theory claims that an adverse effect of torpor could be a rise of oxidative stress and a consequent increase in costly up-regulation of antioxidant defenses (Ruf and Geiser 2015); this hypothesis is controversial, because despite the presence of a pro-apoptotic and oxidative environment during hibernation and the consequent accumulation of DNA damage, the apoptosis is suppressed and necrotic tissue injury is minimal (Sunagawa and Takahashi 2016).

Thermoregulation and Metabolism

Thermoregulation in physiological conditions

Thermoregulation

Thermoregulation is a complex physiological regulatory process that allows the animals to maintain their constant Tb level. This is managed by the body through the regulation of loss and production of heat. The body is highly sensitive to changes in Ta. Animals have a thermo-neutral zone that is defined as the range of Ta without regulatory changes in metabolic heat production or evaporative heat loss (Kingma, Frijns et al. 2012).

Heat can be lost from the surface of the body through radiation, conduction, convection and evaporation. Radiant heat transfer occurs in the absence of contact between objects. Conductive heat transfer occurs between physical objects in each physical state: solid, liquid or gas and they must be in contact with one another. Radiation and conduction are fixed physical phenomena that cannot be manipulated, but are a function of the temperature differential between the body surface and the environment.

Convection is the heat transfer associated with the movement of a fluid (either liquid and gaseous), and evaporation is the conversion of a material from a liquid state to a gaseous state, an example is the heat transfer from the surface of the body. Convection and evaporation in biological systems can be manipulated by adjusting fluid movement (convection) or delivering an expandable fluid to the interface surface (evaporation) (Dennis Grahn 2004).

More than 50 years ago it was theorized that the human body could be divided into two thermo-physiologic compartments: the heat-producing region identified in the homeothermic core, and the heat-loss-regulating poikilothermic shell (Kräuchi 2011). The shell temperature is influenced by skin blood flow, which is increased when core

temperature rises, and by environmental temperature. Usually, the distal skin temperature is measured in hands and feet's (Tansey and Johnson 2015).

The shell size depends directly on Ta, in a warm environment the shell is small, while in a cool environment it is larger and therefore it acts as a bulwark to protect the body core from cooling.

All the peripheral tissues (fat, skin, legs and arms, skeletal muscles) can contribute substantially to the shell size, provided that peripheral blood flow is low (Kräuchi 2011).

Core body temperature (CBT) is the temperature within the "deep" body tissues and organs, which have a high level of basal metabolism. The main ones are the brain and all the abdominal cavity inner organs (e.g., liver, heart, kidney) (Krauchi 2007; Tansey and Johnson 2015).

So, Tb, which depends on CBT, is a critical homeostatic parameter influencing cellular function and organismal survival. Increasing of Tb induces protein denaturation and reduction in membrane fluidity, ion fluxes, and enzyme performance that could dangerously affect the organism's health.

The central neural circuits for thermoregulation orchestrate behavioral and autonomic repertoires that maintain Tb during thermal challenges. Tb is sensed by thermal receptors, either in the external or the internal (e.g., during exercise) environment (Morrison 2016).

In the majority of mammals CBT standard value is set around 37° C (Mekjavic and Eiken 2006; Tansey and Johnson 2015) and the brain CBT is the main target for homeothermy, thus all the behavioral and physiologic processes are regulated on it over a broad environmental temperature range (Mekjavic and Eiken 2006).

General aspects of thermoregulation control

Ta is sensed primarily by the skin, but there are also thermoreceptors in the oral cavity and in the upper respiratory airways (Cliff and Green 1996; Cerri 2017).

The temperature inputs are then elaborated by the central nervous system, mainly by the preoptic area and parabrachial nucleus, to correct any impairment by activating adequate effector mechanisms.

The effector mechanisms for the cold defense, which cause an increasing in the energy costs, includes thermoregulatory behavior to reduce heat loss, cutaneous vasoconstriction (CVC), to conserve heat in the body core, piloerection, non-shivering thermogenesis in brown adipose tissue (BAT) and shivering thermogenesis in skeletal muscle (Morrison and Nakamura 2011).

Animals also show thermoregulatory behaviors that are defined as stereotypical somatic motor acts and are performed in to minimize or optimize heat transfer from the body to the environment. In rodents, such behaviors include postural changes (huddling in the cold or stretching the limbs in the heat), the movement to a more comfortable environment (cold seeking moves to hot environment), or the spreading of saliva on the fur in a hot environment (Morrison and Nakamura 2011).

Since the skin is the first organ that receives the indication of a potential threat to brain and core temperature homeostasis, it is not surprising that thermoregulatory behavior in animals is triggered primarily by cutaneous thermal receptors (Morrison and Nakamura 2011).

There are many theories about the regulation of CBT: the first interpretative theory is named "the open loop theory of thermoregulation" (Romanovsky 2007), which asserts that every thermal effector operates independently from the others, and it is turned on or off by its own neural controller at different temperature thresholds. From this point of view, Tb is just the result of the parallel activity of all the open loops controlling the thermal effectors (Cerri 2017). The main theoretical framework of the thermoregulation physiology is the "set point theory". According to this theory, the

brain controls Tb by changing the reference value of CBT, the so-called set point (Boulant 2006). The thermal effectors will, therefore, work in a coordinated manner to reduce the difference between the core temperature and the set point (Cerri 2017).

Thermoregulation in mammals is under the control of the autonomic nervous system (ANS) which modulates the thermogenic and thermo-dissipative activity of organs to maintain an appropriate Tb for each of the animal's activities (Cerri 2017).

CBT is regulated with thermo-effector thresholds, which are subject to circadian oscillations (Tayefeh, Plattner et al. 1998). Circadian rhythms in mammals are produced by the self-sustaining central pacemaker in the suprachiasmatic nuclei (SCN) of the hypothalamus (Moore and Danchenko 2002). A rostral projection from the SCN to the preoptic anterior hypothalamus (POAH) conveys the circadian signal to the thermoregulatory system (Moore and Danchenko 2002).

The regulation of CBT results from the concerted action of the homeostatic and circadian processes (Kräuchi 2011). In humans, the daily decline of CBT in the evening results from a regulated decline in the thermoregulatory thresholds of heat production and heat loss; the inverse happens in the morning. When heat production is higher than heat loss, body heat content increases and vice versa.

Depending on Ta, about 70 to 90% of body heat content is located in the body core CBT (Kräuchi 2011). The balance in heat production and loss are changed by activities such as muscular exertion and fluid and food intake that is not randomly distributed over the circadian cycle.

Under resting conditions, about 70% of heat production depends on the metabolic activity of inner organs (Kräuchi 2011), whereas body heat loss is initiated by heat redistribution from the core to the shell through blood flow to the distal skin region.

Thermal sensitivity and TRP receptors

The location of thermoreceptors is not homogeneous in all the organs and their role is different in each body part.

Thermal sensitivity can also be divided into peripheral-thermoception and central-thermoception.

As previously stated, Ta is primarily sensed by the peripheral thermoreceptors located in the skin, and warm receptors are less abundant than cold receptors (Cliff and Green 1996). Warm central thermoreceptors are located in the hypothalamus, spinal cord, viscera, and great veins and they are in a higher number than cold thermoreceptors. The activation of central thermoreceptor can modify the CBT inhibiting cold thermoreceptors (Tansey and Johnson 2015).

Major advances in the transduction processes in peripheral thermal sensation have been made since the discovery of the large family of transient receptor potential (TRP) channels in the past fifteen years. Thermoreceptors are part of this family, and different TRP channels provide information regarding specific ranges of temperature, they can be expressed in cell membranes and in membranes of internal structures (Wang and Siemens 2015). Many TRP receptors are polymodal in their activation, but all result in cation influx. TRP channels are involved in thermal sensation and they may contribute by direct activation of sensory fibers (Tansey and Johnson 2015). Nine of them are sensitive to temperature thresholds and their roles have been extensively reviewed (Morrison, Sved et al. 1999; Caterina 2007). In literature the temperature receptors are subdivided into cold noxious, cold, warm, and hot noxious subpopulations on the basis of the temperature stimuli which discriminate (Tansey and Johnson 2015).

Among the most interesting of these channels is the TRPM8 channel, whose natural agonist is menthol; this channel mediates the feeling of cold and it is increasingly activated as temperature drops below 27°C. So it's likely to presume that TRPM8 could mediate innocuous cold sensation (Peier, Moqrich et al. 2002; Tansey and Johnson 2015). Further, TRPA1 channel is activated at temperatures below 17°C and may

contribute to noxious cold sensation, although his role is not completely clear (Cliff and Green 1996).

The feeling of warmth is sensed primarily by the TRPV1 channel (Chen 2015), whose natural agonist is capsaicin, but the TRPV3 channel is also involved (Cliff and Green 1996). TRPV1 and TRPV2 were among the first to be identified with temperature sensitivity. They are activated by temperatures higher than 43 and 52°C, respectively, and may mediate noxious hot sensation (Nakamura and Morrison 2010). TRPV4 and TRPV3 are activated by temperatures above 25 and 31°C, so is likely to assume that they mediate innocuous warm sensation (Smith, Gunthorpe et al. 2002).

Thermoregulatory control network

In non-anesthetized animals, the core and brain temperature doesn't drastically change if they are exposed to a cold environment (Bratincsak and Palkovits 2005). This is an example of a rapid thermo-defensive response that is evoked by detecting changes in environmental temperature through thermoreceptors in primary sensory nerve endings which are distributed across the skin.

The central thermoregulatory control of the sympathetic outflows mediates CVC and BAT thermogenesis. Moreover, regulates the somatic motoneurons that produce shivering, which is effected through parallel but distinct, effector-specific, integrative/efferent circuits (Morrison 2016).

The cutaneous thermoceptors information is transmitted in a feedforward manner to the preoptic area (POA), a sensory-motor integrative site for thermoregulation, located rostral to the hypothalamus (Morrison and Nakamura 2011; Morrison 2016; Cerri 2017). It has been proposed that spontaneous activity in POA neurons could be a pacemaker able to produce action potentials. This neurons are temperature sensitive , this reflects the temperature sensitivity of these membrane currents (Zhao and Boulant 2005; Wechselberger, Wright et al. 2006).

Neurons in the POA are postulated to integrate ascending peripheral signals with local signals to regulate the output of BAT and shivering thermogenesis- promoting neurons in the dorsomedial hypothalamus (DMH) (Nakamura and Morrison 2007) and of CVC-promoting neurons in the median preoptic nucleus (MnPO) (Morrison 2016) (Morrison and Nakamura 2011).

Thermal information from core body receptors is transmitted to the parabrachial nucleus (PBN) in the brainstem (Cerri 2017); the dorsolateral part receives the cold-activated fibers, whereas the dorsomedial part receives the warm ones (Cerri 2017). PBN transmits the thermal information to the ventrolateral portion of the thalamus that delivers the signals to the cerebral cortex, which is the anatomical substrates for the effective cold or warm sensation.

At the same time, thermal information is also sent to the hypothalamus, especially to the MnPO, providing the anatomical substrates for the autonomic control of temperature (Schmieg, Mercer et al. 1980; Xue, Yang et al. 2016; Cerri 2017).

The core body thermoregulatory mechanisms involve many organs like the brain, spinal cord and abdomen (Morrison 2016).

The afferent fibers from cold and warm abdominal thermoreceptors are included among the splanchnic and vagus nerves afferent fibers and their responses to temperature changes are similar to those of cutaneous thermoreceptors (Morrison and Nakamura 2011). It's reasonable to suppose that thermal information derived from core body structures would rise a thermoregulatory response only for extreme thermal situations (Morrison and Nakamura 2011).

Therefore, warm-sensitive POA neurons integrate cutaneous and local thermal information, and project to the medial preoptic region of the hypothalamus (MPO) with has an inhibitory function. MPO neurons are tonically activated at thermoneutral temperatures and suppress both shivering and non-shivering thermogenesis (Morrison and Nakamura 2011). Moreover, it's a current hypothesis that the MnPO neurons integrate all the information (J., T. et al. 2015)

Furthermore, there are many organs that play a direct role in heat production, such as the BAT, liver, and skeletal muscle. Others, such as the heart or the thyroid, play an indirect role (Cerri 2017). The activity of most of the thermoregulatory organs is controlled by the sympathetic branch. The sympathetic preganglionic neurons to these organs are in the intermediolateral column within the spinal cord, whereas the sympathetic premotor neurons are in the brainstem area of the raphe pallidus (RPa) (Cerri 2017).

The activation of neurons within the RPa stimulates thermogenesis having little or no effect on arterial pressure. Thermoregulation is also in relationship with osmoregulation, in particular, dehydration in hot environments suppresses heat dissipation (Doris and Baker 1981). Other conditions that can modulate thermoregulation include the hypoxia (Cadena and Tattersall 2014), diving reflex (Hill, Schneider et al. 1987) and sleep (Parmeggiani 2003).

Nocturnal secretion of melatonin, a pineal hormone, which is under central nervous system (CNS) control, contribute to downregulation of CBT in the evening (Krauchi, Cajochen et al. 2006). Moreover melatonin, acting directly on blood vessel receptors and indirectly through modulation of sympathetic nerve activity, induces distal vasodilation in humans (Krauchi, Cajochen et al. 2006).

Thermogenesis in brown adipose tissue

In consequence to a fall in CBT due to a cold environment or to the presence of pyrogenic cytokines, CNS thermoregulatory networks can stimulate thermogenesis primarily in BAT, skeletal muscle (shivering) and heart (Morrison and Nakamura 2011). Non-shivering or adaptive thermogenesis in BAT is the specific metabolic function of this tissue and it is actuated by the high expression of uncoupling protein-1 (UCP1) in its mitochondrial membranes, which permit to uncouple oxidative metabolism from ATP production and energy expense (Tansey and Johnson 2015).

BAT is a crucial thermoregulatory effector in rodents and small mammals but also for adult humans (Nedergaard, Bengtsson et al. 2007). Recently, it has been confirmed the role of the BAT in the thermoregulation for human adults as well as neonates (van der Lans, Hoeks et al. 2013).

Moreover, BAT has a central role in the process of metabolic balance and it has been recognized to be a potential site for drugs aimed at controlling energy expenditure, so it could potentially be a therapeutic site for the treatment of obesity (Tseng, Cypess et al. 2010).

In response to inputs from peripheral and central thermoreceptors SNS activity can stimulate BAT thermogenesis by catecholamines which bind on β3-adrenergic receptors and activates UCP1. POA neurons are supposed to have an inhibitory action on BAT thermogenesis (Morrison and Nakamura 2011).

In addition, BAT thermogenesis can be modulated by a number of nonthermal factors, including hypoxia, infection, hypoglycemia, and psychological stress (Morrison and Madden 2014).

Metabolism in physiological conditions

BMR indicates the energy supply required to perform the fundamentals metabolic functions, thermoregulation and exercise (Dennis Grahn 2004). Tb is regulated with a proportional increase in heat production that compensates for heat loss at or above a species- or population-specific minimum (Geiser and Ruf 1995). When the heat produced by basal metabolic activity is scarce to provide for the resting animal thermal demands, additional endogenous heat could be generated through different voluntary or involuntary activities, for example with shivering, voluntary exercise or non-shivering thermogenesis (Dennis Grahn 2004).

Likewise, when Tb is higher than the dissipation capacity metabolic efforts will increase to enhance heat dissipation by evaporative heat loss. The thermoneutral zone (TNZ) is limited by a lower critical Tb, below which the resting metabolic rate (RMR) is not enough to compensate for heat loss. Therefore, with acute exposure to severe cold or prolonged exposure to moderate cold, heat loss from the body will be higher than the capacity to produce metabolic heat and the Tb will fall (Dennis Grahn 2004). The entrance into torpor is facilitated with low Ta usually well below the TNZ. The difference between Tb and Ta is usually small 1–3 °C (Geiser 2004) so Ta has a crucial role in determining the value reached by Tb in torpid animals. Another crucial factor promoting the torpid state occurrence is the food scarcity, that in laboratory is mimed with the caloric restriction protocol (see experiment one methods chapter) (Swoap and Gutilla 2009).

If any external interference occurs the hypothalamic temperature set point (Tset) can rise in torpid animals starting thermoregulation, so, the thermoregulation is maintained during torpor. In placental heterotherms BAT is one of the major players involved in endogenous heat production during arousal from torpid states (Geiser 2004). The mean normothermic life parameter values of the laboratory mouse (Mus Musculus) are a body temperature is 37.4 °C and a BMR of 1.47 ml O2/(gh) that decreases respectively

to 19 °C during torpor bouts with a mean torpid metabolic rate value of 0.3 ml O2/(gh) and a Q10 value of 2,4 (Geiser 2004).

Interactions between metabolism and torpor

Body temperature and metabolism

The mechanism that rule different phases of a torpid state isn't clear in literature, in the past 20 years many theories have been formulated by scientists all over the world. Although many experts agree that the reduction of MR during torpor is substantial and is crucial for survival in many species, the mechanisms of how MR is reduced remains controversial.

Several mutually exclusive hypotheses on MR reduction during torpor have been put forward. Several mutually exclusive hypotheses on MR reduction during torpor has been proposed. The traditional, and obsolete, view assert that Tb and MR fall together at the moment of torpor entry, this affirmation is based on the Q10 value, which is the measure of biological system changing rate consequently of a temperature range variation of 10 °C. This theory suggests that the MR reduction during torpor below BMR can be explained by temperature effects, because a Q10 value of 2 was found in torpid animals (Snapp and Heller 1981; Guppy and Withers 1999). Therefore, in this theory the reduction in metabolic rate seems to be explained solely by the temperature effect on the biochemical processes in the body (Strijkstra and Daan 1998) as, for example, the reduction of the enzyme-catalysed reactions rate (the so-called Arrhenius or Q10 effect) (José 2002).

In successive experiments, higher values of Q10 (>3) have found in different species during torpor entry, so the temperature effects itself isn't enough to explain the entrance process into torpor. Therefore, a physiological regulation must be involved in the

reduction of MR (Geiser 1988; Storey and Storey 1990). Others scientist propose that TMR isn't influenced by Tb. They argue that MR is down-regulated at torpor entry and the fall of Tb is a consequence and not the reason for the MR reduction (Storey and Storey 1990; Heldmaier and Ruf 1992; Heldmaier G 1993). Finally, it has been suggested that, as during normothermia, MR during torpor is a function of the Tb-Ta differential (Heldmaier G 1993; Sunagawa and Takahashi 2016).

All the more recent theories agree that Tb fall after MR, this suggests an active, regulated metabolic suppression (Geiser 2004; Staples 2014; Cerri 2017). To better understand the MR-Tb relationship we have to consider that the Tset for Tb is down-regulated during the torpor entrance (Heller, Colliver et al. 1977). The fall of Tset results in a fall of MR from the RMR (that is calculated adding together the energetic cost of thermoregulation and BMR) to BMR because the thermoregulation is supposed to cease during the torpor entry (Geiser 2004). Only when Tb reach the lower Tset during the cooling phase is the metabolic heat production increased in order to keep Tb at or above torpor Tset (Geiser 2004).

An important consideration is that small variation in Tset can radically reduce energy expenditure, because of the thermal inertia, so the animal doesn't need large changes in Tb to save energy during the cooling phase. From this point of view, the transient fall of MR is not due to the fall of Tb but to the fall of Tset. Thus, it is correct to say that the MR has to decrease before the falling of Tb (Geiser 2004).

We have also to consider, that this mechanism is proved to be different between daily heterotherms and hibernators because the main energy supply is different between these two groups. Daily heterotherms, even during the torpor season, remains food collectors and, so, torpor is interrupted to have daily foraging, as opposed to hibernators, whose main fuel source is fat (Geiser 2004). Small daily heterotherms have higher BMRs, and the effects of a reduction of Tb by about 20°C, as commonly observed in daily heterotherms, results in a maximum reduction of the torpor metabolic rate (TMR) to about 25% of BMR assuming a value Q10 around 2 (Geiser 2004).

The reduction in metabolic rate in animals who display daily torpor is largely determined by the decrease in Tb, hibernators seem to apply some kind of extra reduction in metabolic rate (Kräuchi 2011).

Small hibernators undergo prolonged periods of torpor and can survive on stored fat for months.

If hibernators exhibit the same MR reduction as small daily heterotherms their fuel stores would be depleted in a very short term, well before the end of winter. Thus, it is not surprising that the reduction of TMR below BMR in small hibernators is much more pronounced than in daily heterotherms and that the relationship between Tb and TMR of the two groups differs (Geiser 2004).

Circulating and cellular fuels

In the last decade, the improvement of gene analysis technologies allowed to discover new links between gene expression and torpor. Consequently, new theories involving circadian clock genes and torpor have been postulated: new experiments on 43 birds and 141 mammals (Ruf and Geiser 2015) confirmed that Per1, Per2 and Bmal1, are expressed rhythmically during hibernation rather as opposed to constantly (Revel, Herwig et al. 2007; Melvin and Andrews 2009).

The theories described below (about the decrease in MR/Tb) and the new ones about gene expression mechanisms may not be entirely mutually exclusive, because any metabolism-driven changes may still be modulated by the endogenous clock that influences, particularly, the arousal from torpor (Ruf and Geiser 2015).

In any case, it should be mentioned that the endogenous clock modulating Tb and MR in hibernators, if it exists, must differ functionally and anatomically from the circadian clock controlling daily torpor (Malan 2010).

The researches on circulating and cellular fuels are a fundamental part of torpor metabolism study.

In fact, both hibernation and daily torpor episodes are preceded by a period of time in with shortage of food alter the animal nutrient status (Geiser 2004; Swoap and Gutilla 2009). So, the scarcity of fuels in blood and cells could be a trigger for torpor.

A study in mice showed a connection between cellular nutrient status and the circadian clock (Ramsey, Yoshino et al. 2009). An important parameter to measure the cellular nutrient status are the ratios of intracellular [5'-AMP] to [ATP] and [NAD+] to [NADH] (Rodgers, Lerin et al. 2005). These ratios increase proportionally to the decrease of cellular nutrient status.

Shortage of food is a stressful situation leading the cells to switch their metabolism to lipids as the primary energetical source in order to recover the normal nutrient status (Tashima, Adelstein et al. 1970).

So, new theories arose, which links reduced the availability of food in the environment, the energy status of the cell, the mammalian circadian clock and the response to oxidative stress.

R. G. Melvin and Matthew T. A. (Melvin and Andrews 2009) supposed that in a fasted animal occurs a depletion of cellular nutrients and this would increase intracellular concentrations 5'-AMP and NAD+.

Increased [NAD+] would stimulate the activation of the SIRT1 deacetylase that controls the activation of SERT1 itself. SIRT1 can enter into the nucleus and deacetylate lots of targets including the core circadian clock protein, BMAL1 (Takahashi, Hong et al. 2008). SIRT1 could also activate nuclear receptor proteins that promote transcription of enzymes active during lipolysis and in the response to hypoxic stress like HIF-2α (Dioum, Chen et al. 2009). Activation of lipolytic enzymes is part of the switch from carbohydrate to lipid-based metabolism.

Nutrient depletion provokes also increased intracellular [AMP] and results in increased activation of adenosine monophosphate kinase that phosphorylates the nuclear receptor carbohydrate responsive element binding protein, this down-regulate glycolysis and, so, concur to the switch from carbohydrate to lipid based metabolism (Postic, Dentin et al. 2007).

Glucose contributes to the torpid state

As previously mentioned, in mice daily torpor occurs in response to decreased energy availability. The most recent theories, not in order of importance, assume that potential contributors towards daily torpid state are all the players that can cause a drop of power levels. Could be energy-sensitive hormones such as leptin and insulin, as well as the availability of circulating fuels, such as glucose, free fatty acids, and ketones (Melvin and Andrews 2009).

Glucose is the primary fuel used by the brain metabolism, so its deficiency may play an important regulating role in initiating or maintaining torpor. This idea is not new, many experiments on daily torpid animals showed a gradual decline in plasma glucose which precedes or is combined with daily torpor onset (Nestler 1990; Heldmaier, Klingenspor et al. 1999; Dark 2005; Franco, Contreras et al. 2013)

Hibernators similarly to daily torpid animals during deep hibernation shows a reduction in plasma glucose simultaneously with the fall of body temperature and metabolic rate (Sarajas HSS 1967; Galster and Morrison 1970; Atgie, Nibbelink et al. 1990), although this is not true for all the species of hibernators (Musacchia and Deavers 1981; Zimmerman 1982). The role of glucose into torpor triggering emerges also in the pharmacological experiment with the administration of 2-deoxy-glucose (2-DG).

2-DG is an analogue of glucose that can't be metabolized by the enzyme phospho-gluco-isomerase and block the glycolysis cycle (Wick, Drury et al. 1957). The administration of 2-DG in pharmacological in vivo studies on two daily torpid species, the Siberian hamster and the deer mouse, causes a temporary decrease in Tb (Dark, Miller et al. 1994; Stamper and Dark 1996). However, it's important to note that administration of 2-DG induces low body temperature also in rat and human which are not able to undergo in daily torpor (Freinkel, Metzger et al. 1972; Penicaud, Thompson et al. 1986).

Moreover, the autonomic nervous system (ANS) is deeply involved in the regulation of the different phases of the Torpor bout. There is a lot of evidence of a sympathetic downregulation while parasympathetic is upregulated during the torpor entrance and the deep torpor (Morhardt 1970; Milsom, Zimmer et al. 1999; Zosky 2002; Horwitz, Chau et al. 2013).

Even though, sympathetic activity to white fat increases during caloric-restriction-induced torpor and causes the decreasing in clearing leptin and elevates lipolysis. Consequently, the sympathetic activity increases free fatty acid releasing in the blood (Rayner 2001; Swoap, Gutilla et al. 2006; Swoap and Weinshenker 2008).

Moreover, glucose deficiency leads to the inhibition of sympathetic tonus in rats (Young and Landsberg 1979) and garden dormice (Atgie, Nibbelink et al. 1990).

The sympathetic nervous system appears to be activated during arousal from torpor when the heart rate is maximal and brown adipose tissue is activated to produce heat (Hudson and Scott 1979; Swoap and Weinshenker 2008; Oelkrug, Heldmaier et al. 2011).

So, the hepatic glucose dynamics are modified in daily torpor because the liver is involved by the autonomic changes described before.

In physiological conditions the sympathetic activity on the liver provokes the release of glucose while repressing glycogen synthesis; the opposite effect is exerted by the parasympathetic activation via the vagus nerve (Mizuno and Ueno 2017).

Reasonably, the decrease in blood glucose during a day of scarce food availability is a consequence of reduced carbohydrate intake and the extensive reduction of sympathetic outflow that occur during daily torpor episodes, especially for decreased sympathetic outflow to the liver (Lo Martire, Valli et al. 2018).

Sleep and Torpor

Physiology of Sleep

The wake-sleep cycle is the sequence of three principal behavioural states: wakefulness (W), non-rapid eye movement sleep (NREM) and rapid-eye movement sleep (REM).
 From a physiological point of view, sleep can be defined as a reversible behavioural state of perceptual disengagement form and unresponsiveness to the environment. However, this definition is simplistic because it is also true that sleep is a complex mixture of behavioural and physiologic processes (Dement 2011).

The distinction of REM and NREM sleep is based on numerous physiologic parameters, these two states exist in all mammals and birds yet studied, and they are as distinct from one another as each is from wakefulness.

In polysomnography, W is defined by a high electromyographic activity (EMG) and a desynchronized electroencephalographic (EEG) activity with low-voltage rapid waves. NREM sleep (or slow wave sleep) is easily distinguishable from both wakefulness and REM sleep by high voltage and synchronous EEG rhythms, including sleep spindles, K complexes and high-voltage slow waves, associated with low muscle tones and minimal physiological activity. NREM sleep, in human sleep, can be divided into four stages using the EEG (Dement 2011).

Stages 1, 2, 3 and 4 sleep and approximately parallel a depth-of-sleep continuum during NREM sleep, the arousal threshold is generally lower in stage 1 and increase in each consequent stage. NREM sleep is usually associated with minimal or fragmentary mental activity. A shorthand definition of NREM sleep is a relatively inactive yet actively regulating brain in a movable body (Rechtschaffen 1968, repr. 1973.; Dement 2011).

REM sleep, or paradoxical sleep, is identified by episodic bursts of rapid eye movements, suppression of EMG and EEG activation. A relatively low voltage waves characterizes the EEG pattern with a mix of frequency (frequency in θ range is common during REM sleep, particularly in proximity to eye movements). The activity in REM sleep' EEG can be in the α range (1-2 Hz slower than waking activity).

There are not any stages in REM sleep, and it is characterized by the spinal motor neurons inhibition which provokes the suppression of postural motor tonus during REM sleep, although tonic phases may occur in this state.

A normal human adult enters sleep by the NREM state, this principle is important because reflects a highly reliable finding of normal human sleep and this knowledge permit to consider normal versus pathologic sleep. A significant example can be the abnormal entry into sleep through REM sleep that permits to diagnostic in adult patients with narcolepsy (Dement 2011).

Sleep and torpor

Sleep and torpor have blatant common aspects: they are highly regulated, adaptive, and reversible behaviours with a stick out the tendency towards energy conservation (Berger 1984).

Nocturnal hypothermia is the most common pattern of non-seasonal torpor, representing a survival strategy of many small mammals, which allow their metabolic rate to decrease during sleep by 20–30%, and a decrease in Tb of few degrees Celsius. This strategy allows to increases the interval from one meal to the next (Storey and Storey 2010). For instance, the fruit-eating manakins from the tropical rain forest and several species of chickadees and artic willow tits show nightly shallow depressions of body temperature to approximately 27-34°C (REINERTSEN 1983) for few hours.

The daily energy savings derived from nocturnal hypothermia range from about 10% in the willow tit to about 30% in the manakin (REINERTSEN 1983).

Usually, torpid episodes happen in the animals' nest, suggesting that they look for a safe environment to undergo into torpor, this is true also for sleep episodes.

Moreover, animals in torpor seem to be asleep because they maintain a sleep-like posture for the duration of the bout, with elevated arousal thresholds, accompanied by a reduction in muscle tone (Kräuchi 2011; Silvani, Cerri et al. 2018).

Furthermore, they are both characterized by a reduction in Tb, greater in torpor than in sleep, but the mechanism implied in the resetting of the central regulation of Tb during the transition from wakefulness to NREM sleep appears to be homolog with the one of torpor entrance (Heller and Glotzbach 1977).

Analysis of the EEG patterns shows that rodents during torpid bouts stay more in NREM sleep than REM sleep, which is reduced or not present (Walker, Garber et al. 1979; Harris, Walker et al. 1984; Deboer and Tobler 1994; Deboer and Tobler 1995).

In particular, recordings in the deep hibernator hypothalamus indicate that these animals keep alternating between long NREM sleep bouts and short waking bouts (Krilowicz, Glotzbach et al. 1988). These findings support the hypothesis that NREM sleep is an adaptive behaviour for energy conservation, and its function is strengthened during torpor (Berger 1984; Obal, Rubicsek et al. 1985; Heller 1988).

Accordingly, torpor is usually entered through sleep, as demonstrated by the studies conduct by Walker and colleagues (Walker, Glotzbach et al. 1977) in ground squirrels. They showed that Tb starts to decrease during either REM or NREM sleep but never during wakefulness. Walker and colleagues were able to record the EEG during entrance in torpor only if the brain temperature was maintained above 25°C. To correctly analyse the EEG pattern, we have to consider the temperature effect on EEG frequency as Deboer at all proves in hamsters (Deboer and Tobler 1995). They show a systematic downward shift of EEG frequency bands as cortical temperature decreased. Therefore, the EEG slow waves during torpor occurred at frequencies lower than those during euthermia. This is crucial because the lack of physiological EEG slow wave during torpor can represent a long period of sleep deprivation. During the arousal, the animals emerging from torpor immediately enter into deep NREM sleep, irrespective

of whether animals emerge from deep hibernation (Daan, Barnes et al. 1991; Trachsel, Edgar et al. 1991) or daily torpor (Deboer and Tobler 1994).

Therefore, during deep torpor it is likely that the restoring function of sleep cannot be fulfilled, so animals must awaken to recover from the hypothermic sleep deprivation. This statement was confirmed in Djungarian hamster (Deboer and Tobler 2000).

Experiment conducted on golden-mantled ground squirrels showed that the slow-wave activity during NREM sleep, following arousal from torpor, is related only to the minimum brain temperature reached during torpor. So, the sleep debt accumulates during torpor may be a brain-temperature dependent effect (Larkin and Heller 1996).

The synthetic torpor experiment in rats shows a massive increase in EEG slow-wave activity in the euthermic period after deep hypothermia (22°C) (Cerri 2017).

The power of the EEG possibly increases proportionally to the magnitude of the metabolic effort made by the animal to rise from torpor and recover to euthermia. In light of this results in the rat, a great part of the sleep debt could be accumulated during the rewarming phase. In conclusion it is possible that the neural circuits that generate and sustain torpor and NREM are shared, at least in part, mainly because NREM sleep and torpor have in common the outcome of reducing energy expenditure (Silvani, Cerri et al. 2018).

Common Physiological Changes in NREM Sleep and Torpor

The daily temperature trend is characterized by a drop in Tb during the resting phase, which results from an increase in heat dissipation due to cutaneous vasodilation and a concurrent decrease in heat production (Krauchi and Wirz-Justice 1994). NREM sleep in humans is the prevalent component of the rest period and reduces energy expenditure by approximately one-third (Bouma, Kroese et al. 2011; Kayaba, Park et al. 2017). The energy saving characteristic of NREM sleep is observed in small animal models, such as mice, particularly when are considered long, consolidated wake-sleep episodes (Zhang, Zeitzer et al. 2007). Moreover, NREM sleep is characterized, in human and small animal model, by a fall in MR accompanied in concomitance to a decrease in arterial pressure (AP) and heart rate (HR) (Silvani, Bastianini et al. 2014).

It's still not completely clear how AP can decrease but there are two currently main theories in literature: the first assert that the decrease in HR is due to a balance of cardiac sympathetic withdrawal and parasympathetic activation, which cause the AP decrees (Lo Martire, Silvani et al. 2018) in absence of a compensatory increase in stroke volume and/or peripheral resistance (Khatri and Freis 1967). The second theory is based on a recent evidence obtained in mice, which suggest that the diminish AP during NREM sleep depends from a reduction in sympathetic vasoconstriction (Lo Martire, Silvani et al. 2018), itself due to a decrease in sympathetic activity to the vasculature of skeletal muscles (Somers, Dyken et al. 1993), skin (Takeuchi, Iwase et al. 1994), and kidneys (Yoshimoto, Sakagami et al. 2004).

The profound reduction of MR during torpor results in greater energy savings compared with NREM sleep. As in NREM sleep the autonomic nervous system is deeply involved in all stages of a bout of torpor. During entrance and the maintenance of a torpor bout, parasympathetic activity to the heart is markedly increased causing a diminishing in HR. Periodic increases in HR coupled to ventilation are present in torpor bouts due to the instability of parasympathetic action (Morhardt 1970; Milsom,

Zimmer et al. 2001; Zosky 2002; Zosky and Larcombe 2003; Horwitz, Chau et al. 2013). Entrance into torpor is characterized by a sympathetic activity withdraws in concomitance to the parasympathetic dominance (Atgie, Nibbelink et al. 1990). Similarly, in humans NREM sleep decrease in energy expenditure is associated with a decrease in minute ventilation due to the parasympathetic activity, which leads to a rise in the partial pressure of carbon dioxide and a fall in the partial pressure of oxygen (Douglas, White et al. 1982). These effects of NREM sleep on respiratory control are also seen in small model organisms: in mice NREM sleep decreases the respiratory rate and blunts the chemoreflex responses to hypoxia (Nakamura and Morrison 2007). Approaching the onset of torpor, the ventilation in mice occurs in concert with the spike of EMG activity and tachycardia (Milsom and Jackson 2011; Swoap, Kortner et al. 2017). Likewise in NREM sleep the ventilation during torpor decreases more than metabolic rate does, leading to a modest respiratory acidosis (Milsom, Zimmer et al. 2001; Milsom and Jackson 2011).

Orexin, Sleep and Torpor

Physiology of Orexin system

In 1998 two research groups, using different techniques, independently discovered two neuropeptides produced by neurons in the lateral and posterior hypothalamus (de Lecea, Kilduff et al. 1998; Sakurai, Amemiya et al. 1998) and gave them different names. Sakurai et al. called them orexins, from the Greek word "orexis" which means appetite, whereas De Lecea et al. called them hypocretins. Therefore, Orexin A and B (ORX A-B) is respectively Hypocretin 1 and 2 (HCRT-1, HCRT-2).

Sakurai et al. discovered a multiple orphan G-protein-coupled cell surface receptors (GPCRs) and did a systematic biochemical search for its ligands: he used a cell-based reporter system wherewith identified the Orexins (ORXS), a new family of neuropeptides that can bind two closely-related orphan GPCRs.

In the lateral hypothalamus, and adjacent areas, a large expression of mRNA for the orexin's precursor was found. This brain portion is known to be implied in energy homeostasis and regulation of feeding behaviour. ORXS implication in food control networks was discovered when was proved the infusion in rat brains increased food consumption; further analysis demonstrated that ORXS production was influenced by the nutritional state of the animal.

De Lecea et al. identified a specific C-DNA from 38 clones which was expressed in the posterior hypothalamus, this sequence encoded for two putative peptides: the secretin, a gut hormone, and the ORXS.

In mice the ORXS mRNA is a product of a gene on chromosome 11 and accumulate in neuronal cell bodies of the dorsal and lateral hypothalamus after the third week of life (de Lecea, Kilduff et al. 1998).

"Orexin" and "Hypocretin" is considered synonymous in many papers but for the sake of clarity the term Orexin is used throughout this script.

ORX A is a peptide of 3,562 Da composed by 33-amino acid with two intra-chain disulfide bonds and carboxy (C)-terminal amidation and an amino (N)-terminal pyroglutamyl residue; its structure is conserved throughout many mammalian species like human, rat, mouse, cow, sheep, dog and pig (Sakurai 2007).

ORX B is a C-terminally amidated linear peptide of 2,937 Da composed by 28-amino acid. Human ORX B has two amino acid substitutions compared to rodent sequence and four as compared to pigs and dogs one.

ORX A and B are 46% identical, the C-terminal part is very similar whereas the N-terminal is more variable (Sakurai 2007). They are originated by a common precursor peptide: the prepro-orexins (prepro-ORXS) polypeptide. The prepro-ORXS gene encodes for a 130-residue (rodent)

or 131-residue (human) polypeptide (Sakurai, Moriguchi et al. 1999).

The prepro-ORXS gene consists of two exons and one intron of 818 bp distributed over 1432 base pairs gene localized in the chromosome 11 in mice and in 17q21 in humans A fragment of the human prepro-ORXS gene, which contains a 3.15-kb 5'-flanking region and the whole length of the 5'-noncoding regions of the first exon is sufficient to direct the expression of the Escherichia coli β-galactosidase (lacZ) gene in ORXS neurons without ectopic expression in transgenic mice. The lacZ-positive neurons were positively stained with the anti-ORXS antibody, suggesting that this genomic fragment contains all the necessary elements for appropriate expression of the gene (Ohno and Sakurai 2008).

This fragment of the human prepro-ORXS gene could function as a promoter and it has been used to induce expression of exogenous molecules in ORXS neurons and create transgenic mice. A good example is the ORXS neuron-ablated mice and rats (Hara, Beuckmann et al. 2001) in which ORXS neurons specifically express the calcium-sensitive fluorescent protein (yellow cameleon Yc2.1) or green fluorescent protein (Yamanaka, Beuckmann et al. 2003). In vivo experiments with these rodents permitted to better understand the different roles of ORXS system and its biochemistry.

The action of ORXS is related by two G protein-coupled receptors named respectively orexin A receptor (ORX-1R) and orexin B receptor (ORX-2R); it's interesting that ORX-1R is structurally similar to the Y2 neuropeptide Y (NPY) receptor (26% similarity), a hormone deeply involved in Torpor regulation (Paul, Freeman et al. 2005).

Humans ORX-1R and ORX-2R have a 64% amino acid sequence in common, the structure of this receptor is conserved in rats (94% for ORX-1R and 95% for ORX-2R) (Ohno and Sakurai 2008).

Competitive radioligand binding assays showed that ORX-1R is a high-affinity agonist for ORX-2R. The concentration of cold ORX-1R required to displace 50% of specific radioligand binding (IC50) was 20 nM.

Human ORX B is an agonist of ORX A, however it's not efficient because ORX B has a significantly lower affinity for the receptor ORX-1R than ORX A: the calculated IC50 in the competitive binding assay was 250 nM for human ORX B, two orders of magnitude lower if compared with the affinity of ORX A.

On the other hand, binding experiments proved that ORX-2R is a high affinity receptor for human ORX B with IC50 of 20 nM but it's not selective because also ORX A had a similar value of IC50 (Ohno and Sakurai 2008).

ORX-1R and ORX-2R are G protein-coupled receptors and conduct the information into cells by activating heterotrimeric G proteins. Distinct protein G may activate different signaling pathways and lead to the diverse physiological roles of ORXS in neurons.

The G protein-coupled neurotransmitter receptors can modulate both voltage-dependent calcium channels and G protein-gated inwardly rectifier potassium channels (GIRKs or Kir3 channels), this difference is a degree of selectivity in the coupling to one or another of these channels in neurons.

ORX-1R transmit signals through the $G\alpha 11$ class of G protein, which trigger the activation of phospholipase C and subsequently the phosphatidylinositol cascade that terminate into an influx of extracellular $Ca2+$.

ORX-2R use the same activation pathway described for ORX-1R: the cascade of reactions is triggered by a Gα11 G protein and inhibited by a Gi G protein (Zhu, Miwa et al. 2003).

ORXS neurons originate from the posterior and lateral hypothalamus (Peyron, Tighe et al. 1998) and project widely to the entire neuroaxis, excluding the cerebellum.

They have a variable shape (spherical, fusiform or multipolar) and size (the cell body diameter ranges from 15‑40 µm). In rat brain have been counted around 3000 ORXS neurons have been counted, which are doubled in the human brain (Peyron, Tighe et al. 1998; Nambu, Sakurai et al. 1999).

The lateral hypothalamic area (LHA), in which orexins are produced, is known as the feeding center so orexins are identified as regulators of feeding behaviour, this is supported by the brain co-localization with melanin-concentrating hormone, an orexigenic peptide, and by the results of an in vivo intracerebroventricular (ICV) injection of ORXS in rats and mice which has triggered feeding behaviours (Sakurai, Moriguchi et al. 1999).

ORXS is also important to regulate the circadian cycle, particularly the wakefulness and their deficiency causes narcolepsy in animals and humans. A crucial contribution to the discover of the ORXS roles came from the animal models of ORXS deficiency. Many types of genetically modified lines have been studied, like prepro-ORXS gene or ORX-2R gene knockout (KO) mice, double ORX 1R and 2R KO mice, and mice and rats treated with hypocretin-ataxin-3-transgene which induced the loss of ORXS neurons (Hara, Beuckmann et al. 2001; Willie, Chemelli et al. 2003; Silvani, Bastianini et al. 2014). In the last decade, with the international renown of optogenetic, also the transgenic mice that conditionally express Trpv1 in Cre-expressing cells are a new model for understanding the effects of orexins in hunger behaviour (Dietrich, Zimmer et al. 2015).

Orexins and circadian cycle

ORXS neurons project to the entire neuroaxis, excluding the cerebellum. The most relevant projection discovered are the nerves ending in the paraventricular nucleus of the thalamus (PVNT), the arcuate nucleus, the locus coeruleus (LC), dorsal raphe (DR) and tuberomammillary nucleus (TMN).

The LC contains noradrenergic neurons, the DR contains serotonergic neurons and the TMN histaminergic ones (Nambu, Sakurai et al. 1999; Peyron, Faraco et al. 2000).

All these regions are crucial for the maintenance of wakefulness and most of them are supposed to be implied in the regulation of torpor (Cerri 2017). The DR and the ventral tegmental area (VTA) contain both ORX-1R and ORX-2R mRNA (Marcus, Aschkenasi et al. 2001). These colocalization highlight the role of these monoaminergic regions as effectors of ORXS, resulting in increased arousal and wakefulness (Sakurai 2007).

This hypothesis is supported by experiments in vitro, in which histaminergic cells of the TMN, dopaminergic cells of the VTA noradrenergic cells of the LC and serotonergic cells of the DR have all been shown to be activated by ORXS (Liu, van den Pol et al. 2002; Yamanaka, Tsujino et al. 2002).

The activities in the TMN, LC and DR are known to be associated with regulation of sleep and wakefulness: the neurons fire tonically during wakefulness, decrease their activity during NREMS, and stop firing during REMS (Sakurai 2007).

ORXS neurons are activated during wakefulness and excite these wake-active neurons sustaining their activity. A rebuttal to this hypothesis is the absence of ORXS neurons activity during NREMS and REMS (Sakurai 2007).

The ventrolateral preoptic nucleus (VLPO) neurons are generally active during sleep and have two inhibitory neurotransmitters: galanin and GABA. In vivo lesions of the VLPO showed a reduction in time spent in NREMS and REMS by more than 50% (Lu, Greco et al. 2000).

The VLPO also receives inhibitory afferents from each of the major monoaminergic and histaminergic systems. Both noradrenaline and serotonin inhibit VLPO neurons. Therefore, the VLPO can be inhibited by ORXS (Saper, Scammell et al. 2005).

Experiments on transgenic mice showed a role of ORXS in shaping EEG activity during REM sleep (Bastianini, Lo Martire et al. 2016).

In conclusion, the ORXS neurons are crucial for the correct regulation of circadian rhythm and the loss of ORXS neurons in the hypothalamus cause the insurgence of the Narcolepsy with cataplexy, a lifelong disorder, which often appear in childhood and is characterized by the intrusion of sleep during wakefulness, loss of muscular tone evoked by intense emotions (cataplectic attacks), metabolic dysfunctions, an altered control of HR and arterial pressure profile during sleep (Silvani, Bastianini et al. 2014).

Orexin regulation of glucose level and metabolism

The integration of metabolic, autonomic, endocrine, and environmental factors results in the control of feeding behaviour. It's well known that the hypothalamus plays a critical role in maintaining energy homeostasis by integrating those factors and coordinating behavioural, metabolic, and neuroendocrine responses (Willie, Chemelli et al. 2001; Suzuki, Jayasena et al. 2012). In mammals, the LHA is crucial for both feeding and behavioural arousal, it was discovered in animal models with lesions of the LHA which exhibit hypophagia, increased metabolic rate and diminished arousal. Frequently this condition leads to the death of the animal by starvation. Therefore, the LHA has been considered as the hypothalamic "feeding center" and represent an important component of the ANS with projections to the other regions of the hypothalamus and throughout the entire neuroaxis (Willie, Chemelli et al. 2001).

The hypothalamic nuclei and circuits have also the key role of sense and integrate the information from multiple circulating peripheral signals such as leptin, insulin, glucagon, adiponectin, and various other gut hormones.

The adipose tissue produces leptin proportionally with the fat mass. High leptin levels suppress ORXS expression and down regulate ORXS neuron firing.

The ghrelin is a hormone secreted by the stomach before the meals and during fasting that activates ORXS neurons.

Therefore, ORXS show up an important role in the control of feeding, also confirmed by in vivo experiments conducted by Hara and colleagues in which intracerebroventricular (ICV) administration of ORX 1R selective antagonist reduced the food intake. Moreover, the prepro-orexin knockout mice and transgenic mice lacking ORXS neurons ate significantly less than the control wild-type mice (Hara, Beuckmann et al. 2001).

The interaction of the metabolic sensors and specific hypothalamic region, both centrally as well as peripherally, is crucial for the maintenance of glucose homeostasis. The deregulation of this circuits is considered an important key factor for the onset and progression of various metabolic disorders such as obesity, dyslipidemia and type 2 diabetes mellitus (Koshiyama, Hamamoto et al. 2006; Gooley 2016; Kim, Toda et al. 2017; Sieminski, Szypenbejl et al. 2018).

Moreover, ORXS are known to play an important role in the central and peripheral regulation of glucose homeostasis.

The central regulation of glucose homeostasis happens by the interaction of various hypothalamic regions such as perifornical (Yi, Serlie et al. 2009), ventromedial hypothalamus (VMH) (Shiuchi, Haque et al. 2009), and suprachiasmatic Nucleus (SCN) (Otlivanchik, Le Foll et al. 2015; Foppen, Tan et al. 2016).

The central role of ORXA in glucose elevation is supported by in vivo experiments in which ICV injection of ORX A is displayed in conscious rodents resulting in the increases of the blood glucose levels (at 60 and 90 min) while intravenous administration of the same dose of ORX A doesn't show any effect (Matsumura, Tsuchihashi et al. 2001; Yi, Serlie et al. 2009).

In contrast, Shiuchi et al., demonstrate that ORX A injection into the VMH do not changes the insulin levels and plasma glucose in the normal rats (Shiuchi, Haque et al. 2009).

The central effects of ORXA on glucose homeostasis is mediated the sympathetic nervous system. Matsumara et al. demonstrate that ICV ORXA administration raised the renal sympathetic nerve activity which results in an augmented sympathoadrenal outflow, that in turn increases the blood glucose levels (Matsumura, Tsuchihashi et al. 2001; Yi, Serlie et al. 2009).

Yi and colleagues have reported that a continuous ICV infusion of ORX A into rats fasted for 5 h results in increased plasma glucose levels and abolished daytime decrease of endogenous hepatic glucose production (EGP). Hepatic sympathetic, but not parasympathetic, denervation blocks the orexin induced apparent enhancement of EGP. In addition, when the bicuculline, a γ-aminobutyric acid receptor antagonist, is injected in the perifornical area in order to activate ORXS neurons, basal EGP raise and, in consequence, insulin-mediated suppression of EGP diminish (Yi, Serlie et al. 2009).

Recent studies have confirmed that ORXS actions in glucose homeostasis is under the control of the ANS (Tsuneki, Murata et al. 2008; Harada, Yamazaki et al. 2013; Tsuneki, Nagata et al. 2016).

Therefore, the release of hypothalamic ORX A can activate the hepatic branch of the vagus nerve and reduce plasma glucose levels by restoring the insulin sensitivity (Rani, Kumar et al. 2018).

The role of ORXS is not only limited to glucose central homeostasis but it play an important role also peripherally: there are shreds of evidence that ORXS can induce glucose production in the liver (Stanley, Pinto et al. 2010) and promote glucose uptake in skeletal muscle in order to decrease glycemia (Yi, Serlie et al. 2009).

In addition, it has shown that ORX A and B regulates glucagon release from the pancreas (Bass and Takahashi 2010).

The ORXS neurons can interact with glucose-sensitive neurons within the LHA, which are inhibited by rising glucose concentration (Shiraishi, Oomura et al. 2000), in particular, in particular ORX A specifically stimulates the glucose-sensitive cells (Liu, Morris et al. 2001).

Muroya et al. (Muroya, Uramura et al. 2001) hypothesized that some glucose-sensitive neurons directly express ORXS. In the medulla, ORXS neurons innervate the ventral area (Zheng, Patterson et al. 2005) and the nucleus of the solitary tract (Ciriello, McMurray et al. 2003) which is an important relay station that receives sensory signals from the viscera, such as portal vein glucose level and gastric distension. These signals are transmitted to the hypothalamus (Ter Horst, de Boer et al. 1989) in which the LHA ORXS neurons and NPY/agouti-related peptide (AgRP) neurons in the arcuate nucleus ARC (Venner, Karnani et al. 2011) contribute to controls glucose utilization in insulin-sensitive organs as well as whole-body energy metabolism (Sudo, Minokoshi et al. 1991; Haque, Minokoshi et al. 1999). A recent discovery confirmed this statement: ORX 1R and 2R are expressed in the pancreatic islets, with a higher expression of ORX lR than ORX 2R (Nowak, Mackowiak et al. 2000; Rani, Kumar et al. 2018).

LHA is an important station also to the control of the metabolic rate.

Animal with lesions in the LHA consistently become hypercatabolic and remain so, even after they reach a lower body weight set-point (Lubkin and Stricker-Krongrad 1998). Using indirect calorimetry, Lubkin and colleagues found that ORX A injection during the light phase rises oxygen consumption and the respiratory quotient by an augmented utilization of carbohydrates (Lubkin and Stricker-Krongrad 1998). Significant shreds evidence has been accumulated in support of ORXS contribution in the regulation of energy metabolism and autonomic function (Willie, Chemelli et al. 2001).

As well, ORXS increases feeding behaviour in a dose-dependent manner (Sakurai, Amemiya et al. 1998) and rises oxygen consumption in mice pointing out an increased metabolic rate (Lubkin and Stricker-Krongrad 1998) and, as said before, ORXS influences sympathetic outflow. Altogether these effects result in increased energy consumption.

New studies support the role of ORXS in peripherical glucose homeostasis, in vivo subcutaneous injection of ORX A has been associated with increased blood glucose levels and insulin levels in both normal fed and fasted rodents (Nowak, Mackowiak et al. 2000; Ehrstrom, Naslund et al. 2004; Sieminski, Szypenbejl et al. 2018). Therefore,

ORX A plays an important role in the metabolism homeostasis, not only via regulating the secretion of insulin, glucagon, leptin and ghrelin but ORXA itself is regulated by these metabolic hormones (Ouedraogo, Naslund et al. 2003; Arafat, Kaczmarek et al. 2014). Recent studies have also described the co-localization of ORX 1R in the alpha and beta pancreatic islet cells of animals (Kirchgessner and Liu 1999; Adeghate, Fernandez-Cabezudo et al. 2010; Tian, Zhao et al. 2011; Park, Shim et al. 2015; Rani, Kumar et al. 2018) and in vivo studies have reported that ORXS physiologically regulates the insulin secretion (Nowak, Mackowiak et al. 2000; Switonska, Kaczmarek et al. 2002; Tsuneki, Murata et al. 2008), supporting the role of ORXS in the peripheral glucose homeostasis.

In conclusion, several studies demonstrate that ORXS are involved in the control of central and peripheral homeostasis of glucose.

Body temperature regulation and orexins

Energy homeostasis is maintained with long-term and short-term regulatory processes. In the first, metabolic requirements and food intake must be proportional, so an unbalanced intake-consumption produces variation in body weight. The second regulatory process regard the equilibrium between MR (actual energy production) and energy dissipation, in function of temperature regulation; any imbalance results as a modification in Tb (Szekely, Petervari et al. 2002).

Loss of ORXS neurons causes a dysregulation in energy and metabolic homeostasis, raising the possibility of obesity insurgence (Kok, Overeem et al. 2003) and the potential for altered thermoregulation (Plazzi, Moghadam et al. 2011).

ORXS receptors and connection fibers have been described in RPa, a region of the ventromedial medulla. RPa is the principal site of sympathetic and somatic premotor neurons for the regulation of thermal effectors (Morrison and Nakamura 2011).

Is well known the role of RPa neurons in the thermoregulation: it promotes the activation of BAT thermogenesis and the cardiovascular adaptations to thermogenic needs (i.e., cutaneous vasoconstriction and increase in heart rate).

Nano injection of ORX A into the rostral raphe pallidus produced a great increase in BAT sympathetic outflow and in BAT thermogenesis (Tupone, Madden et al. 2011). Therefore, RPa is a key relay site that controls thermoregulatory sympathetic outflow and is supposed to have a key role in enters into torpor because its neurons must be inactivated (Cerri, Mastrotto et al. 2013).

Moreover, ORXS neurons receive afferent projections from the pre-optic area (POA), and express c-Fos when, the GABA-A agonist, muscimol is injected into the POA (Rusyniak, Zaretsky et al. 2011)

So, GABAergic neurons in the POA could provide inhibitory signals to ORXS-synthesizing neurons and causing an increase in Tb, HR and BP (Satoh, Matsumura et al. 2004).

Interactions between Torpor and orexins

To enter torpor, the animal must sense an energy deficit, which, as explained previously, is relayed by the hypothalamus circuit and the ORXS neuron in LHA and the AgRp neurons in the ARC are two fundamental players. Bolcking the ARC with monosodium glutamate prevents mice from sensing their energy status, preventing torpor following caloric restriction (Gluck, Stephens et al. 2006). In the same way, the administration of peripheral ghrelin lengthens and deepens torpor bouts but ghrelin itself does not cause hypothermia in fed mice (Gluck, Stephens et al. 2006).

Similarly, low leptin levels create a permissive environment for torpor entrance but are not sufficient to initiate torpor.

Moreover, mice with permanently low levels of leptin readily enter torpor upon fasting (Himms-Hagen 1985; Gavrilova, Leon et al. 1999; Swoap 2001).

The Ob/ob mice are carrier of a mutation in the leptin gene and, consequently, they are obese (Gavrilova, Leon et al. 1999). Despite having large energy stores in the form of white adipose tissue, ob/ob mice enter bouts of torpor upon fasting (Himms-Hagen 1985; Swoap 2001).

This finding suggests that a drop in basal leptin levels, rather than actual energy stores available, can be the signal for the organism that it should enter torpor.

Similarly, A-ZIPyF-1 mice, which lack white adipose tissue and so shows reduced leptin levels, rapidly enter torpor upon fasting compared to control mice (Gavrilova, Leon et al. 1999).

However, decreased leptin levels or leptin signaling is not sufficient to initiate torpor bouts given that ob/ob and a mouse model missing a functional leptin receptor (db/db mice) are not permanently torpid (Heller and Hammel 1972).

Therefore, leptin levels influence torpor physiology, but high levels of leptin do not prevent torpor entrance. Interestingly, leptin administration to ob/ob mice, but not A-ZIPyF-1 mice, prevents torpor entrance, which suggests that there are leptin-dependent

and leptin-independent mechanisms that contribute to torpor regulation (Gavrilova, Leon et al. 1999).

In addition, torpor is also regulated by NPY. This has been demonstrated in Mice deficient in NPY (NPY-/-) which cannot sustain torpor bouts when fasted (Gluck, Stephens et al. 2006). Moreover, intracerebroventricular injection of NPY leads to hypothermia in Siberian hamsters (Paul, Freeman et al. 2005).

Hypothalamic ORXS neurons contribute to stress-induced thermogenesis through activation of beta-3 receptors probably activating the sympathetic nerves which control the brown adipose tissue (Zhang, Sunanaga et al. 2010). In vivo experiment conduct by Futatsuki (Futatsuki, Yamashita et al. 2018) and colleagues showed a strong relation between ORXS and Torpor: double transgenic mice for ORX A and B (ORX-AB mice) during the first 24 h of food deprivation have a decrease in Tb and a greater length of time spend in hypothermia than in control mice (WT). This can indicate a protective role for orexin neurons in fasting-induced hypothermia. Moreover, ORXS neuronal activity raises during the hours preceding the hypothermic episode and is kept high also during the recovery period towards the end of hypothermia. The Authors hypothesized that the regulatory actions of orexin neurons on Tb could be mediated by the sympathetic nervous system, which activates the BAT (Zhang, Sunanaga et al. 2010; Takahashi, Zhang et al. 2013). This theory is supported by the results obtained from the administration of orexin peptide into the medullary Rpa which, as mentioned before, activates the sympathetic nerves controlling the brown adipose tissue (Tupone, Madden et al. 2011). In RPa are located the sympathetic premotor neurons controlling brown adipose tissues (Nakamura, Matsumura et al. 2004). Therefore, they propose that orexin neurons have a protective role against hypothermia by limiting the decrease in Tb and accelerating the recovery, probably through sympathetic activation (Futatsuki, Yamashita et al. 2018).

Another probable trigger for the torpid state is the Adenosine, a direct metabolite of ATP. It has been implicated as a signal of metabolic state and could be an important molecule required for entering torpor (Swoap, Rathvon et al. 2007). Namely, mice lacking the adenosine A1 receptors and those lacking both the adenosine A1 and A3

receptors (Carlin, Jain et al. 2017) still showed fasting-induced hypothermia, but not CHA-induced hypothermia (Vicent, Borre et al. 2017). Therefore, it could not be by itself the trigger for torpor and a more complicated mechanism must be involved (Carlin, Jain et al. 2017). It has been recently demonstrated that it's possible to induce a completely reversible suspended animation status in rats (Rattus norvegicus) by the suspension of the thermoregulatory central control with the inhibitions of RPa neurons by muscimol (Cerri, Mastrotto et al. 2013).

Perspectives

For non-hibernating mammals, including man, the negative consequences of hypothermia are the effects on cellular reactions, which are debilitating, often lethal, and occur with a less than 10 °C drop in core Tb (Storey and Storey 2010).

The human experience of natural hypometabolism is quite limited. Some metabolic suppression can occur in deep meditative states (Chaya, Kurpad et al. 2006) and small reductions in thermogenesis occur in newborn exposed to hypoxia or during starvation (Hochachka 2000; Zimmermann-Belsing, Brabant et al. 2003). Furthermore, an ancestral capacity for hypometabolism might be hidden into clinical depression and other mood disorders (Tsiouris 2005).

However, the hypometabolism persists in lineages quite close to man, for example within the primates several Madagascar's lemur species which experience both daily torpor and seasonal hibernation (Giroud, Blanc et al. 2008; Kobbe and Dausmann 2009). So, there is the opportunity to believe that an ancestral capacity for torpor still disguise in the human genome and could potentially be restored (Storey and Storey 2010).

Humans may benefit from active hypometabolism. For example, in stroke, it is important to begin treatment as quickly as possible after the onset of symptoms (Boulant 1998) because outcomes worsen as time passes due to hypoxia in the brain. During the hypothermia, the demand for oxygen is lower. So, the progress of brain damage slow down and this could increase the progress of brain damage slow down; this could increase the survival rate (Sunagawa and Takahashi 2016).

Torpor can be used also to improve the ''shelf life'' of tissues organs removed for transplantation bypassing the damage that occur with the cold shock. The torpid mechanism could be applied to coordinate metabolic rate depression and have higher ischemia resistance and hypothermia tolerance (Cerri 2017).

Inducible metabolic suppression could also be applied in situations where individuals need to be transported over long distances to medical care, such as in the case of

battlefield injury or, ultimately, to long distance space explorations (Cerri, Tinganelli et al. 2016).

The technique used nowadays is the mild or moderate hypothermia (32–35 °C) is widely used as a clinical intervention in man, but deep hypothermia (<30 _C) is rapidly lethal (Peier, Moqrich et al. 2002; Chen 2015) and activate the compensatory physiological mechanisms which cause the major cellular damages.

Torpid and hibernating spices also show little or no atrophy of their skeletal muscles despite being virtually immobile for a great amount of time, hence, they may illustrate mechanisms that can be applied to minimize atrophy in human muscle under situations of long-term bed rest. Also, they are studied as models of neuroprotection during a stroke (Lee and Hallenbeck 2006; Polderman 2009). Finally, strong seasonal cycles of lipid accumulation followed by months without feeding also make hibernators promising models for studying obesity regulation (Storey and Storey 2010).

Aims

This study aimed at describing physiological changes that characterize spontaneous daily torpor in mice, and at investigating the role of the ORXS in the mechanisms of entry, maintenance and exit from the condition of torpor. As far as physiological changes are concerned, we mainly focused on sleep changes and on the dynamics of blood glucose variations, evaluating the relationship that these variations have with those of Tb and motor activity. We chose the mouse model because is a facultative heterotherm, and it is, also, the most common animal model for biological experiments. The possibility of having genetically modified animals represents, in fact, an important added value in addressing the study of regulatory mechanisms.

More in detail, the study consisted of two main parts:

i. *The Characterization of the role of orexins system and the study of sleep changes related to Torpor*;

Hypothalamic ORXS neurons have diffused projection to the entire neuroaxis.

The ORXS are important neurotransmitters, involved not only is wake-sleep control, but also in cardiovascular regulation, thermoregulation and energy metabolism regulation. We hypothesized that hypothalamic ORXS system could play a role in regulating the entry and exit from the torpid state.

Furthermore, we investigated sleep changes related to torpor because there are many studies, reviewed in the introduction, investigating the relationship between sleep and torpid state, but there are inconsistent results. A deepening is therefore necessary.

The i. experiments have been performed at Bologna University, under the supervision of Professor G. Zoccoli in PRISM laboratory.

ii.   *Study of Glucose dynamics during Torpid stat*e;

Glucose is the main source of energy for the brain neurons and a crucial one for the entire metabolism both in human and animals. Because mice enter into the torpid state only when calorically challenged, we hypothesized that one of the inputs for the initiation of a torpor bout could be the lack of the primary fuel (glucose) used to power brain metabolism. Using glucose telemetry in mice, we tested the hypotheses that: a) circulating glucose changes related to torpor are significantly interrelated with changes in body temperature, and activity, and b) the level of blood glucose at the onset of torpor differs from blood glucose when there is no torpor.

The ii. experiments have been performed at Williams College (Williamstown, MA, USA) in Professor Swoap' Laboratory.

The study is original because there aren't in literature research that evaluates the entire mechanism which drive the entry and exit from the torpid state in the mouse model and which consider the role of ORXS system, glucose and sleep. The scientific interest of this study is high because the knowledge of this mechanisms can be the first, indispensable, step towards the development of procedures for the induction of a stable hypothermia state in non-hibernating animal species.

The understanding of the mechanisms underlying spontaneous torpor in mouse model is crucial for the development of methods which allow the endogenous hypothermia induction in human subjects. Today, as already mentioned in perspectives paragraph, therapeutic hypothermia is used in pathological conditions such as stroke and heart attack, which in Western countries are among the most frequent causes of hospitalization and premature death (Drew, Buck et al. 2007; Bouma, Verhaag et al. 2012; Fattore, Torbica et al. 2012). While it has been shown that this procedure is effective in increasing the survival rate to these events (Arrich, Holzer et al. 2016),

Nowadays, therapeutic hypothermia is produced by exogenous cooling, which induces defensive reactions by the body that limit its benefits (Sessler 2009). Such adverse effects could be avoided by the development of procedures that induce a condition of endogenous hypothermia, like the spontaneous torpor of the mouse.

First experiment

"The Characterization of the role of orexins system and the study of sleep changes related to Torpor"

Material and methods

Sleep, orexins and daily torpor in mice

There are many similarities between sleep and torpor. Both conditions require an adequate posture in a safe place (i.e. a burrow hole or the nest) and are accompanied by a reduction in muscle tone, autonomic activity, energy metabolism. They are characterized by a decreased reactivity to the external environment.

On these bases, it has been suggested that sleep is a behaviour that is evolved to favors energy conservation, and torpor may represent an its extension (Heller and Ruby 2004). Torpor may be entered through sleep as proved by Walker and Colleagues (1977) which recorded EEG during entrance in hibernation in ground squirrels and showed that the brain temperature started to decrease during either REM or NREM sleep, but never during wakefulness. These Authors were able to record the characteristic EEG of NREM and REM sleep until the brain temperature was maintained above 25 °C.

The percentage of time spent in a sleep state by the animal increased (until 88% of the recording time) proportionally to the decreasing of the brain temperature. The structure of sleep was changed: NREM sleep was predominant while REM sleep tends to decrease until it disappears at a brain temperature below 25°C (Walker, Glotzbach et al. 1977).

Similar findings have been found in the pocket mouse and round-tailed ground squirrel (Walker, Garber et al. 1979; Harris, Walker et al. 1984).

In Djungarian hamster torpor is also entered via NREM sleep. During torpor episode sleep predominates, with a progressive decrease in the amount of REM sleep, which is absent at a brain temperature of 24 °C (Deboer and Tobler 1995). Moreover, Deboer et al found a systematic shift of EEG frequencies as cortical temperature decreased. Spectral analysis showed that prominent peaks in power density measured at 35°C

during REM sleep (7 Hz) and NREM sleep (4.5 Hz) shifted towards lower frequencies during hypothermia. Slow waves in hypothermia correspond largely to frequencies outside the traditionally normal range in euthermia, which are therefore substantially absent during the torpor episode. This could therefore represent an equivalent of sleep deprivation.

Sleep after exit from torpor has also been extensively investigated. EEG recordings performed on the Djungarian hamster showed that daily torpor was followed by an increase in NREM sleep, similar to the increase observed after sleep deprivation. The increase in slow wave activity (SWA) was positively correlated with the length of torpor episode; subsequently SWA declined with time spent asleep (Deboer and Tobler 1996; Palchykova, Deboer et al. 2002). This increase in SWA supports the hypothesis that sleep following a torpor bout is homeostatic regulated: animal in torpor incurs a sleep debt, possibly due to the low brain temperatures that hampers sleep restorative process (Heller and Ruby 2004). This hypothesis was strengthened by EEG data obtained in Ground squirrels which predominantly sleep during the arousal process from hibernation. They also pass a great part of inter bouts time asleep, with a progressive decrease in SWA that is characteristic of a declining requirement for sleep (Daan, Barnes et al. 1991) (Trachsel, Edgar et al. 1991).

Consistent data were obtained in European ground squirrels by Strijkstra & Daan (1997) (Strijkstra and Daan 1998). These authors showed that the SWA enhancing effects are restricted to low brain temperatures (in this case below 15°C) and suggested that this evidence could be related to the absence of hypothalamic neuronal activity below 14–18°C (Krilowicz, Glotzbach et al. 1988). In this regard, it is interesting to note that even when hypothermia and low brain temperature (22°C) are pharmacologically induced in a non-hibernator, the rat, in the subsequent euthermic period was found a similarly massive increase in SWA (Cerri, Mastrotto et al. 2013). However, in this study, the size of SWA apparently mostly depends on the degree of the metabolic effort of the animal to recover euthermia, suggesting that a relevant part of the sleep debt is accumulated during rewarming phase.

Moreover, Orexin neuropeptides control sleep, body temperature, and food intake. It has been demonstrated that hypothalamic orexin neurons contribute to stress-induced thermogenesis through

activation of beta-3 receptors probably on the sympathetic nerves controlling the brown adipose tissue (Zhang, Sunanaga et al. 2010). Orexins also protect against hypothermia induced by cold environments (Takahashi, Zhang et al. 2013) and isoflurane anesthesia (Kuroki, Takahashi et al. 2013) and in vitro their production is regulated by glucose and leptin (Nakagawa, Ogawa et al. 2003), adenosine (Liu and Gao 2007), and hyperthermia (Parsons, Belanger-Willoughby et al. 2012). However, it is still unclear whether orexins mediate the relationship between torpor and sleep in mice. Here, we investigated whether i) sleep alterations mark the onset of torpor in mice ii) these alterations are orexin-dependent.

Experimental procedures

Ethical approvals

Experiments performed in Bologna were conducted in accordance to the DL 26/2014 and the European Union Directive 2010/63/EU under the supervision of the Central Veterinary Service of the University of Bologna, after the approval by the National Health Authority (decrees: 291/2013-B; 124/2015-PR; 219/2013-B).

8 C57BL/6J (wild-type, WT) female mice and knock-out mice for the pre-pro-orexin gene (KO-HCRT, (- / -), homozygotes due to the lack of the gene) (Chemelli, Willie et al. 1999), were grown in the animal facility of the Department of Biomedical and Neuromotor Science of the University of Bologna (DIBINEM), with controlled condition of temperature (23°C), humidity and a light/dark cycle of 12:12 hour, with

lights on at 9.00 am (i.e. ZT0). Mice had free access to food (standard diet 4RF21, Mucedola, Settimo Milanese, Italy) and water.

The experiments have been performed on 32 weeks old WT mice and age matched KO-HCRT. The KO-HCRT model has been studied for over 10 years in various laboratories around the world (Anaclet, Parmentier et al. 2009; Bastianini, Silvani et al. 2011). This genetically modified mouse strain develops behavioural alterations homologues those of human narcolepsy-cataplexy, essentially represented by an altered distribution of waking and sleep periods in 24 hours (Chemelli, Willie et al. 1999). The KO-HCRT mice were reproduced by mating homozygous (- / -) female and male mice which generate 100% of the mutation-carrying mice (KO-HCRT).

The KO-HCRT mice are completely congenic (≥ 9 generation of backcrossing) to the C57Bl / 6J genotype, therefore C57Bl / 6J mice were used as control group (WT) for KO-HCRT mice.

The genotype of animals was confirmed by PCR amplification of DNA extracted from connective biopsies (Bastianini, Silvani et al. 2011).

Torpor was induced in mice exposing them to a moderate reduction of the ambient temperature (20 °C) and caloric intake (caloric restriction (CR), 70% of normal food intake) (Swoap and Gutilla 2009).

Caloric restriction protocol

From the age of 29 weeks the animals were housed individually to monitor daily their body weight and food amount for seven days. This procedure was performed to establish the daily intake of food consumed by each mouse and to calculate the quantity of food to administer during the following protocol of caloric restriction (CR) specifically for each animal.

Surgery

The surgery was performed under general anesthesia (isoflurane, Abbott, Latina, Italy, 1-2% and balance O2, constant flow of 1 l/min) (Bastianini, Silvani et al. 2011), a stable Tb (37 °C) was ensured using a heating pad. Post-operative pain has been prevented by intraoperative administration of analgesic (Carprofen 4 mg/kg subcutaneously. Norocarp; Pfizer Italy, Latina)

A telemetric blood pressure transducer (TA11PA-C10, DSI, Tilburg, the Netherlands; 1.4 g weight) was implanted subcutaneously on the right flank, with the catheter inserted through the right femoral artery into the abdominal aorta (Silvani, Bastianini et al. 2009; Bastianini, Silvani et al. 2011).

Moreover, animals were implanted with a cortical thermistor (22 G diameter cannula, C313G, Plastics One, USA) to detect a real time value of brain temperature, necessary to identify periods of spontaneous torpor (Baracchi, Zamboni et al. 2008).

The mouse was placed in a stereotaxic device (51600 Lab Standard Stereotaxic Instrument, 2Biological Instrument, Varese), shaved on the top of the head and the surgeon dissect the skin and removed the periosteum with a delicate abrasion to exhibit the cranial suture. The cross of the sutures made two points used as landmarks: the anterior one is Bregma and the caudal one is Lambda. The thermistor has been positioned at -2 and +1 mm from Bregma (Figure 1). A pair of Teflon-coated stainless-steel electrodes (Cooner Wire, Chatsworth, CA, USA) were welded to two stainless-steel screws which were positioned in contact with the dura mater through burr holes: 2 mm anteriorly and 2 mm lateral to the bregma (frontal) and 2 mm anteriorly and 2 mm lateral to the lambda (parietal), to obtain a differential EEG signal. A second pair of electrodes was inserted bilaterally in the nuchal muscles to obtain a differential electromyographic (EMG) signal. All electrodes were connected to a miniature plastic connector, which was cemented to the skull with stainless-steel anchor screws (2.4 mm length, Plastics One, Roanoke, VA, USA). The thermistor and the electrodes were fixed using a dental cement (Rely X ARC, 3M ESPE, Segrate, Milano, Italy), and

dental acrylic (Respal NF, SPD, Mulazzano, Italy) (Silvani, Bastianini et al. 2009; Bastianini, Silvani et al. 2011). (Figure 1).

At the end of the surgery, an antibiotic prophylaxis (Rubrocillina Veterinaria, Intervet, Schering-Plough Animal Health, Milano. 12500 U.I./Kg benzylpenicillin benzatinic + 5 mg/kg dihydrostreptomycin sulphate diluted in physiologic solution, subcutaneously) was performed. After the surgery, the mice were housed at 25 °C, light/dark cycle 12:12 hours, with the lights turning on at 9 o'clock (ZT0) with free access to food and water. The animals have been kept in an individual cage for all the duration of the experiment (2-3 weeks) to prevent injuries caused by conspecifics in presence of the surgical implants.

Torpor induction

After a week of post-operative recovery, the mice were subjected to caloric restriction protocol and exposed to a lower ambient temperature (20 °C). The CR protocol consisted in the administration of 70% of each animal daily intake of food (Vicent, Borre et al. 2017), given at 12 a.m. (ZT3). This protocol has already been used to induce extremely reproducible episodes of spontaneous torpor, which lasted 2-4 hours and happened in the second part of the successive dark period (Vicent, Borre et al. 2017).

Experimental protocol

The last two days of the post-operative recovery period was used to accustom the animals to the registration apparatus. Successively, the baseline recording was performed by the continuous acquisition of the Tb, EEG, EMG and BP signals for 4 days. The animals were free to move in their habitual housing environment.

The transmission of the signals from the EEG / EMG electrodes to the recording apparatus was done by an ultra-thin cable and rotating electrical connectors, which could avoid the spontaneous movement of the mice. EEG was acquired at 0.3-300 Hz and EMG at 100-1000 Hz. We choose to use the cable recording for the acquisition of EEG and EMG signals because, in the mouse model, represented the golden standard and its used in the main international sleep laboratories.

The mice were sacrificed under deep anesthesia (isoflurane, Abbott, Latina, Italy; 5% diluted in O2, flow 1 l/min) (Figure 2).

Data analysis

Data analysis was performed with MatLab (Mathworks, Natick, MA, USA). To define univocally the torpor bout we used the brain cortical temperature (Tb) values as the main physiological variable and the baseline was divided in 5 sequences: 1) we defined "cooling periods" as time periods during which Tb monotonically decreased more than 0.5°C per time bin and results in an overall reduction of Tb > 5 °C with respect to the starting point of each period. In figure 3 is highlighted with a blue line. 2) Similarly, "rewarming periods" was defined as the time periods during which Tb monotonically increased more than 0.5°C per time bin, resulting in an overall Tb increase of > 5 °C. In figure 3 is highlighted with a red line. 3-4) In order to robustly identify cooling and rewarming periods un the face of short-lasting low-amplitude perturbations of Tb, instances of one or two time bins in which the absolute change in temperature was lower than 0.5 °C were considered not to interrupt the period in case the preceding and following time bins were both characterized by an increase (rewarming) o decrease (cooling) in Tb of more than 0.5 °C. For each cooling period it was found a baseline sequence from 6 to 4 hours before the onset of the cooling period, which was not part of other cooling or rewarming periods. Similarly, for each rewarming period, it was found a reference sequence from 1 to 2 hours after the end of the rewarming period, which was not part of other cooling or rewarming periods. These baseline and reference sequences are respectively highlighted with a green and a pink line in figure 3. The yellow sequence in figure 3 is the interval of stable deep torpor in which Tb did not vary more than 0.5°C per time bin and the absolute value of Tb was < 25°C.

So, in this work, the onset of torpor was defined as the beginning of the first cooling period and ends at the ending of the rewarming period.

The raw data were averaged in windows of 10 min because there was a high variability. We decided to see if there were differences between control and KO-HCRT group for the physiological variables during a torpor bout, so we evaluate the variation of Tb, heart rate (HR), activity (ACT) and systolic blood pressure (SBP).

To consider all the sequences in different animal/torpid bouts it was taken in consideration separately the three phases of the torpor bout, so the data are presented in a 120-minute window (independently from the total length of the cooling/rewarming sequence) centered at the beginning of the cooling and at the end of rewarming period, and a single time point for the deep torpor. All the sequences of the WT group (controls) and KO-HCRT group (lacking orexin) were averaged within the group and compared between the groups with the ANOVA and t-test analysis.

The second batch of analyses was performed on this dataset using the same data organization: the slope of the cooling and rewarming sequence was calculated averaging all the animals within the groups (WT and KO-HCRT). The slope of Tb, ACT, HP and SBP was compared with ANOVA analysis.

The wake-sleep state was scored manually by trained and qualified personnel and the same principles applied for the physiological analysis was used in the sleep one. For the analysis of the relationship of torpor and sleep we considered the percentage of time spent in: NREM sleep (%NREM), REM sleep (%REM) and indeterminate state (%IND) (a state that is not scorable as wake or sleep) and the EEG SWA during NREM sleep. The ANOVA on the slope for the sleep analysis was calculated, as said before, for the variables of %NREM, %REM.

Statistical analysis

Statistical analysis was performed with SPSS (SPSS, Armonk, NY, USA). Data were analyzed with ANOVA with Huyn-Feldt correction and with t-tests with statistical significance for $P < 0.05$.

Data were reported as means ± SD.

Results

Physiological variables during cooling, deep torpor and rewarming

An example of the raw data collected in a WT mouse during 24 h of baseline recording under caloric restriction and exposed at an ambient temperature of 20 °C is shown in Figure 3. Brain cortical temperature (Tb), heart period (HP), activity (ACT) and systolic blood pressure (SBP), the percentage of time spent in NREM sleep (%NREM) and in wakefulness (%W) are all plotted vs time of recording.

In the Tb graph is plotted a typical torpor bout and cooling, deep torpor and rewarming periods are highlighted respectively in blue, yellow and red (Figure 3). The baseline (B) precedes the torpor bout of 30 minutes and is represented in green. The pink sequence is the referring sequence for the rewarming period: we have used it to exclude the circadian effects on the analysis performed during the rewarming period.

The variables are analyzed comparing WT and KO-HCRT groups during cooling, stable torpor and rewarming conditions (n= 8 WT vs 8 KO-HCRT).

In figure 5, panel A, Tb is plotted vs time. During the cooling period, as expected, Tb decreases reaching the minimum value in the last two points of the cooling sequence (between 40 and 60 min). At these time points, Tb significantly differs from the B in both KO-HCRT and WT mice (ANOVA, $P < 0.05$).

Tb reaches the absolute minimum value during the deep torpor (T) when, as expected, its value statistically differs from B (ANOVA, $P < 0.05$). In the first part of the rewarming period (between -60 and -30 min) Tb is significantly lower in KO-HCRT mice than in WT (ANOVA, $P < 0.05$), and Tb result lower during the entire duration of the rewarming period compared to B in both the experimental groups. Tb gradually rises until the end of the post rewarming sequence in which reaches the B value. The trend is similar for the two groups and the KO-HCRT mice result to have a lower Tb compared to B value until the last point of the post rewarming sequence.

In the figure 5 panel B the ACT is plotted vs time and it doesn't show a significative difference between KO-HCRT and WT.

ACT in the pre-cooling phase (from -60 to 0 min) rises until it reaches a maximum value which is significantly higher than in B (P< 0.05, ANOVA). After the cooling onset and for all the duration of the cooling period ACT decreases, as expected, and reaches the lower value at the end of the sequence (60 min) when it is significantly lower than in B (P< 0.05, ANOVA). The ACT value during T is significantly lower compared to the B value (P< 0.05, ANOVA) but never goes to 0 AU. During the rewarming phase ACT is stable with values comparable to those observed in B, or barely higher right before the end of rewarming (-10 to 0 min) (P< 0.05, ANOVA).

In the figure 5 panel C, HP is plotted vs time and there aren't statistical differences between KO-HCRT and WT.

As expected, HP increases compared to B value during cooling period (P< 0.05, ANOVA). The maximum value of HP is reached during T and, as expected, it's significantly higher than during B (P< 0.05, ANOVA). Thereafter, the HP decreases until it reaches the same value observed in B during the rewarming sequence, reaching a value higher than that recorded in B (time point -60 min) (P< 0.05, ANOVA).

In the figure 5 panel D, SBP is plotted vs time and there are no significative differences between WT and KO-HCRT mice.

During the pre-cooling phase (-60 to 0 min) the SBP decreases as long as the torpor becomes deeper and after the onset of the cooling, the values of the SBP are statistically lower than in B (P< 0.05, ANOVA).

SBP reaches the minimum value during T and its value is significantly lower than in B (P< 0.05, ANOVA). During the rewarming period the SBP rises and in the first time point of rewarming has a value statistically significantly lower than in baseline (P< 0.05, ANOVA). During rewarming the SBP rises until it reaches a peak at the end of rewarming (from 0 to 10 min) and in the post rewarming shows lower value than in B (P< 0.05, ANOVA).

Slope of changes in physiological variables during cooling and rewarming sequences

Table 1 show the results concerning the length (L) (min) of the cooling (L-c) and rewarming (L-r) periods, the slope of Tb during cooling (Tb-c) and rewarming (Tb-r), the slope of the ACT during cooling (ACT-c) and rewarming (ACT-R), the slope of HP during cooling (HP-c) and rewarming (HP-R) and the slope of SBP during cooling (SBP-c) and rewarming (SBP-r).

All the values are calculated from averaging all the animal's values within each experimental group.

There are no statistical differences between the WT and KO-HCRT mice.

The rewarming (L-r) appears to have a shorter length than cooling (L-c) ($P<0.05$, ANOVA). During rewarming the Tb-r rises faster than the Tb-c decreases during cooling ($P<0.01$, ANOVA) whereas the ACT-r rise slower ($P<0.05$, ANOVA) than ACT-c decreases during cooling. The SBP and HP slopes do not show any significative difference during cooling and rewarming sequences ($P>0.05$, ANOVA).

Sleep parameters during cooling, deep torpor and rewarming phases:

The wake-sleep cycle is divided into three stages: active wakefulness (W), non-rapid eye movement sleep (NREM) and rapid eye movement sleep (REM). They can be discriminated using the analysis of the electroencephalographic signals (scoring) performed by trained personnel or automatically (Bastianini, Berteotti et al. 2014).

In this case, the analysis of sleep parameters includes the percentage of time spent in the indeterminate state (%IND) which is a state not assimilable to any of the wake-sleep cycle. As showed in figure 4 during T the characteristics of the EEG and EMG are unique. Particularly, during deep torpor, the EEG appears to be desynchronized, similar to that observed during W, whereas the EMG appear to be lower than in W, similar to that recorded during NREM sleep.

In figure 6 panel A is plotted the percentage of time spent in NREM (%NREM) vs time; there aren't significative differences between KO-HCRT and WT.

The % NREM sleep before the onset of the cooling sequence decreases significantly compared to B ($P<0.05$, ANOVA) reaching values near to 0. After the onset of the

cooling sequence the %NREM sleep increases and reaches a peak at the end of the cooling, when it results significantly higher than during baseline (P<0.05, ANOVA). In T the % NREM sleep is 0 and is significantly different with the respect to baseline (P<0.05, ANOVA).

At the beginning of the rewarming sequence, the %NREM sleep shows values significantly lower than in B (P<0.05, ANOVA) and gradually increases.

During the post rewarming period the % NREM sleep is comparable to baseline values and its trend seems to have a decrescent evolution because in the PR the %NREM has lower values than B.

The SWA plotted as a function of time does not show any significant difference between KO-HCRT and WT.

In the pre-cooling, the SWA seems to decrease reaching the minimum value at the cooling onset, during the cooling it seems to rise but it never reaches the statistical significance with respect to B.

During the rewarming for the SWA trend for WT group appear to be more stable than KO-HCRT but there isn't any statistical difference. At the end of the rewarming and during the post rewarming the WT has an SWA barely higher than B.

In panel C has plotted the percentage of time spent in REM sleep (%REM) vs time. In the pre-cooling, the %REM is significantly lower in WT with the respect to KO-HCRT mice. During the cooling period, the %REM is still significantly higher in KO-HCRT than WT (P<0.05, ANOVA). At the end of the cooling period, KO-HCRT %REM decreases until it reaches the WT %REM value (60 min).

In deep torpor, the %REM is 0 for both the experimental groups. At the end of the rewarming period, the KO-HCRT trend shows a pick (from 0 to 10 min) while the WT trend rises linearly, but the difference doesn't reach the statistical significance. In the post rewarming, the %REM of WT and KO-HCRT have values comparable to B.

In panel D, is plotted the percentage of time spent in the indeterminate state (%IND) vs time: no significative differences between KO-HCRT and WT are present.

During the pre-cooling, the value of %IND decrease until it reaches 0 rightly before the onset of the cooling.

During the cooling the %IND rise until reaches a peak (60 min) in which is significantly higher than in B (P<0.05, ANOVA). The %IND is maximum during T.

In the first part of rewarming (-60 to -30 min), the KO-HCRT group shows significantly higher %IND with the respect to WT (P<0.05, ANOVA), and both groups show a higher %IND during the first part of rewarming compared to B (P<0.05, ANOVA). From the end of the rewarming to the end of post-rewarming the %IND is stable and has values comparable to B and there aren't differences between the groups.

Analysis of the baseline slope for the sleep parameters: percentage of time spent in NREM sleep and REM sleep.

In Table 2 are reported the slope of the percentage of NREM for the cooling (%NREM-c) and rewarming (%NREM-r) and the slope of %REM for the cooling (%REM-c) and rewarming (%REM-r) (% time) for WT and KO-HCRT mice.

There %NREM doesn't differ between the two groups whereas %REM inCreases faster in KO-HCRT mice compared to WT during the cooling period (P<0.05, ANOVA).

In the rewarming, the slope of the percentage of NREM is significantly higher than during cooling (P<0.05, ANOVA).

Discussion

In this study, I examined the possible role of orexinergic neurons in the entrance and arousal from torpor. Torpor was induced with the caloric restriction protocol and the exposure to low ambient temperature (for more detail see the methods chapter).

We analysed the Tb, the ACT, the HP and the SBP during the phases preceding and the following torpor (cooling and rewarming periods), and during deep torpor.

Tb significantly differs between WT and KO-HCRT mice only at the beginning of the rewarming period. During the cooling and deep torpor phases, there is no significative difference between the two experimental groups. We expected to see difference in Tb between the KO-HCRT and WT animals because experiments conducted in KO-HCRT mice showed a difference in the Tb with respect to WT in sleep state (Kuwaki 2015), moreover the orexin neuron-ablated mice (TG-HCRT) showed a lower temperature than WT during the deep hypothermia induced by food deprivation (Futatsuki, Yamashita et al. 2018). Probably, this aspect depends on the restricted number of animals involved in the study (8 WT vs 8 KO-HCRT) which doesn't allow us to describe little biological effects (Figure 5 panel A). The analysis of the ACT, SBP and HP don't provide any significative difference between the WT and KO-HCRT mice during the different torpor phases (Figure 5 panel B, C, D and Table 1).

However, it's interesting the overall trend of ACT which shows a peak right before the onset of cooling. It is unusual that this peak in activity was reached right before the entry in the "energy saving mode" (cooling sequence=entry into torpor), (Figure 5 panel B and table 1). We give two possible explanation: the first is that the peak in activity is the last extreme attempt for the mouse to not enter in torpor looking for food in their environment. Evolutionally the daily torpid animals deduce an energetically advantage from the torpid state, and to enter in torpor the assume a specific sleep-like position and they need to stay in a safe ambient (like their nest) because they are more exposed to predators (Geiser 1998) (Ruf and Geiser 2015), so they can attempt to not

enter into torpor if they can find food nearby . The second is that the animal tries to keep their euthermia activating the voluntary shivering production of heat.

This ACT peak is aligned with the finding in the Dormice that shows a similar spot before hibernation (Elvert and Heldmaier 2005) and in TG-HCRT mice before the entry in fasting-induced torpor (Futatsuki, Yamashita et al. 2018).

We can say that the cooling is a slower event than the rewarming because it has a greater length and the Tb decreases slower than its increase during rewarming (table 1 and 2). We can speculate that the increase of the activity of the sympathetic nervous system (SNS) during the rewarming is faster compared to the increase in parasympathetic nervous system (PNS) activity during cooling (Geiser 2004; Swoap and Gutilla 2009).

The analysis of the physiological parameter doesn't provide significative differences between the WT and KO-HCRT mice during the different torpor phases (Figure 5 panel A, B, C, D and Table 1) so we can conclude that ORXS doesn't have a central role during the entry, the arousal and the maintenance of deep spontaneous torpor in laboratory mice.

Our results are in contrast with those of Futatsuki et al. which suggested a protective role of orexins in fasting-induced hypothermia in mice (Futatsuki, Yamashita et al. 2018). Futatsuki et al define torpor as Hypothermic episodes in which the body temperature decreases below the minimum value obtained during the day of free access to food. In this way, they admit torpor episodes with a minim Tb of 29 °C that we exclude because of our torpor definition (see the data analysis paragraph for more detail). So, it could be that the ORXS have a protective role only in the shallow hypothermia and not in deep torpor.

We have also analysed the %NREM, the % REM sleep, the %IND and the SWA during the phases of rewarming, cooling and deep torpor.

The caloric restriction protocol permits to induce highly reproducible multiday torpor bouts, the time in which the episode occurs depend on the feeding time (Swoap and Gutilla 2009). In our experimental design, the pre-cooling and cooling phases happen in the dark period (night) of recording and the rewarming and post rewarming start in the first part and ends during the morning. The mice are nocturnal animals, so they are active during the night (the predominant state wakefulness) and they sleep during the day. Therefore, during the entry (pre-cooling and cooling) we expect to have a predominance of wakefulness and in the arousal (rewarming and post-rewarming) a sleep prevalence.

The sleep pattern during torpor isn't deeply conditioned by the orexins, which is unexpected because ORXS has a central role in regulating the sleep-wake cycle (Zhang, Zeitzer et al. 2007).

However, during the pre-cooling and cooling sequence, the KO-HCRT mice show more REM sleep with the respect to WT (Figure 6 panel C, table 2). During the pre-cooling phase, WT mice spend in NREM and REM nearly the 0 % of time over the total time of recordings, whereas KO-HCRT mice in the same period show a peak in the percentage of REM sleep. We can speculate that the cooling phase promotes REM sleep in mice lacking orexins since we don't find a significative difference between KO-HCRT and WT in the % REM during B. This finding is in accordance with the previous sleep experiments showing that KO-HCRT mice spent a major percentage of the recording period in REM sleep during the dark period (Chemelli, Willie et al. 1999; Willie, Chemelli et al. 2003). For the sake of clarity, we have also to consider the possibility that the lack of a significant difference in B between the WT and KO-HCRT groups could depend on the small number of animals involved in the experiment.

Both the groups show a peak in %NREM at the end of the cooling sequence rightly before the occurrence of T (Figure 6, panel A). So, we can speculate that sleep time, in particular, NREM sleep time, is increased in mice entering into torpor.

This finding is in accordance with results showing that, in a large number of species, NREM sleep is increased during the period preceding the torpor bout. (Walker, Garber et al. 1979; Harris, Walker et al. 1984; Deboer and Tobler 1994; Deboer and Tobler 1995) but in rare cases also the REM sleep can precede the deep torpor (Walker, Glotzbach et al. 1977).

Surprisingly, the SWA doesn't present any significant difference between the two groups even though its overall tendency is to increase during cooling, without reaching a statistically significant difference compared to B. During rewarming SWA looks stable and comparable with the B (Figure 6, panel B). This is in contrast with previous results in Djungarian hamster and rats showing that SWA radically increases at the arousal from torpor (Deboer and Tobler 2000; Deboer and Tobler 2003; Cerri 2017). This discrepancy could be due to the different torpor induction's protocol used in the previous experiments: in the Djungarian hamster torpor was combined with sleep deprivation and in rat torpor was pharmacologically induced. We can also presume that the small number of animals involved in our experiment could have blunted this effect. During T, the %IND has a peak while the %NREM and %REM are almost 0 (Figure 6, panel A, C, D). Moreover, the sleep pattern is uncommon because EEG is like active wakefulness and EMG is almost flat, similarly to NREM sleep (Figure 4). This unusual sleep pattern coincides with the minimum Tb recorded (Figure 6 panel D and figure 5 panel A).

This result is in contrast with the Deboer et al. results showing a systematic downward shift of EEG frequency bands as long as cortical temperature decreases (Deboer and Tobler 1995).

More experiments are needed but, in presence of an EEG spectrum similar to active wakefulness we can speculate that torpor could represent a long period of sleep deprivation as Deboer et al. suggested in 1995 and 2003 (Deboer and Tobler 1995; Deboer and Tobler 2003).

Second experiment

"Study of Glucose dynamics during Torpid state"

Material and methods

Glucose dynamics during daily torpor in mice

The metabolic signals that can provoke a torpor bout and that arise from restricted caloric intake are not well understood. Daily torpor occurs in the mouse in response to decreased energy availability, so the potential contributors include a drop in levels of energy-sensitive hormones such as leptin and insulin, as well as in the availability of fuels, such as glucose, free fatty acids, and ketones from the circulation (Melvin and Andrews 2009). The idea that glucose might be involved with, or influence, torpor is not a new one, many recent articles examines this relationship but the results are conflicting: some daily torpid animals show a gradual decline in plasma glucose at daily torpor onset (Nestler 1991; Dark, Lewis et al. 1999; Heldmaier, Klingenspor et al. 1999; Franco, Contreras et al. 2013) but this is not true for hibernators (Musacchia and Deavers 1981; Zimmerman 1982). Moreover, the results of pharmacological studies sustain the meaningful role of Glycemia in the signaling of daily torpor.

2-DG, a glucose analog that blocks glycolysis, causes a transient decrease in Tb in different species displaying daily torpor (Dark, Miller et al. 1994; Stamper and Dark 1996; Westman and Geiser 2004). However, it is important to note that 2-DG also induces a low Tb in animals that do not use torpor, such as the rat and human (Freinkel, Metzger et al. 1972; Penicaud, Thompson et al. 1986). Taken together, the available evidence raises the hypothesis that the low glycemia may play a role in the onset and/or maintenance of daily torpor.

The available results in literature have been hampered by technical limitations of periodic and repeated blood sample collection, which may induce stress and influence physiological behavior of the animal. Recent technical developments have led to the commercial availability of a telemetry system for continuous and simultaneous monitoring of blood glucose concentration (GLC), Tb, and activity (ACT). A system like this allows for a much greater temporal resolution of changes in GLC, with

minimal animal handling. Indeed, this system has been recently applied in a longitudinal study of a mouse model of diabetes mellitus (Korstanje, Ryan et al. 2017). We took advantage of the high temporal resolution of GLC, Tb, and ACT from these telemeters to test: 1) whether GLC, Tb, and ACT are significantly interrelated, and 2) that the level of circulating glucose at the onset of torpor differs from both glucose during arousal from torpor, and from feeding conditions that do not lead to torpor (Lo Martire, Valli et al. 2018).

This paragraph is from Lo Martire, Valli et all. (Lo Martire, Valli et al. 2018)

Ethical approvals

Experiments in Williamstown were approved by the Williams College Institutional Animal Care and Use Committee (protocol # SS-N-17) and were performed in accordance with the guidelines described by the US National Institutes of Health Guide for the Care and Use of Laboratory Animals.

6 C57BL/6J male mice were purchased from Jackson Laboratories (Bar Harbor, Maine). The animals were housed in the animal facility of Williams College on a 12:12 hours light/dark cycle, with lights on at 5.00 a.m. (i.e., ZT0), at an ambient temperature of 30 °C with free access to food (10% kcal from fat, Research Diets, D12450B) and water until surgery.

Experimental procedures

The experiment was performed on 16 weeks old male mice. Male mice aren't commonly used in torpor experiments because female is more sensitive to torpid environment and reach lower brain temperature during torpor, but we choose to use male mice because we felt the likelihood of success would be greater due to the larger body mass compared to younger or female mice, and the glucose telemeter, once activated, can't be reused. The body weight (BW) at surgery was 27.7 ± 0.2 g (Lo Martire, Valli et al. 2018) which granted a good percentage of surgery success. A real-time telemetric glucose transducer has been implanted in the carotid artery to obtain real-time glycemia.

The mice were left in their home cage and free to move for all the duration of the experiment.

Surgery

Surgery was performed on a heating pad to keep the body temperature constant under isoflurane anesthesia (2.5% isoflurane in O2, constant flux 1 l/min). Thermistors (model HD-XG, Data Science International, USA) can measure the blood glucose and peritoneal temperature. The glucose sensor was inserted in the carotid arch via a left carotid artery cannulation following manufacturer instructions. The catheter connected to the sensor was tunneled subcutaneously to the peritoneal cavity, where the telemeter body was implanted and sutured to the body wall. An analgesic was administered subcutaneously at the end of the procedure (Meloxicam at 5 mg/kg BW, Henry Schein, USA). Mice were maintained in their cage on the heating pad for 48 hours after the end of surgery and then housed individually at 30°C and fed ad libitum with a standard diet for 7 more days to allow post-operative recovery (Lo Martire, Valli et al. 2018).

Experimental protocol

The implanted telemetry devices were calibrated in vivo over the course of the study against measurements of plasma glucose obtained using a glucometer (Nova Stat-Strip blood glucose monitor, Data Sciences International). An initial 2-point calibration was performed at the beginning of the recordings by measuring glucose in duplicate from a nick in the tail tip of the mouse, both before an intraperitoneal bolus injection of glucose (3 mg/g BW at ~ ZT10) and 5 minutes after the subsequent peak in the telemeter glycemia (GLC) signal. The intraperitoneal glucose injection increased GLC by at least 200 mg/dl. Single-point calibrations were then made with duplicate blood glucose measurements twice per week at the same time of the day (ZT10). The calibration algorithm in the acquisition software converted the raw telemetry data recorded in nA to mg/dL.

A baseline recording was performed for three days with mice fed ad libitum and exposed to an ambient temperature of 30°C (Figure 7). Mice were then fasted for 24 h starting from ZT10, with free access to water and exposed to an ambient temperature of 23°C, which was maintained constant for the rest of the experimental protocol. Then, mice underwent a caloric restriction protocol, with 2 grams of diet administered at ZT10. This amount represents about 70% of normal intake for male mice at this ambient temperature in our laboratory. Mice were calorically restricted until a bout of torpor was achieved, between 2 and 7 days of caloric restriction. Mice were then refed ad libitum for 4 days. The experimental schedule of fasting, caloric restriction, and refeeding was repeated twice for each mouse, to increase the recording database for analysis. During recordings, all interactions with the mice, consisting of food administration/removal, bedding change, and GLC calibration, were performed in the last 2 hours of the light period (i.e., from ZT10 to ZT12). The GLC, core body temperature (Tb), and activity (ACT) signals were acquired (Dataquest ART - DSI, St. Paul, MN, USA) typically every 10 seconds, with occasional sampling every 20

seconds if required when data acquisition was crowded with several data streams. The ACT signal was based on the change in telemeter signal strength as the mouse moved about in its cage (Lo Martire, Valli et al. 2018).

Data analysis

This paragraph is from Lo Martire, Valli et all. (Lo Martire, Valli et al. 2018)

Data analysis was performed with MatLab (Mathworks, Natick, MA, USA). The values of GLC, Tb, and ACT were averaged over consecutive 5-minute periods, and then, for analyses of day-night rhythm, further averaged over 2-hour periods. ACT was expressed in arbitrary units (AU) normalized per minute of recording. The last two hours of the light period of each recording day (i.e., from ZT10 to ZT12) were excluded from the analysis to avoid interference due to experimenter interaction with the mice. In order to compare directly the day-night fluctuations in GLC with those in Tb during ad lib feeding, a z-score value was calculated for each of the two variables on 2-hour bins. Particularly, the difference between each 2-hour bin value and the average of the eleven 2-hour bin values (the 2-hour bin from ZT10 to ZT12 was excluded from the analysis, see above) was divided by the standard deviation of the eleven 2-hour bin values.

To assess the link between GLC and Tb in association with torpor bouts, we defined "cooling periods" as time periods during which Tb monotonically decreased (on 5-minute average values) resulting in an overall Tb reduction of ≥ 5 °C with respect to the starting point of each period. Similarly, "rewarming periods" was defined as the time periods during which Tb monotonically increased (on 5-minute average values) resulting in an overall Tb increase of ≥ 5 °C. In this work, the onset of torpor was defined as the beginning of the first cooling period (if there was a sequence of them), and the beginning of the rewarming period. The dynamics of GLC, Tb, and ACT during torpor onset and arousal were analyzed on a 60-minute window centered at the onset of the cooling period or the onset of the rewarming period, respectively. For each mouse, each instance of torpor onset or arousal was compared with the average of all 60-minute windows recorded in different days at an ambient temperature of 23°C, centered at the same ZT of the torpor onset/arousal instance, devoid of any cooling or

rewarming sequence, and with Tb at ≥ 34 °C for at least 2 hours before and 2 hour after the window center (i.e., during stable euthermia).

Estimates of the maximum and minimum values of GLC (GLC-MAX and GLC-MIN), including those associated with cooling and rewarming periods, were compared on 5-minute average values over all recording days at an ambient temperature of 23 °C, considering the value of Tb. In order to make these estimates robust to the sporadic occurrence of unusually high or low GLC readings, we defined GLC-MAX and GLC-MIN as the upper and lower adjacent values of GLC, which correspond to the GLC values indicated by Tukey's boxplot whiskers. In particular, GLC-MAX was estimated as the highest GLC reading within the upper inner fence, which is 1.5 times the interquartile range (3rd quartile – 1st quartile) above the 3rd quartile of GLC. GLC-MIN was estimated as the lowest GLC reading within the lower inner fence, which is 1.5 times the interquartile range (3rd quartile – 1st quartile) below the 1st quartile of GLC. For each mouse, boxplots were computed for all 5-minute average values of GLC and, separately, for 5-minute average values of GLC included in cooling or rewarming periods, subdivided as a function of 3 arbitrarily-defined Tb ranges: ≤ 30 °C, 30-34 °C, and ≥ 34 °C .

Statistical analysis

Statistical analysis was performed with SPSS (SPSS, Armonk, NY, USA). Data were analyzed with ANOVA with Huyn-Feldt correction and with t-tests with statistical significance for $P < 0.05$. The linear correlation between the z-scores of GLC and Tb was determined with the Pearson's correlation coefficient. Data were reported as means $\pm$ SEM.

Results

This paragraph is from Lo Martire, Valli et all. (Lo Martire, Valli et al. 2018)

Daily rhythm of GLC, Tb, and ACT in baseline conditions of ad libitum feeding and thermoneutrality

Figure 8A shows the raw data collected in a typical mouse in a 22-h period in baseline conditions of ad libitum feeding and at an ambient temperature of 30 °C. GLC, Tb, and ACT all varied significantly with time (P < 0.05, ANOVA), with values significantly higher during the dark period than during the light period (P < 0.05) (Figure 8 B, C, D). Analyses of the z-scores of Tb and GLC revealed that the two variables significantly differed at specific times of the day (P = 0.001, ANOVA, variable x time interaction). GLC increased less than Tb at the dark-light transition and increased at the end of the light period in the face of a fall in Tb (P < 0.05, t-tests). Nevertheless, Pearson's correlation analysis indicated that the daily values of TB were significantly (P < 0.001) and linearly correlated with those of GLC, with 56% of shared variance (Figure 8E).

GLC, Tb, and ACT during fasting, caloric restriction, and refeeding at 23 °C ambient temperature

When mice are fasted or calorically restricted at an ambient temperature of 23 °C, they often engage in a bout of torpor that initiates before the onset of the light phase and typically lasts through the first few hours of the light phase (Figure 9 A). As Figure 9 shows, Tb and GLC dropped significantly during fasting and caloric restriction as compared to refeeding (P<0.001, t-tests). However, ACT was not significantly different among the three conditions until the second half of the light period where ACT was elevated in the CR condition (P=0.011, t-tests), likely a result of food anticipatory behavior in these mice. Circadian rhythms of higher Tb, GLC, and ACT

during the dark phase vs. the light phase were re-established during the refeeding periods (P < 0.001 t-test).

ACT, Tb, and GLC during cooling/rewarming periods

The recordings of ACT, Tb, and GLC during ad libitum feeding at an ambient temperature of 30 °C, and then during fasting, caloric restriction and refeeding periods at an ambient temperature of 23 °C in one representative mouse are shown in Figure 10 A, highlighting the cooling (blue lines) and rewarming (red lines) periods. As shown by this mouse, torpor bouts became prominent after two days of caloric restriction and ceased during the refeeding periods. Recordings during three days of caloric restriction with prominent torpor bouts are displayed at higher magnification in Figure 10 B.

The results of the quantitative analysis of cooling and rewarming periods are shown in Figure 11. The 60-minute windows centered on the onset of the cooling periods showed significant time-dependent differences in ACT and Tb compared with control windows (P ≤ 0.009, ANOVA, time x cooling interaction). In particular, Tb was significantly lower with respect to the control windows in the 30 minutes preceding the onset of cooling (P = 0.028, t-test) but not in the 30 minutes afterward (P = 0.092, t-test; Figure 11A). On the other hand, GLC in the 60-minute window centered on the onset of the cooling period (Figure 11B) differed significantly from values in control windows (ANOVA, main effect of the cooling vs. control window, P = 0.010), but did not differ significantly as a function of time (ANOVA, P = 0.275 for the main effect of time; P = 0.193 for the time x condition interaction). Accordingly, GLC was significantly lower than in control sequences during the periods preceding and following cooling onset (P ≤ 0.019, t-test; Figure 11B). ACT values were significantly higher with respect to control windows both before and after the onset of the cooling period (P ≤ 0.041, t-test; Figure 11C).

The 60-minute windows centered on the onset of the rewarming periods showed significant time-dependent differences in ACT, Tb, and GLC compared with control

windows (P ≤ 0.009, ANOVA, time x rewarming interaction). Both Tb (Figure 11D) and GLC (Figure 11E) were significantly lower before and after the onset of the rewarming period than during the control windows (P ≤ 0.004, t-test). During the 30 minutes before the onset of the rewarming period, ACT was virtually zero, and significantly lower than in control windows (P = 0.006, t-test). ACT levels then increased after the onset of rewarming to values similar to those in control windows (P = 0.759, t-test; Figure 11F).

The results of the analysis of the GLC-MAX and GLC-MIN associated with cooling and rewarming periods as a function of Tb are shown in Figure 12. Figure 12 A and 12 B show boxplots of GLC as a function in Tb considering all time points (i.e., 5-minute average values, Figure 12 A) or only the time points included in cooling or rewarming periods (Figure 12 B). As detailed in the Methods section, the values of GLC-MAX and GLC-MIN for each mouse and Tb category were computed as those of the upper and lower boxplot whiskers, respectively. The values of GLC-MAX computed considering all-time points differed significantly among Tb categories (≤ 30 °C, 30-34 °C, > 34 °C; P < 0.001, ANOVA), whereas those of GLC-MIN did not (P = 0.130, ANOVA; Figure 12 C). Accordingly, the values of GLC-MAX were significantly lower at values of Tb ≤ 30 °C and 30-34 °C than at values of Tb > 34 °C (P ≤ 0.024, t-test). The same analysis performed focusing only on the cooling and rewarming periods is represented in Figure 12 D. As expected from the results of Figure 12 C, the values of GLC-MAX differed significantly as a function of Tb, whereas those of GLC-MIN did not (ANOVA main effect, P = 0.015 and P = 0.062, respectively). Both the values of GLC-MAX and those of GLC-MIN were significantly higher during rewarming than during cooling periods (ANOVA main effect, P = 0.006 and P = 0.003, respectively), without significant interaction effects between cooling/rewarming and the Tb category (ANOVA, P = 0.918 and P = 0.233, respectively).

Discussion

This paragraph is from Lo Martire, Valli et all. (Lo Martire, Valli et al. 2018)

Using a recent technical development of a telemetry system for continuous and simultaneous monitoring of GLC, Tb, and ACT, we tested: 1) whether and how day-night rhythms of GLC, Tb, and ACT are interrelated in mice at thermoneutrality; 2) whether GLC and ACT values at the onset of a torpor bout and arousal from the torpor bout differ from those in control conditions when torpor does not occur. We found a strong positive and linear correlation between circulating glucose and Tb during ad libitum feeding at thermoneutrality (Figure 8). Further, mice that were calorically restricted entered torpor bouts readily. Circulating blood glucose was low during torpor entry but did not drop precipitously as Tb did at the onset of a torpor bout. Blood glucose significantly increased during arousal from torpor during times when the mice were not feeding, indicating the presence of endogenous glucose production (Figure 11 panel E). Finally, while low blood glucose itself was not predictive of a bout of torpor, the onset of torpor was associated with the combination of low blood glucose and hyperactivity (Figure 11 panel B and C).

GLC showed the expected robust circadian rhythm in these mice as reported in the literature for humans (Boden, Chen et al. 1996; Van Cauter, Polonsky et al. 1997), and rodents (Kalsbeek, la Fleur et al. 2014). It should be noted that previous reports for GLC have been measured at standard laboratory temperatures, and the current work extends this finding to thermoneutrality. GLC peaks at the light/dark transition (Figure 8), in agreement with previous research in rodents (Kalsbeek, la Fleur et al. 2014). However, because we handled the mice before the onset of the dark period, our findings are confounded by a potential sympathetic response to animal handling. We show here that GLC and Tb were clearly interrelated (Figure 8). It is likely that the measurements made here at baseline (ACT, GLC, and Tb) are primarily influenced by the sleep/wake

state of the mouse. Mice are feeding, are generally active, and have greater sympathetic drive when awake, all which would drive up Tb and GLC.

However, we did not assess the sleep/wake state of these mice, although the temporal resolution of these telemeters will allow for future studies in just this area. In addition, we speculate that the higher increase in GLC at the end of the light/dark transition could be partly due to the decrease in glucose tolerance during the circadian rest period and during sleep. Studies on human subjects constantly infused with glucose to avoid endogenous glucose production have demonstrated that glucose tolerance varies across the day, reaching its minimum during the night, which corresponds to the rest period for humans (Van Cauter, Desir et al. 1989). The reduced glucose utilization during sleep is also supported by the high levels of plasma glucose measured during NREM sleep (Scheen, Byrne et al. 1996).

We compared GLC, Tb, and ACT values during cooling and rewarming periods with those in temporally matched periods of stable euthermia. This analytical approach made it possible to consider ZT and Tb in evaluating the relationship between GLC and torpor (Figure 9). GLC did not precipitously drop before the onset of torpor (Figure 9 A and Figure 10 B), suggesting that torpor is not preceded by a dramatic drop in GLC. On the other hand, we found that GLC was always lower in the cooling and rewarming periods with the respect to control conditions. It is intriguing that in the 30 minutes preceding the onset of the cooling period when mice had low GLC, both Tb and ACT substantially increased (Figure 11, panel A and C). This elevation in ACT and Tb parallels the finding in dormice where the pre-torpor period is associated with elevated sympathetic and metabolic activity as evidenced by an increase in ventilation, heart rate and metabolic rate (Elvert and Heldmaier 2005).

Peaks in metabolic and respiratory rate prior to entrance into torpor have also been observed in many hibernators like pocket mice, Djungarian hamsters and alpine marmots (Withers 1977; Heldmaier, Klingenspor et al. 1999; Ortmann and Heldmaier 2000).

Accordingly, the peak metabolic rate was chosen for the definition of torpor onset in experiments performed in Djungarian hamsters (Heldmaier, Klingenspor et al. 1999).

Taken together with this previous work, our present results raise the hypothesis that an increase in ACT in the face of hypoglycemia plays a role in torpor onset in calorically restricted mice.

During a fast, hepatic production of glucose is the primary source of circulating glucose and are under the control of the autonomic nervous system as well as circulating hormones such as glucagon and insulin.

The autonomic nervous system is intimately involved with both torpor induction and arousal (Atgie, Nibbelink et al. 1990; Swoap, Gutilla et al. 2006; Swoap and Weinshenker 2008; Swoap and Gutilla 2009; Braulke and Heldmaier 2010; Silvani, Cerri et al. 2018). Our results suggest that mice, either fasted or calorically restricted, were metabolizing circulating glucose, or at least taking it up from circulation, without full hepatic replacement of GLC.

Upon arousal from torpor, we found that GLC increased (Figures 9, 10, and 11). The rise in GLC during arousal from torpor is coincident with changes in other physiological functions that are also under the autonomic influence (Swoap and Gutilla 2009; Silvani, Cerri et al. 2018).

Hence, we can hypothesize that the rise in GLC upon arousal from torpor results from increased sympathetic drive to the liver. It is important to note that other pathways besides glycogenolysis can support metabolism during the arousal from torpor. Fat reserves may provide the necessary energy to arouse from torpor as suggested by the respiratory quotient (Nestler 1990; Heldmaier, Klingenspor et al. 1999). Indeed, an increased production of ketones from the liver, heart, and plasma is observed during arousal from torpor in mice (Nestler 1991).

For any given category of Tb defined here, we found that GLC was higher during rewarming than during cooling (Figure 12, panel D). This relationship between GLC and Tb during the torpor bout has also been observed with other physiological parameters. For example, heart rate and metabolic rate are both much greater during arousal as compared to torpor entry (Swoap and Gutilla 2009; Geiser, Currie et al. 2014).

This relationship between GLC and Tb may simply be a result of the thermal inertia of the animal and the telemeter. That is, the changes in Tb are slow relative to the changes in GLC because the mass of the animal/telemeter necessitates more time to be reflected in the measurement than does GLC.

However, this hysteretic GLC/ Tb relationship in torpor may also reflect substantially different physiological states of the organism as it enters and arouses from torpor. These possibilities are not mutually exclusive in that the animal may truly be in a much different physiological state, and our perception of that difference is amplified due to the nature of the parameter being measured. In conclusion, our results demonstrate that GLC and Tb are interrelated across the day-night period, both in baseline and in conditions predisposing to torpor onset. It may follow from this relationship between GLC and Tb that high glucose levels are not permissive for torpor induction. Further, high ACT and low GLC precede torpor onset, suggesting that this may be involved in triggering torpor necessitates more time to be reflected in the measurement than does GLC.

However, this hysteretic GLC/TB relationship in torpor may also reflect substantially different physiological states of the organism as it enters and arouses from torpor. These possibilities are not mutually exclusive in fact the animal may truly be in a much different physiological state, and our perception of that difference is amplified due to the nature of the parameter being measured. We also found that the minimum GLC was not different in cooling or rewarming periods. In other words, the mice had several instances where they had low GLC with a normal Tb, suggesting that low glucose is not likely a trigger for torpor induction.

In conclusion, our results demonstrate that GLC and Tb are interrelated across the day-night period, both in baseline and in conditions predisposing to torpor onset. It may follow from this relationship between GLC and Tb that high glucose levels are not permissive for torpor induction. Further, high ACT and low GLC precedes torpor onset, suggesting that this combination may be predictive of torpor onset.

Conclusion

These studies aimed to investigate the neural and metabolic mechanisms ruling spontaneous torpor in mice, which haven't been completely elucidated.

The first experimental part was aimed to understand the role of orexinergic transmission in torpor regulation. ORXS neurons are localized in the hypothalamus (de Lecea, Kilduff et al. 1998; Sakurai, Amemiya et al. 1998) and they widely project into the brain. In particular, the ORXS neurons are localized in the lateral hypothalamus together with the feeding-center (Sakurai, Amemiya et al. 1998), and they are involved in the regulation of food intake and of energetic metabolism. On this basis, it has been hypothesized that ORXS could participate in the regulatory mechanisms of the torpid state. Furthermore, ORXS neurons responds to peripheric signaling involved in torpor regulation, such as glucose, leptin and adenosine (Hara, Beuckmann et al. 2001).

Moreover, ORXS are implied in the circadian regulation and promote wakefulness (Hara, Beuckmann et al. 2001; Willie, Chemelli et al. 2003; Silvani, Bastianini et al. 2014).

Other potential contributors towards the regulatory mechanisms of torpor include a drop-in level of energy-sensitive hormones, such as leptin and insulin, as well as in the availability of glucose and other fuels, such as free fatty acids, and ketones from the circulation (Melvin and Andrews 2009).

The relationship between plasma glucose levels and the onset of torpor has never been directly investigated, even if previous studies suggested that glycemia levels could be involved in torpor regulation (Nestler 1991; Dark, Lewis et al. 1999; Heldmaier, Klingenspor et al. 1999; Franco, Contreras et al. 2013).

Particularly, pharmacological studies showed that a state similar to torpor can be induced with the administration of the 2-deoxyglucose, a glucose analog that blocks glycolysis by inactivating the enzyme phospho-gluco-isomerase (Dark, Miller et al. 1994; Stamper and Dark 1996; Westman and Geiser 2004). On the contrary,

mercaptoacetate, which blocks fatty acid oxidation, doesn't induce a torpor-like state in mice (Dark, Miller et al. 1994; Stamper and Dark 1996).

Considering these evidences, the second experimental part of this project was aimed to clarify if changes in glycemia (GLC) are correlated with the induction of torpor in mice.

A shared definition of torpor is still lacking so, in this study, we described the cooling and rewarming phases, which are the moments of transition between euthermia and hypothermia, and the deep torpor which is the phase in-between the previous ones (for more detailed definition see the methods chapter) (Lo Martire, Valli et al. 2018). In both the experimental parts, the analysis was focused on the physiological variables' dynamic changes during the three torpor phases.

The main result obtained in the first experimental part is that the dynamic changes showed by all the studied variables during the different torpor phases are very similar in WT and mice lacking orexins (KO-HCRT). So, KO-HCRT show normal patterns of the variables studied during the different phases of torpor. Although some specific differences exist, we can conclude that the key features of torpor are clearly preserved in KO-HCRT mice.

Another interesting result is that in both experimental groups a peak in ACT precedes the decrease in Tb (figure 5 panel A, figure 11 panel C). This significant increase in motor activity is accompanied by a significant sleep reduction, suggesting that an increase in ACT and a decrease in sleep propensity may represent a hallmark of torpor onset. We also found that the %REM sleep is significantly higher in KO-ORX mice compared to WT mice before and during cooling period. The onset of torpor is always during the dark period because of the experimental time feeding. A rise of the time spent in REM sleep during dark period by the KO-HCRT mice has been already described in the literature both in the KO-HCRT (Chemelli, Willie et al. 1999; Willie, Chemelli et al. 2003) and in the mice lacking orexinergic neurons (TG-HCRT) (Lo Martire, Silvani et al. 2012), and it is confirmed in this study. We also found that during stable deep torpor both %REM sleep and %NREM sleep is 0, and almost all the time is spent in an indeterminate state, that does not respond to standard EEG and EMG

criteria for wake or sleep scoring in euthermia (Figure 4). This represents a difference with respect to previous studies performed in hamster (Deboer and Tobler 2000; Deboer and Tobler 2003), showing and high % NREM sleep during torpor. The reasons of this difference remain to be clarified. All the mice involved in the first experiment show a peak in time spent NREM sleep rightly before the torpor onset, so we can speculate that mice enter into torpor trough sleep and in particular from NREM sleep. This finding is in accordance with other studies showing that the animals enter into torpor through sleep both during hibernation and daily torpor (Withers 1977; Heldmaier, Klingenspor et al. 1999; Ortmann and Heldmaier 2000; Elvert and Heldmaier 2005).

As far as the second experiment is concerned, we had two main findings. The first is that during ad libitum feeding GLC, Tb and ACT showed a robust circadian rhythm, with a strong positive and linear correlation between GLC and Tb. The second is that the high motor activity before the onset of torpor already described in the first experiment was accompanied by low GLC. We speculated that a condition of hyperactivity while the GLC low can be predictive of torpor onset. Moreover, GLC was low during torpor, while it is significantly increased during arousal from torpor. This increase of GLC during the rewarming phase (figure 11 panel E) suggests that there is an endogenous glucose production. In fact, GLC is low before the entry into torpor and keeps low and stable level during all the torpor bout (Figure 11, panel B). The GLC rising during the rewarming period could be explained by a sympathetic activation on the liver. The direction of changes during rewarming period of all the physiological variables studied (Figure 5, panel A, B, C, and D) suggests that the sympathetic nervous system is intensively activates, in accordance with previous hypothesis (Swoap and Gutilla 2009; Silvani, Cerri et al. 2018).

Interestingly, high GLC is not permissive for the entry into torpor, but low GLC itself can't be the torpor trigger; in fact, low GLC level were also recorded during euthermic periods.

So, torpor can be defined as a complex and multifactorial phenomenon used by different species to survive to extreme environmental conditions.

Our results are in concert with the literature. I can conclude there is not a unique torpor trigger but rather an involvement of metabolic, genetic and neural factors ruling during the entrance and the exit from torpor.
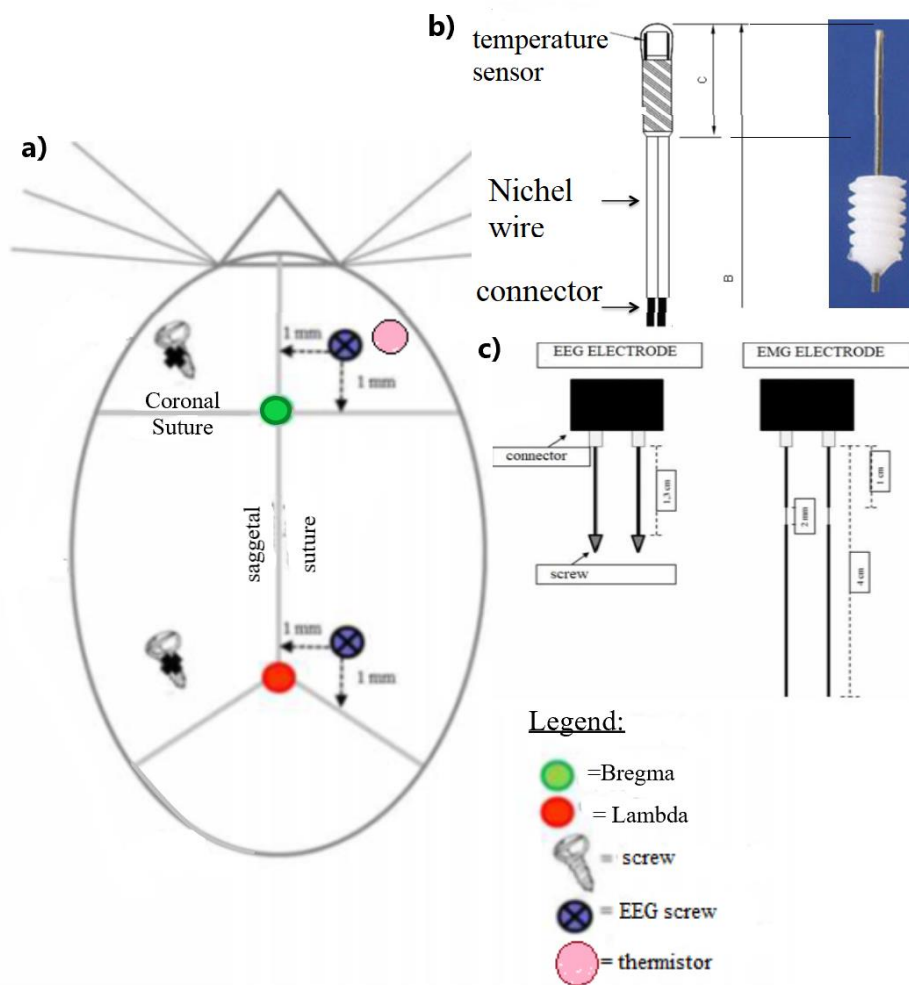
Figures

Figure 1. Scheme of: the cranial surgery, electroencephalographic (EEG) and electromyographic (EMG) electrodes and thermistor.

In the image A) is represented by a stylized mouse head, the grey lines represent the cranial suture and the green point is the cranial cross (Lambda). The red point is the caudal cross of the cranial sutures (Bregma). These two points are used as landmarks to take the stereotaxic coordinates. The thermistor (Figure B) has been positioned at -2 and +1 mm from Bregma (pink point). It is composed by a guide cannula in which is fixed a temperature sensor connected to a copper wire. This wire is weld to a plastic pin to detect the real-time brain temperature. The two EEG screws are implanted in contact with the dura mater through burr holes (Figure A, purple points) to obtain a differential EEG signal. The EEG and EMG electrodes are assembled in PRISM laboratory (Figure C). Stainless-steel anchor screws positioned as in the (Figure A, screws) to give stability to the structure (2.4 mm length, Plastics One, Roanoke, VA, USA). The thermistor and the electrodes were fixed using a dental cement (Rely X ARC, 3M ESPE, Segrate, Milano, Italy), and dental acrylic (Respal NF, SPD, Mulazzano, Italy).
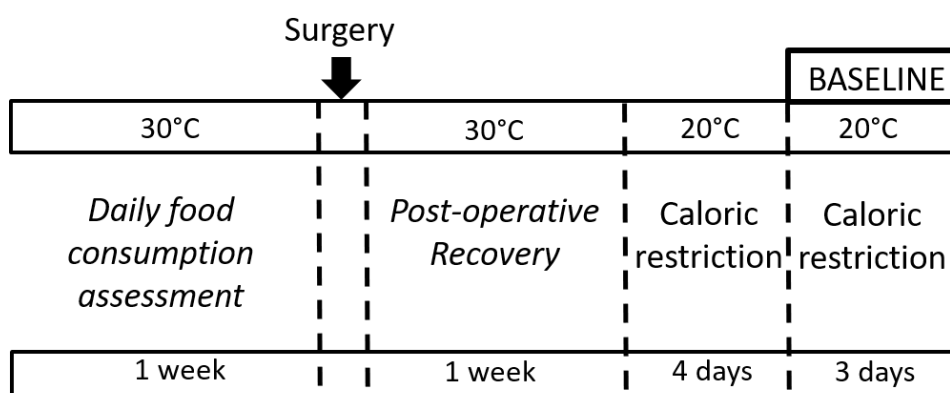
Figure 2. Schedule of surgery and conditions during which the bio-signals were recorded.

See Experimental protocol, recordings, and data acquisition of experiment one for details.
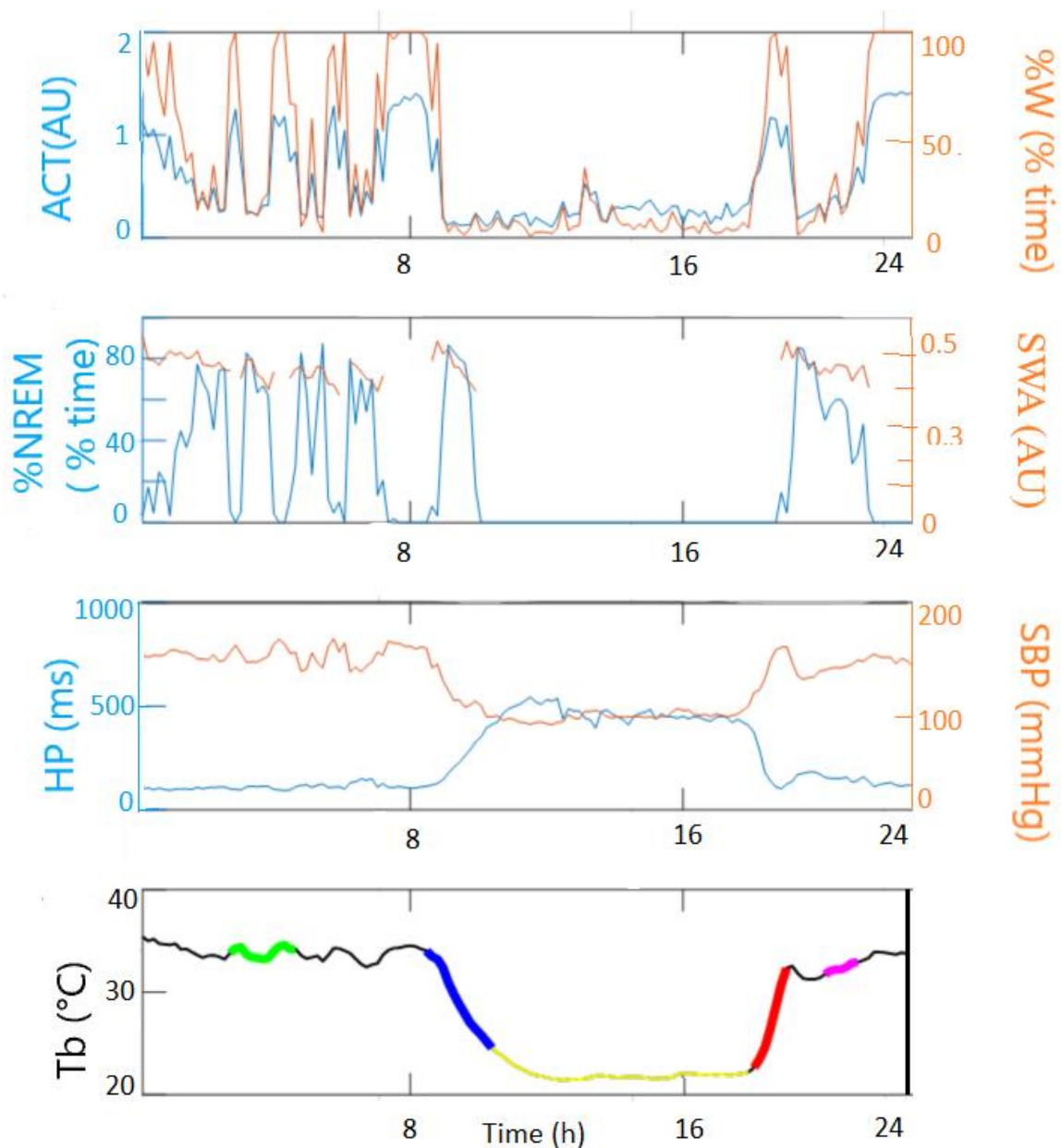
Figure 3. **Raw data collected in a typical mouse in a 24 h interval of the baseline record**
The raw data collected in a typical mouse in a 24 h interval of the baseline recording calorically
restricted and with the ambient temperature set at 20 °C. In the first graph is plotted the activity
(ACT, in blue), the amount of time spent awake (W, in orange) vs time of recording (h).
In the second graph is plotted in blue the percentage of time spent by the animal in quiet sleep
(NREM, in blue) and the slow wave amplitude (SWA, AU) in orange vs time of recording (h).
In the third graph is plotted the heart period (HP, in blue) and the blood pressure (BP, in orange) vs
time.
In the 4th graph is plotted the brain cortical temperature (Tb, in black) vs time of recording (h).
The cooling sequence is highlighted in blue, the baseline is highlighted in green, the rewarming
sequence is highlighted in red. The pink line is a reference sequence for the rewarming sequence and
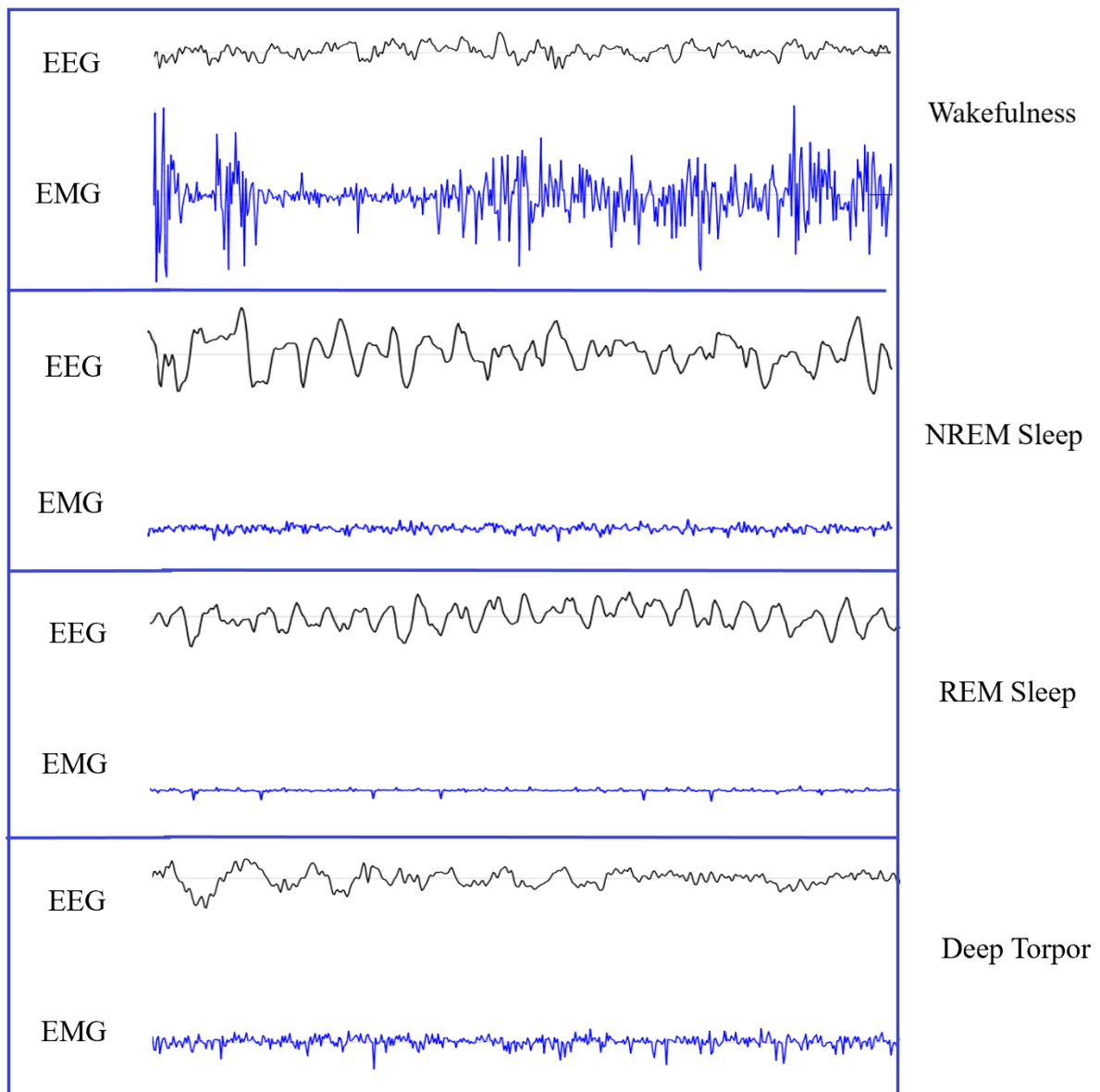the yellow line is the interval of stable-deep torpor.

Figure 4. The electroencephalographic and electromyographic signals during wakefulness, NREM sleep, REM sleep, and deep torpor.

The wake-sleep cycle is divided into three phases: the wakefulness (W) and, within sleep, two separate states are defined based on multiple physiologic parameters: rapid eye movement (REM) and non-REM (NREM). In wakefulness, the electroencephalographic (EEG) pattern is desynchronized (low amplitude and high frequencies waves) and electromyographic (EMG) pattern is of maximum activity. The EEG pattern in NREM sleep is commonly described as synchronous (high-voltage, low frequencies slow waves) and EMG activity lower than wakefulness. REM sleep, by contrast, is defined by EEG activation (High frequencies and low voltage waves), muscle atonia, and episodic bursts of rapid eye movements. Deep torpor is an indefinite condition because there is an EEG pattern similar to active wakefulness while the EMG is low as in NREM sleep.
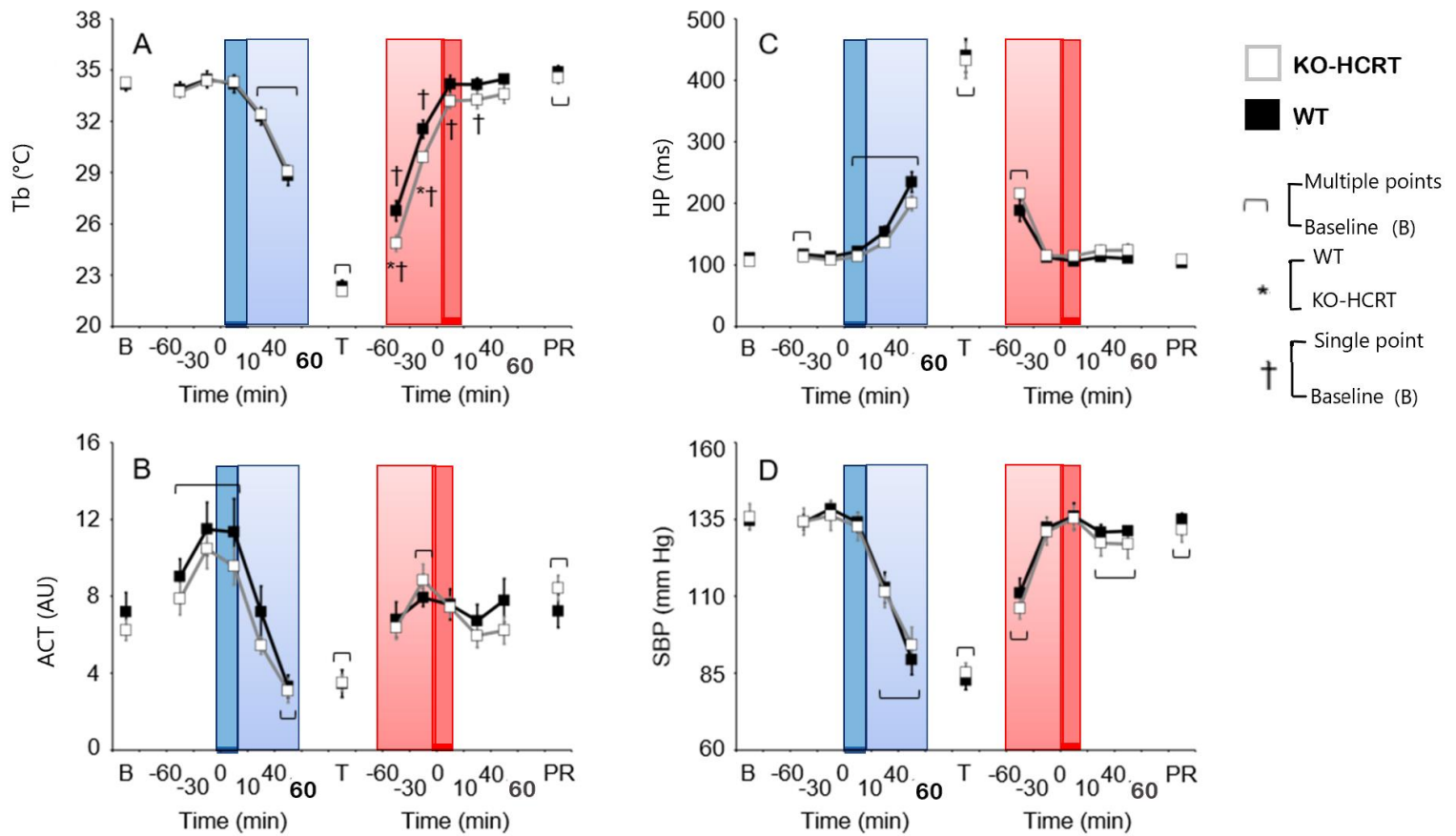
Figure 5. Brain cortical temperature, activity, Heart period and Systolic blood pressure during cooling deep torpor and rewarming.

The panel A shows brain cortical temperature (Tb, °C), the panel B the activity (ACT, AU), the panel C the Heart Period (HP, ms) and the panel D the systolic blood pressure (SBP, mmHg). Time zero is the onset of the cooling and the end of rewarming sequences, marked with the monochrome blue and red rectangle. The shading rectangle represents the duration of the cooling (blue) and rewarming (red) sequence. We have analyzed 60 minutes before and after the event onset. The deep torpor is in correspondence with the T in the X axes. The B represents the mean value of the baseline and the PR represent the reference value for the rewarming.

The black and gray line represent respectively the results obtained in the wild-type (WT) and in the mice knock out for the pre-pro orexin gene (KO-HCRT) groups.

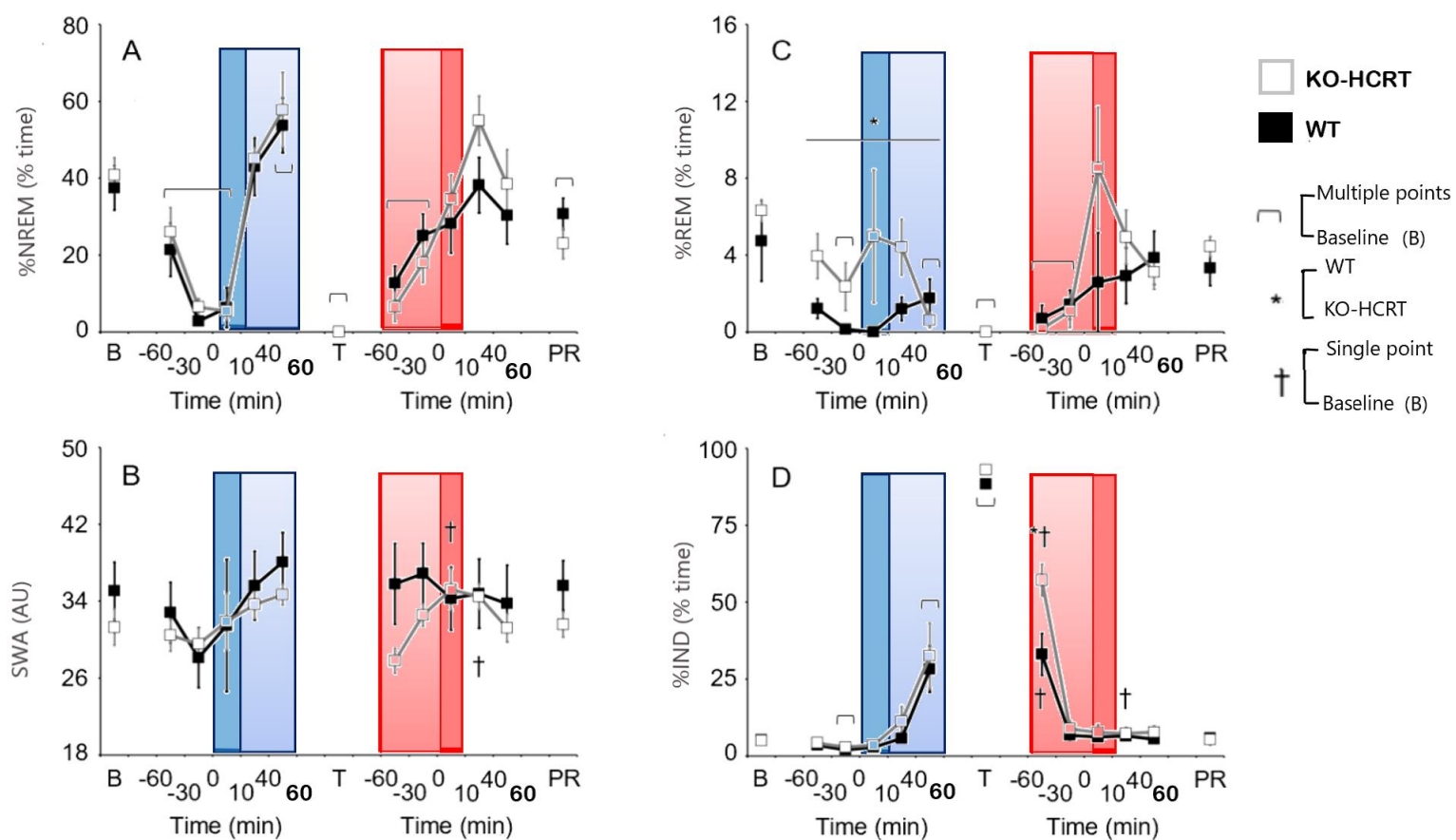Data are reported as means ± SD with n = 8 WT vs 8 KO-HCRT.

Figure 6. Percentage of time spent in NREM, in REM sleep, Slow-wave activity in NREM and Percentage of time spent in the undetermined state.

The panel A shows the percentage of time spent in NREM sleep (%NREM, %time), the panel B the NREM sleep slow wave activity (SWA, AU), the panel C the percentage of time spent in REM sleep (%REM, %time) and the panel D the percentage of time spent in undetermined state (%IND, %time). Time zero is the onset of the cooling and rewarming sequences, highlighted respectively in the blue and red rectangle. We have considered 60 minutes before and after the event onset. The deep torpor is in correspondence with the T in the X axes. The B represents the mean value of the baseline (for the cooling and rewarming sequences) and the PR represent the reference value for the rewarming. The black and gray line represent respectively the results obtained in the wild-type (WT) and in the mice knock out for the pre-pro orexin gene (KO-HCRT) groups.

Data are reported as means ± SD with n = 8 WT vs 8 KO-HCRT.

variable	group	mean	Standard deviation
L-c (min)	WT	110.28	26.85
	KO-HCRT	114.10	10.18
L-r (min)	WT	76.67	7.70
	KO-HCRT	77.25	4.83
Tb-c	WT	0.090	0.013
	KO-HCRT	0.085	0.006
Tb-r	WT	0.134	0.022
	KO-HCRT	0.127	0.017
ACT-c	WT	0.007	0.003
	KO-HCRT	0.005	0.003
ACT-r	WT	0.005	0.004
	KO-HCRT	0.004	0.004
HP-c	WT	2.422	0.721
	KO-HCRT	2.007	0.721
HP-r	WT	2.402	0.657
	KO-HCRT	2.212	0.390
SBP-c	WT	0.567	0.266
	KO-HCRT	0.441	0.091
SBP-r	WT	0.514	0.267
	KO-HCRT	0.489	0.057

Table 1. Length, Slope of cortical brain temperature, activity, heart period and systolic blood pressure during cooling and rewarming sequences.

The length (min) of the cooling (L-c) and rewarming (L-r) sequences are presented as a means of all the wild-type animals (WT) and ko mice for the pre-pro orexin gene (KO-HCRT). The rewarming has a shorter duration than cooling sequences ($P< 0.001$, ANOVA).

The slope of cortical brain temperature during cooling (Tb-C) and during the rewarming sequences (Tb-R) for the WT and mice KO-HCRT shows no significative difference between the experimental groups but the Tb-r rise faster than the Tb-c decrease ($P<0.001$, ANOVA).

The variation of the activity during the cooling sequences (ACT-c) and rewarming sequences (ACT-r) for the WT and KO-HCRT mice doesn't show statistic differences between the experimental groups but that ACT-c decrease significantly faster than ACT-r rise, ($P<0.05$, ANOVA).

The values for the variation of heart period during the cooling (HP-c) and rewarming sequence (HP-r) and the systolic blood pressure during cooling (SBP-c) and rewarming sequence (SBP-r) respectively for WT and KO-HCRT mice shows no significative differences ($P>0.05$, ANOVA).

Data are reported as means $\pm$ SD with n = 8 WT vs 8 KO-HCRT.

variable	group	mean	Standard deviation
%NREM-c	WT	0.065	0.111
	KO-HCRT	0.058	0.055
%NREM-r	WT	0.329	0.297
	KO-HCRT	0.404	0.310
%REM-c	WT	0.007	0.020
	KO-HCRT	0.038	0.075
%REM-r	WT	0.031	0.068
	KO-HCRT	0.111	0.087

Table 2. **The slope of the percentage of time spent in NREM and REM sleep during cooling and rewarming sequence.**

The slope of percentage of time spent in NREM for the cooling (%NREM-c) and rewarming (%NREM-r) for the wild-type (WT) and mice KO pre-pro orexin gene (KO-HCRT) shows no significative difference between the two experimental groups but the increase of %NREM-r is significantly faster than %NREM-c ($P<0.05$, ANOVA).

The slope of the percentage of time spent in REM for the cooling (%REM-c) and rewarming (%REM-r) for the WT and mice KO-HCRT mice show that the KO-HCRT enters more rapidly in REM during the cooling than the WT, ($P<0.05$, ANOVA).

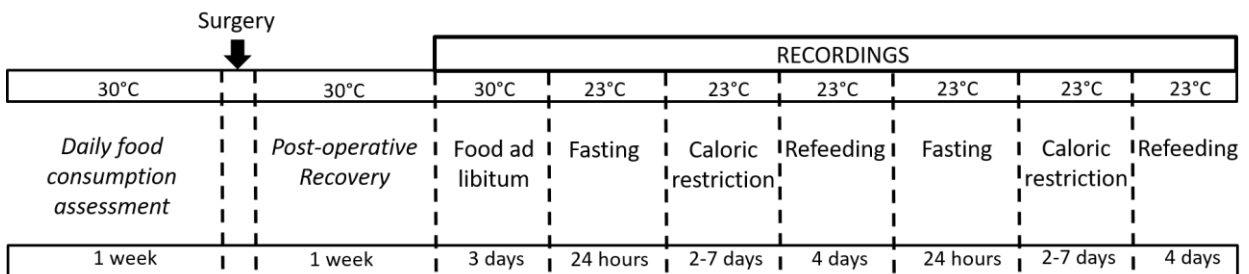Data are reported as means $\pm$ SD with n = 8 WT vs 8 KO-HCRT.

Figure 7. Schedule of surgery and conditions during which the bio-signals were recorded.

See Experimental protocol, recordings, and data acquisition of the experiment two for detail
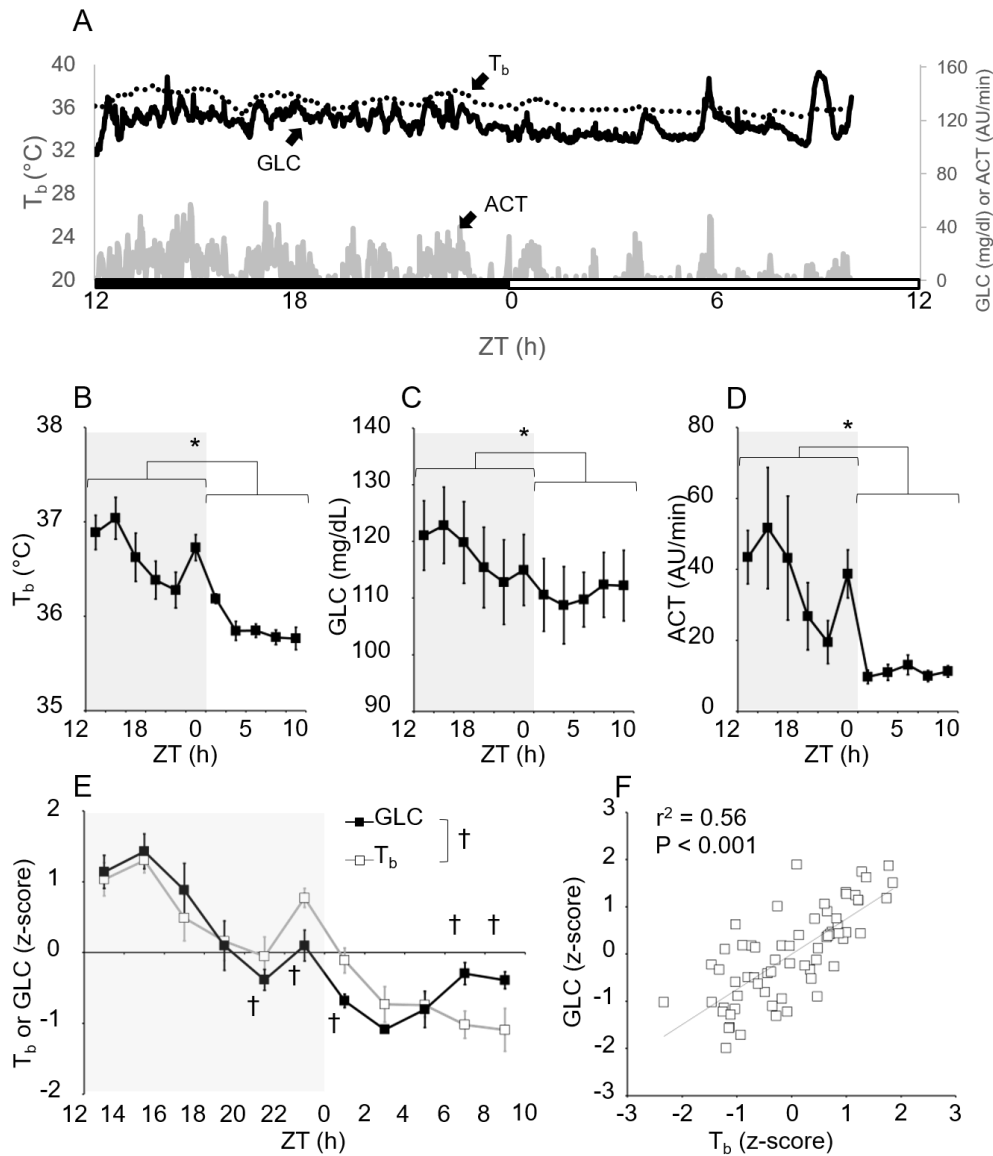
Figure 8. Blood glucose, core body temperature, and activity in ad lib fed C57Bl/6J male mice in thermoneutrality.

Panel A shows the raw data collected in a 22-h period in a typical mouse in ad-libitum feeding condition at 30°C Ta. ACT, activity, expressed in arbitrary units (AU) per 1-min recording; Tb, core body temperature; GLC, blood glucose concentration. Lights were on at 5 a.m., which corresponded to Zeitgeiber time ZT=0, whereas ZT=12 corresponded to lights off (5 p.m.). The black bar indicates the dark period and the white bar corresponds to the light period. Panel B, C and D show Tb, GLC, and ACT, respectively, averaged over two-hour bins for the six mice under study. Data are reported as means ± SEM. *, P < 0.05, light vs dark period (t-test). Panel E shows the z-score values of Tb and GLC averaged over 2-hour intervals, in a 22-h period in ad libitum feeding condition at 30 °C Ta. †, P < 0.05, Tb z-score vs GLC z-score. Panel F shows the relationship between GLC and Tb z-scores calculated through Pearson's linear correlation analysis. r2, coefficient of determination (Lo Martire, Valli et al. 2018). Data are reported as means ± SEM with n = 6.
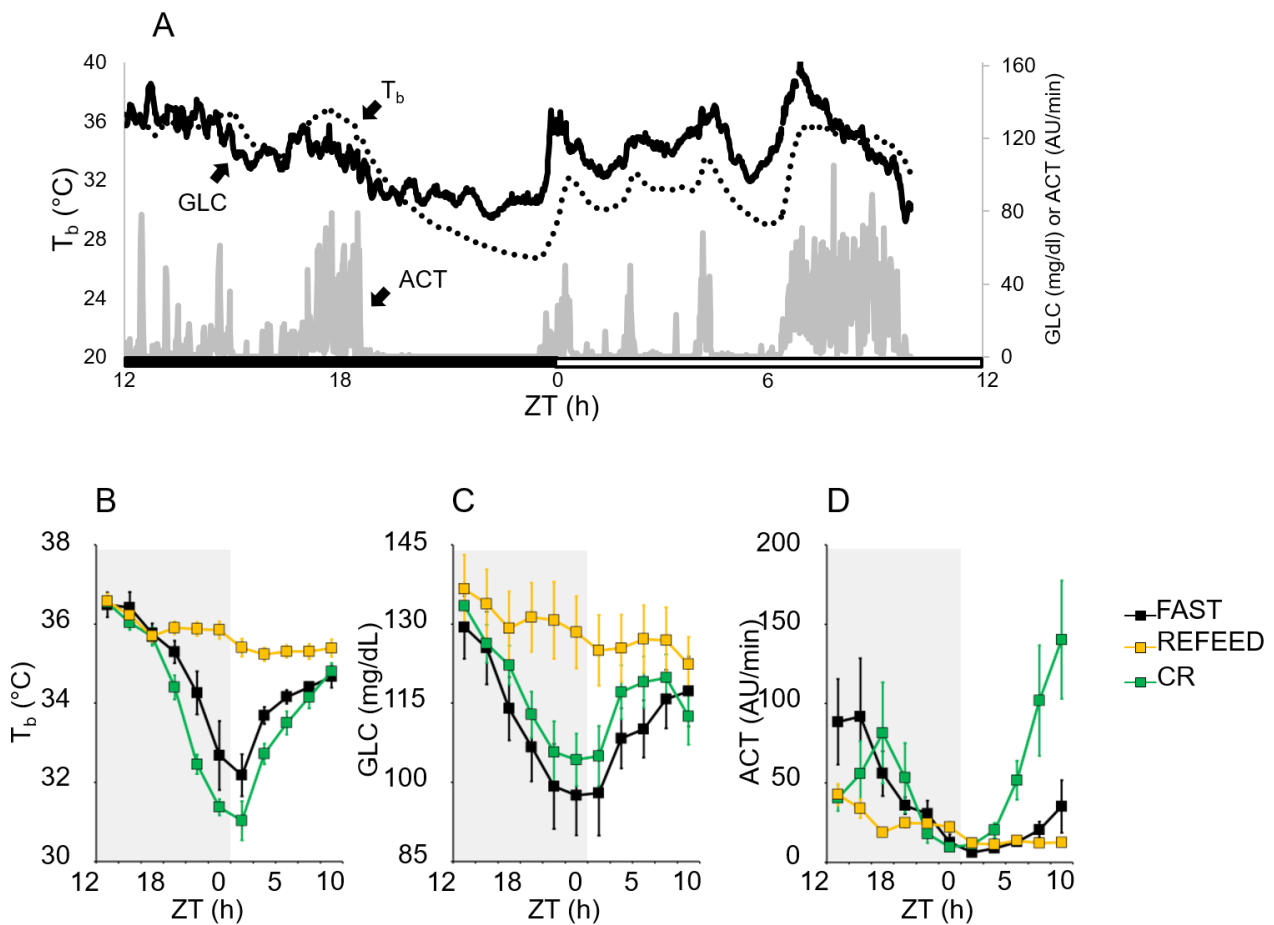
Figure 9. Blood glucose, core body temperature, and activity during fasting, caloric restriction, and refeeding.

Panel A shows core body temperature (Tb), blood glucose concentration (GLC), and activity (ACT, expressed in arbitrary units, AU, per 1-min recording) on the 3rd day of caloric restriction for one of the mice. Lights were on at 5 a.m., which corresponded to Zeitgeiber time ZT=0, whereas ZT=12 corresponded to lights off (5 p.m.). The black bar indicates the dark period, the white bar corresponds to the light period. From tracings like these, the values of Tb (panel B), GLC (panel C), and ACT (panel D) were averaged over consecutive 2-hour periods during fasts, days of caloric restriction, and during refeeding. Data are reported as means ± SEM with n = 6 (Lo Martire, Valli et al. 2018).
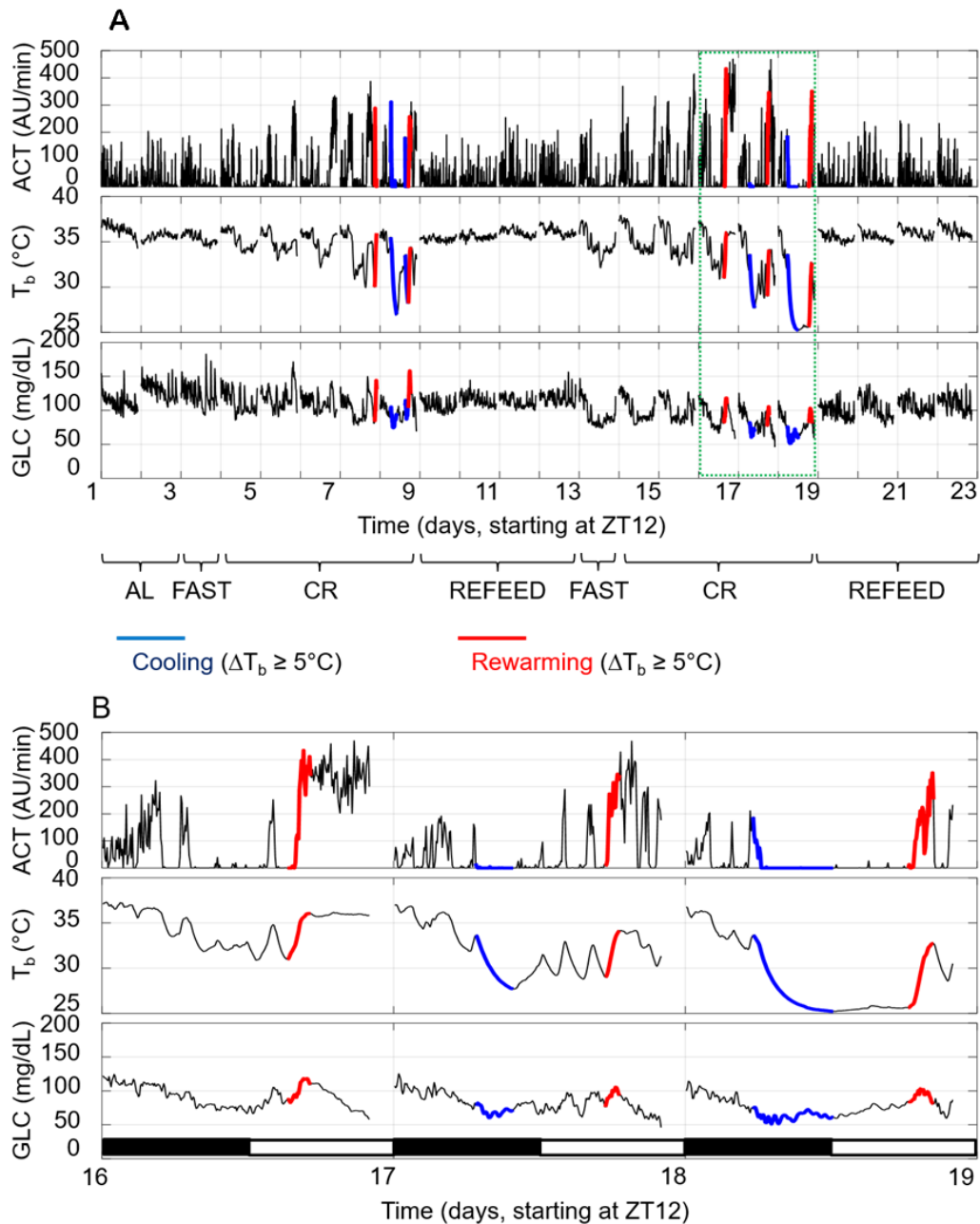
Figure 10. Blood glucose, core body temperature, and activity over 23 days of continuous recording.

Panel A shows the recordings of activity (ACT, in arbitrary units, AU, per 1-min recording), core body temperature (Tb) and blood glucose concentration (GLC) during ad-libitum feeding at 30 °C Ta, and then, at 23 °C Ta, during fasting, caloric restriction (70% of normal food intake), and ad libitum refeeding periods from one representative mouse. The cooling and rewarming periods (cf. Methods for details) are represented in blue and red, respectively. A magnified view of three days of caloric restriction when torpor was prominent can be seen in panel B (Lo Martire, Valli et al. 2018).
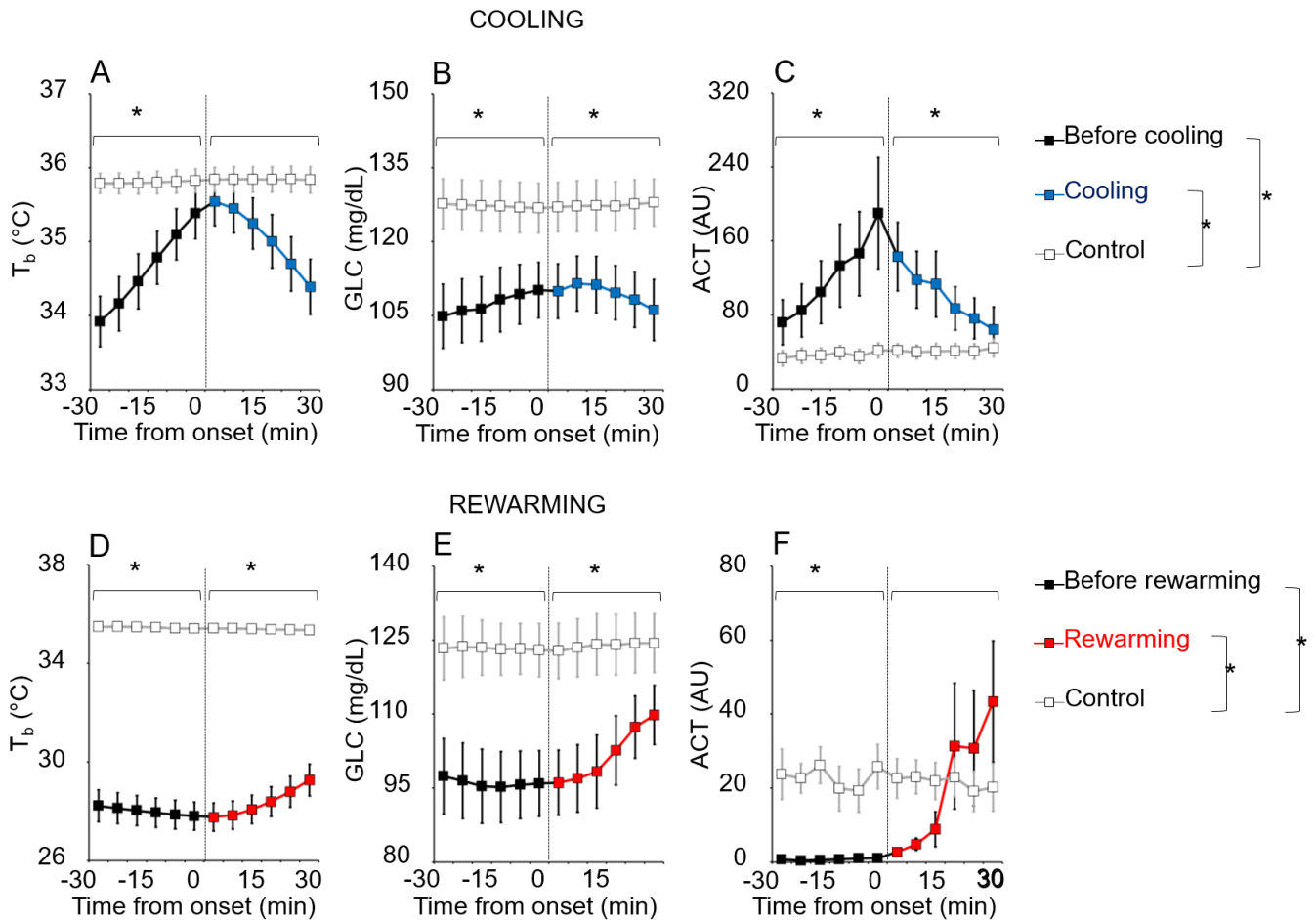
Figure 11. Blood glucose, core body temperature, and activity before/after the onset of cooling and rewarming periods.

Panels A, B, and C show the comparison of core body temperature (Tb), blood glucose concentrations (GLC), and activity (ACT, in arbitrary units, AU, per 1-min recording), averaged over 5-minute intervals, between cooling periods (black lines before cooling onset, blue lines after cooling onset) and temporally matched periods of stable euthermia (control periods, gray lines). Panels D, E, and F compare the same variables between rewarming periods (black lines before rewarming onset, red lines after rewarming onset) and temporally matched periods of stable euthermia (control periods, gray lines). Time 0 indicates the onset of the cooling/rewarming periods. Data are reported as means ± SEM with n = 6. *, $P < 0.05$, cooling or rewarming vs. control periods (t-test) (Lo Martire, Valli et al. 2018).
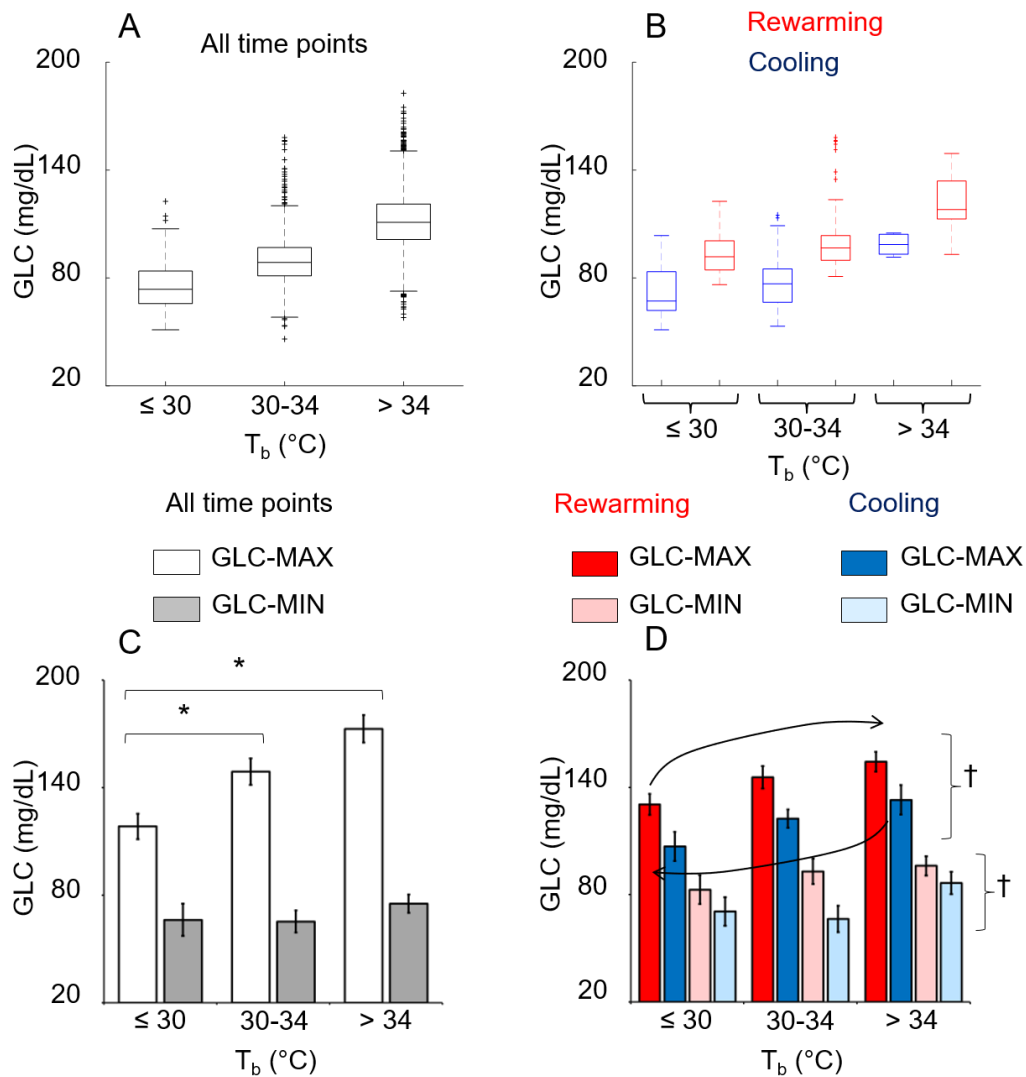
Figure 12. The relationship between blood glucose and core body temperature during periods of body cooling and rewarming.

Panel A and B shows boxplots of the distribution of GLC values (averages over 5-minute intervals) in one representative mouse throughout the whole recording period at 23 °C, including all time points (panel A) or only the cooling (blue) and rewarming (red) periods (panel B; cf. Methods for details), as a function of Tb ($\leq$ 30°C, 30-34°C, > 34 °C). Boxplot whiskers were taken as estimates of the maximum and minimum values of GLC robust to the effect of extreme values in the distribution (MAX and MIN, respectively). Panels C and D shows means $\pm$ SEM (n = 6 mice) of MAX and MIN of GLC on all time points (panel C) or only for cooling (blue) and rewarming (red) periods (panel D) as a function of Tb ($\leq$ 30 °C, 30-34 °C, >34 °C). The black arrows in panel D highlight the hysteresis in the relationship between GLC and Tb during cooling and rewarming periods. *, P < 0.05 for values at 30-34 °C Tb vs. values at $\leq$ 30 °C or > 34 °C Tb (t-test). †, P < 0.05, cooling vs. rewarming periods irrespective of Tb (ANOVA main effect) (Lo Martire, Valli et al. 2018).

Bibliography

Adeghate, E., M. Fernandez-Cabezudo, et al. (2010). "Orexin-1 receptor co-localizes with pancreatic hormones in islet cells and modulates the outcome of streptozotocin-induced diabetes mellitus." PLoS One **5**(1): e8587.

Anaclet, C., R. Parmentier, et al. (2009). "Orexin/hypocretin and histamine: distinct roles in the control of wakefulness demonstrated using knock-out mouse models." J Neurosci **29**(46): 14423-14438.

Andrews, M. T. (2007). "Advances in molecular biology of hibernation in mammals." Bioessays **29**(5): 431-440.

Arafat, A. M., P. Kaczmarek, et al. (2014). "Glucagon regulates orexin A secretion in humans and rodents." Diabetologia **57**(10): 2108-2116.

Arrich, J., M. Holzer, et al. (2016). "Pre-hospital versus in-hospital initiation of cooling for survival and neuroprotection after out-of-hospital cardiac arrest." Cochrane Database Syst Rev **3**: CD010570.

Atgie, C., M. Nibbelink, et al. (1990). "Sympathoadrenal activity and hypoglycemia in the hibernating garden dormouse." Physiol Behav **48**(6): 783-787.

Baracchi, F., G. Zamboni, et al. (2008). "Cold exposure impairs dark-pulse capacity to induce REM sleep in the albino rat." J Sleep Res **17**(2): 166-179.

Bass, J. and J. S. Takahashi (2010). "Circadian integration of metabolism and energetics." Science **330**(6009): 1349-1354.

Bastianini, S., C. Berteotti, et al. (2014). "SCOPRISM: a new algorithm for automatic sleep scoring in mice." J Neurosci Methods **235**: 277-284.

Bastianini, S., V. Lo Martire, et al. (2016). "High-amplitude theta wave bursts characterizing narcoleptic mice and patients are also produced by histamine deficiency in mice." J Sleep Res **25**(5): 591-595.

Bastianini, S., A. Silvani, et al. (2011). "Sleep related changes in blood pressure in hypocretin-deficient narcoleptic mice." Sleep **34**(2): 213-218.

Berger, R. J. (1984). "Slow wave sleep, shallow torpor and hibernation: homologous states of diminished metabolism and body temperature." Biol Psychol **19**(3-4): 305-326.

Boden, G., X. Chen, et al. (1996). "Evidence for a circadian rhythm of insulin sensitivity in patients with NIDDM caused by cyclic changes in hepatic glucose production." Diabetes **45**(8): 1044-1050.

Boulant, J. A. (1998). "Hypothalamic neurons. Mechanisms of sensitivity to temperature." Ann N Y Acad Sci **856**: 108-115.

Boulant, J. A. (2006). "Neuronal basis of Hammel's model for set-point thermoregulation." J Appl Physiol (1985) **100**(4): 1347-1354.

Bouma, H. R., H. V. Carey, et al. (2010). "Hibernation: the immune system at rest?" J Leukoc Biol **88**(4): 619-624.

Bouma, H. R., F. G. Kroese, et al. (2011). "Low body temperature governs the decline of circulating lymphocytes during hibernation through sphingosine-1-phosphate." Proc Natl Acad Sci U S A **108**(5): 2052-2057.

Bouma, H. R., E. M. Verhaag, et al. (2012). "Induction of torpor: mimicking natural metabolic suppression for biomedical applications." J Cell Physiol **227**(4): 1285-1290.

Bratincsak, A. and M. Palkovits (2005). "Evidence that peripheral rather than intracranial thermal signals induce thermoregulation." Neuroscience **135**(2): 525-532.

Braulke, L. J. and G. Heldmaier (2010). "Torpor and ultradian rhythms require an intact signalling of the sympathetic nervous system." Cryobiology **60**(2): 198-203.

Cadena, V. and G. J. Tattersall (2014). "Body temperature regulation during acclimation to cold and hypoxia in rats." J Therm Biol **46**: 56-64.

Cannon, B. and J. Nedergaard (2004). "Brown adipose tissue: function and physiological significance." Physiol Rev **84**(1): 277-359.

Careau, V. (2013). "Basal metabolic rate, maximum thermogenic capacity and aerobic scope in rodents: interaction between environmental temperature and torpor use." Biol Lett **9**(2): 20121104.

Carey, H. V., M. T. Andrews, et al. (2003). "Mammalian hibernation: cellular and molecular responses to depressed metabolism and low temperature." Physiol Rev **83**(4): 1153-1181.

Carlin, J. L., S. Jain, et al. (2017). "Hypothermia in mouse is caused by adenosine A1 and A3 receptor agonists and AMP via three distinct mechanisms." Neuropharmacology **114**: 101-113.

Caterina, M. J. (2007). "Transient receptor potential ion channels as participants in thermosensation and thermoregulation." Am J Physiol Regul Integr Comp Physiol **292**(1): R64-76.

Cerri, M. (2017). "The Central Control of Energy Expenditure: Exploiting Torpor for Medical Applications." Annu Rev Physiol **79**: 167-186.

Cerri, M., M. Mastrotto, et al. (2013). "The inhibition of neurons in the central nervous pathways for thermoregulatory cold defense induces a suspended animation state in the rat." J Neurosci **33**(7): 2984-2993.

Cerri, M., W. Tinganelli, et al. (2016). "Hibernation for space travel: Impact on radioprotection." Life Sci Space Res (Amst) **11**: 1-9.

Chaya, M. S., A. V. Kurpad, et al. (2006). "The effect of long term combined yoga practice on the basal metabolic rate of healthy adults." BMC Complement Altern Med **6**: 28.

Chemelli, R. M., J. T. Willie, et al. (1999). "Narcolepsy in orexin knockout mice: molecular genetics of sleep regulation." Cell **98**(4): 437-451.

Chen, J. (2015). "The evolutionary divergence of TRPA1 channel: heat-sensitive, cold-sensitive and temperature-insensitive." Temperature (Austin) **2**(2): 158-159.

Ciriello, J., J. C. McMurray, et al. (2003). "Collateral axonal projections from hypothalamic hypocretin neurons to cardiovascular sites in nucleus ambiguus and nucleus tractus solitarius." Brain Res **991**(1-2): 133-141.

Claudia, B., L. Karin, et al. (2014). "Body mass dependent use of hibernation: why not prolong the active season, if they can?" Functional Ecology **28**(1): 167-177.

Cliff, M. A. and B. G. Green (1996). "Sensitization and desensitization to capsaicin and menthol in the oral cavity: interactions and individual differences." Physiol Behav **59**(3): 487-494.

Daan, S., B. M. Barnes, et al. (1991). "Warming up for sleep? Ground squirrels sleep during arousals from hibernation." Neurosci Lett **128**(2): 265-268.

Dark, J. (2005). "Annual lipid cycles in hibernators: integration of physiology and behavior." Annu Rev Nutr **25**: 469-497.

Dark, J., D. A. Lewis, et al. (1999). "Hypoglycemia and torpor in Siberian hamsters." Am J Physiol **276**(3 Pt 2): R776-781.

Dark, J., D. R. Miller, et al. (1994). "Reduced glucose availability induces torpor in Siberian hamsters." Am J Physiol **267**(2 Pt 2): R496-501.

Dausmann, K. H., J. Glos, et al. (2004). "Physiology: hibernation in a tropical primate." Nature **429**(6994): 825-826.

Dave, K. R., S. L. Christian, et al. (2012). "Neuroprotection: lessons from hibernators." Comp Biochem Physiol B Biochem Mol Biol **162**(1-3): 1-9.

de Lecea, L., T. S. Kilduff, et al. (1998). "The hypocretins: Hypothalamus-specific peptides with neuroexcitatory activity." Proceedings of the National Academy of Sciences **95**(1): 322-327.

Deboer, T. and I. Tobler (1994). "Sleep EEG after daily torpor in the Djungarian hamster: similarity to the effect of sleep deprivation." Neurosci Lett **166**(1): 35-38.

Deboer, T. and I. Tobler (1995). "Temperature dependence of EEG frequencies during natural hypothermia." Brain Res **670**(1): 153-156.

Deboer, T. and I. Tobler (1995). "Temperature dependence of EEG frequencies during natural hypothermia." Brain Res **670**(1): 153-156.

Deboer, T. and I. Tobler (1996). "Natural hypothermia and sleep deprivation: common effects on recovery sleep in the Djungarian hamster." Am J Physiol **271**(5 Pt 2): R1364-1371.

Deboer, T. and I. Tobler (2000). "Slow waves in the sleep electroencephalogram after daily torpor are homeostatically regulated." Neuroreport **11**(4): 881-885.

Deboer, T. and I. Tobler (2003). "Sleep regulation in the Djungarian hamster: comparison of the dynamics leading to the slow-wave activity increase after sleep deprivation and daily torpor." Sleep **26**(5): 567-572.

Dement, M. A. C. a. W. C. (2011). Normal Human Sleep: An Overview, Elsevier saunders.

Dennis Grahn, P. a. H. C. H., PhD. (2004). "The Physiology of Mammalian Temperature Homeostasis." ITACCS Critical Care Monograph: 18.

Dietrich, Marcelo O., Marcelo R. Zimmer, et al. (2015). "Hypothalamic Agrp Neurons Drive Stereotypic Behaviors beyond Feeding." Cell **160**(6): 1222-1232.

Dioum, E. M., R. Chen, et al. (2009). "Regulation of hypoxia-inducible factor 2alpha signaling by the stress-responsive deacetylase sirtuin 1." Science **324**(5932): 1289-1293.

Doris, P. A. and M. A. Baker (1981). "Effects of dehydration on thermoregulation in cats exposed to high ambient temperatures." J Appl Physiol Respir Environ Exerc Physiol **51**(1): 46-54.

Doucette, L. I., R. M. Brigham, et al. (2012). "Prey availability affects daily torpor by free-ranging Australian owlet-nightjars (Aegotheles cristatus)." Oecologia **169**(2): 361-372.

Douglas, N. J., D. P. White, et al. (1982). "Respiration during sleep in normal man." Thorax **37**(11): 840-844.

Drew, K. L., C. L. Buck, et al. (2007). "Central nervous system regulation of mammalian hibernation: implications for metabolic suppression and ischemia tolerance." J Neurochem **102**(6): 1713-1726.

Ehrstrom, M., E. Naslund, et al. (2004). "Pharmacokinetic profile of orexin A and effects on plasma insulin and glucagon in the rat." Regul Pept **119**(3): 209-212.

Elvert, R. and G. Heldmaier (2005). "Cardiorespiratory and metabolic reactions during entrance into torpor in dormice, Glis glis." J Exp Biol **208**(Pt 7): 1373-1383.

Fattore, G., A. Torbica, et al. (2012). "The social and economic burden of stroke survivors in Italy: a prospective, incidence-based, multi-centre cost of illness study." BMC Neurol **12**: 137.

Foppen, E., A. A. Tan, et al. (2016). "Suprachiasmatic Nucleus Neuropeptides and Their Control of Endogenous Glucose Production." J Neuroendocrinol **28**(4).

Franco, M., C. Contreras, et al. (2013). "Profound changes in blood parameters during torpor in a South American marsupial." Comp Biochem Physiol A Mol Integr Physiol **166**(2): 338-342.

Freinkel, N., B. E. Metzger, et al. (1972). "The hypothermia of hypoglycemia. Studies with 2-deoxy-D-glucose in normal human subjects and mice." N Engl J Med **287**(17): 841-845.

Futatsuki, T., A. Yamashita, et al. (2018). "Involvement of orexin neurons in fasting- and central adenosine-induced hypothermia." Sci Rep **8**(1): 2717.

Galster, W. A. and P. Morrison (1970). "Cyclic changes in carbohydrate concentrations during hibernation in the arctic ground squirrel." Am J Physiol **218**(4): 1228-1232.

Gavrilova, O., L. R. Leon, et al. (1999). "Torpor in mice is induced by both leptin-dependent and -independent mechanisms." Proc Natl Acad Sci U S A **96**(25): 14623-14628.

Geiser, F. (1988). "Reduction of metabolism during hibernation and daily torpor in mammals and birds: temperature effect or physiological inhibition?" J Comp Physiol B **158**(1): 25-37.

Geiser, F. (1998). "Evolution of daily torpor and hibernation in birds and mammals: importance of body size." Clin Exp Pharmacol Physiol **25**(9): 736-739.

Geiser, F. (2004). "Metabolic rate and body temperature reduction during hibernation and daily torpor." Annu Rev Physiol **66**: 239-274.

Geiser, F. (2010). Hibernation, Daily Torpor and Estivation in Mammals and Birds: Behavioral Aspects. Encyclopedia of Animal Behavior. M. D. B. a. J. Moore. Burlington, MA, USA, Academic Press

2: PP. 77-83.

Geiser, F., S. E. Currie, et al. (2014). "Torpor and hypothermia: reversed hysteresis of metabolic rate and body temperature." Am J Physiol Regul Integr Comp Physiol **307**(11): R1324-1329.

Geiser, F. and T. Ruf (1995). "Hibernation versus Daily Torpor in Mammals and Birds: Physiological Variables and Classification of Torpor Patterns." Physiological Zoology **68**(6): 935-966.

Geiser, F. and C. Turbill (2009). "Hibernation and daily torpor minimize mammalian extinctions." Naturwissenschaften **96**(10): 1235-1240.

Giroud, S., S. Blanc, et al. (2008). "Chronic food shortage and seasonal modulations of daily torpor and locomotor activity in the grey mouse lemur (Microcebus murinus)." Am J Physiol Regul Integr Comp Physiol **294**(6): R1958-1967.

Gluck, E. F., N. Stephens, et al. (2006). "Peripheral ghrelin deepens torpor bouts in mice through the arcuate nucleus neuropeptide Y signaling pathway." Am J Physiol Regul Integr Comp Physiol **291**(5): R1303-1309.

Gooley, J. J. (2016). "Circadian regulation of lipid metabolism." Proc Nutr Soc **75**(4): 440-450.

Guppy, M. and P. Withers (1999). "Metabolic depression in animals: physiological perspectives and biochemical generalizations." Biol Rev Camb Philos Soc **74**(1): 1-40.

Haque, M. S., Y. Minokoshi, et al. (1999). "Role of the sympathetic nervous system and insulin in enhancing glucose uptake in peripheral tissues after intrahypothalamic injection of leptin in rats." Diabetes **48**(9): 1706-1712.

Hara, J., C. T. Beuckmann, et al. (2001). "Genetic ablation of orexin neurons in mice results in narcolepsy, hypophagia, and obesity." Neuron **30**(2): 345-354.

Harada, S., Y. Yamazaki, et al. (2013). "Orexin-A suppresses postischemic glucose intolerance and neuronal damage through hypothalamic brain-derived neurotrophic factor." J Pharmacol Exp Ther **344**(1): 276-285.

Harris, D. V., J. M. Walker, et al. (1984). "A Continuum of Slow-Wave Sleep and Shallow Torpor in the Pocket Mouse Perognathus longimembris." Physiological Zoology **57**(4): 428-434.

Heldmaier, G., M. Klingenspor, et al. (1999). "Metabolic adjustments during daily torpor in the Djungarian hamster." Am J Physiol **276**(5 Pt 1): E896-906.

Heldmaier, G., S. Ortmann, et al. (2004). "Natural hypometabolism during hibernation and daily torpor in mammals." Respir Physiol Neurobiol **141**(3): 317-329.

Heldmaier, G. and T. Ruf (1992). "Body temperature and metabolic rate during natural hypothermia in endotherms." Journal of Comparative Physiology B **162**(8): 696-706.

Heldmaier G, S. R., Ruf T.; (1993). Suppression of metabolic rate in hibernation

Heller, H. C. (1988). "Sleep and hypometabolism." Canadian Journal of Zoology **66**(1): 61-69.

Heller, H. C., G. W. Colliver, et al. (1977). "Thermoregulation during entrance into hibernation." Pflugers Arch **369**(1): 55-59.

Heller, H. C. and S. F. Glotzbach (1977). "Thermoregulation during sleep and hibernation." Int Rev Physiol **15**: 147-188.

Heller, H. C. and H. T. Hammel (1972). "CNS control of body temperature during hibernation." Comp Biochem Physiol A Comp Physiol **41**(2): 349-359.

Heller, H. C. and N. F. Ruby (2004). "Sleep and circadian rhythms in mammalian torpor." Annu Rev Physiol **66**: 275-289.

Hill, R. D., R. C. Schneider, et al. (1987). "Heart rate and body temperature during free diving of Weddell seals." Am J Physiol **253**(2 Pt 2): R344-351.

Himms-Hagen, J. (1985). "Food restriction increases torpor and improves brown adipose tissue thermogenesis in ob/ob mice." Am J Physiol **248**(5 Pt 1): E531-539.

Hochachka, P. W. (2000). "Pinniped diving response mechanism and evolution: a window on the paradigm of comparative biochemistry and physiology." Comp Biochem Physiol A Mol Integr Physiol **126**(4): 435-458.

Horwitz, B. A., S. M. Chau, et al. (2013). "Temporal relationships of blood pressure, heart rate, baroreflex function, and body temperature change over a hibernation bout in Syrian hamsters." Am J Physiol Regul Integr Comp Physiol **305**(7): R759-768.

Hudson, J. W. and I. M. Scott (1979). "Daily torpor in the laboratory mouse *Mus musculus* var. albino." Physiological Zoology **52**: 205-218.

J., M. M., Y. S. T., et al. (2015). "The median preoptic nucleus: front and centre for the regulation of body fluid, sodium, temperature, sleep and cardiovascular homeostasis." Acta Physiologica **214**(1): 8-32.

Jastroch, M., S. Giroud, et al. (2016). "Seasonal Control of Mammalian Energy Balance: Recent Advances in the Understanding of Daily Torpor and Hibernation." J Neuroendocrinol **28**(11).

José, V. (2002). "Biochemical adaptation: Mechanism and process in physiological evolution." Biochemistry and Molecular Biology Education **30**(3): 215-216.

Kalsbeek, A., S. la Fleur, et al. (2014). "Circadian control of glucose metabolism." Mol Metab **3**(4): 372-383.

Kayaba, M., I. Park, et al. (2017). "Energy metabolism differs between sleep stages and begins to increase prior to awakening." Metabolism **69**: 14-23.

Kennedy, P. M. and W. V. Macfarlane (1971). "Oxygen consumption and water turnover of the fat-tailed marsupials Dasycercus cristicauda and Sminthopsis crassicaudata." Comp Biochem Physiol A Comp Physiol **40**(3): 723-732.

Khatri, I. M. and E. D. Freis (1967). "Hemodynamic changes during sleep." J Appl Physiol **22**(5): 867-873.

Kim, J. D., C. Toda, et al. (2017). "Hypothalamic Ventromedial Lin28a Enhances Glucose Metabolism in Diet-Induced Obesity." Diabetes **66**(8): 2102-2111.

Kingma, B., A. Frijns, et al. (2012) "The thermoneutral zone: implications for metabolic studies." Frontiers in bioscience (Elite edition) **4**, 1975-1985 DOI: 10.2741/518.

Kirchgessner, A. L. and M. Liu (1999). "Orexin synthesis and response in the gut." Neuron **24**(4): 941-951.

Kobbe, S. and K. H. Dausmann (2009). "Hibernation in Malagasy mouse lemurs as a strategy to counter environmental challenge." Naturwissenschaften **96**(10): 1221-1227.

Kok, S. W., S. Overeem, et al. (2003). "Hypocretin deficiency in narcoleptic humans is associated with abdominal obesity." Obes Res **11**(9): 1147-1154.

Korstanje, R., J. L. Ryan, et al. (2017). "Continuous Glucose Monitoring in Female NOD Mice Reveals Daily Rhythms and a Negative Correlation With Body Temperature." Endocrinology **158**(9): 2707-2712.

Koshiyama, H., Y. Hamamoto, et al. (2006). "Hypothalamic pathogenesis of type 2 diabetes." Med Hypotheses **67**(2): 307-310.

Krauchi, K. (2007). "The thermophysiological cascade leading to sleep initiation in relation to phase of entrainment." Sleep Med Rev **11**(6): 439-451.

Krauchi, K., C. Cajochen, et al. (2006). "Thermoregulatory effects of melatonin in relation to sleepiness." Chronobiol Int **23**(1-2): 475-484.

Krauchi, K. and A. Wirz-Justice (1994). "Circadian rhythm of heat production, heart rate, and skin and core temperature under unmasking conditions in men." Am J Physiol **267**(3 Pt 2): R819-829.

Kräuchi, K. D., T. (2011). Body Temperatures, Sleep, and Hibernation., Elsevier Health Sciences.

Krilowicz, B. L., S. F. Glotzbach, et al. (1988). "Neuronal activity during sleep and complete bouts of hibernation." Am J Physiol **255**(6 Pt 2): R1008-1019.

Kuroki, C., Y. Takahashi, et al. (2013). "The impact of hypothermia on emergence from isoflurane anesthesia in orexin neuron-ablated mice." Anesth Analg **116**(5): 1001-1005.

Kuwaki, T. (2015). "Thermoregulation under pressure: a role for orexin neurons." Temperature (Austin) **2**(3): 379-391.

Landry-Cuerrier, M., D. Munro, et al. (2008). "Climate and resource determinants of fundamental and realized metabolic niches of hibernating chipmunks." Ecology **89**(12): 3306-3316.

Larkin, J. E. and H. C. Heller (1996). "Temperature sensitivity of sleep homeostasis during hibernation in the golden-mantled ground squirrel." Am J Physiol **270**(4 Pt 2): R777-784.

Lee, Y. J. and J. M. Hallenbeck (2006). "Insights into cytoprotection from ground squirrel hibernation, a natural model of tolerance to profound brain oligaemia." Biochem Soc Trans **34**(Pt 6): 1295-1298.

Liu, R. J., A. N. van den Pol, et al. (2002). "Hypocretins (orexins) regulate serotonin neurons in the dorsal raphe nucleus by excitatory direct and inhibitory indirect actions." J Neurosci **22**(21): 9453-9464.

Liu, X. H., R. Morris, et al. (2001). "Orexin a preferentially excites glucose-sensitive neurons in the lateral hypothalamus of the rat in vitro." Diabetes **50**(11): 2431-2437.

Liu, Z. W. and X. B. Gao (2007). "Adenosine inhibits activity of hypocretin/orexin neurons by the A1 receptor in the lateral hypothalamus: a possible sleep-promoting effect." J Neurophysiol **97**(1): 837-848.

Lo Martire, V., A. Silvani, et al. (2018). "Modulation of sympathetic vasoconstriction is critical for the effects of sleep on arterial pressure in mice." J Physiol **596**(4): 591-608.

Lo Martire, V., A. Silvani, et al. (2012). "Effects of ambient temperature on sleep and cardiovascular regulation in mice: the role of hypocretin/orexin neurons." PLoS One **7**(10): e47032.

Lo Martire, V., A. Valli, et al. (2018). "Changes in blood glucose as a function of body temperature in laboratory mice: implications for daily torpor." Am J Physiol Endocrinol Metab.

Lu, J., M. A. Greco, et al. (2000). "Effect of lesions of the ventrolateral preoptic nucleus on NREM and REM sleep." J Neurosci **20**(10): 3830-3842.

Lubkin, M. and A. Stricker-Krongrad (1998). "Independent feeding and metabolic actions of orexins in mice." Biochem Biophys Res Commun **253**(2): 241-245.

Malan, A. (2010). "Is the torpor-arousal cycle of hibernation controlled by a non-temperature-compensated circadian clock?" Journal of biological rhythms **25**(3): 166-175.

Marcus, J. N., C. J. Aschkenasi, et al. (2001). "Differential expression of orexin receptors 1 and 2 in the rat brain." J Comp Neurol **435**(1): 6-25.

Matsumura, K., T. Tsuchihashi, et al. (2001). "Central orexin-A augments sympathoadrenal outflow in conscious rabbits." Hypertension **37**(6): 1382-1387.

Mekjavic, I. B. and O. Eiken (2006). "Contribution of thermal and nonthermal factors to the regulation of body temperature in humans." J Appl Physiol (1985) **100**(6): 2065-2072.

Melvin, R. G. and M. T. Andrews (2009). "Torpor induction in mammals: recent discoveries fueling new ideas." Trends Endocrinol Metab **20**(10): 490-498.

Milsom, W. K. and D. C. Jackson (2011). "Hibernation and gas exchange." Compr Physiol **1**(1): 397-420.

Milsom, W. K., M. B. Zimmer, et al. (1999). "Regulation of cardiac rhythm in hibernating mammals." Comp Biochem Physiol A Mol Integr Physiol **124**(4): 383-391.

Milsom, W. K., M. B. Zimmer, et al. (2001). "Vagal control of cardiorespiratory function in hibernation." Exp Physiol **86**(6): 791-796.

Mizuno, K. and Y. Ueno (2017). "Autonomic Nervous System and the Liver." Hepatol Res **47**(2): 160-165.

Moore, R. Y. and R. L. Danchenko (2002). "Paraventricular-subparaventricular hypothalamic lesions selectively affect circadian function." Chronobiol Int **19**(2): 345-360.

Morhardt, J. E. (1970). "Heart rates, breathing rates and the effects of atropine and acetylcholine on white-footed mice (Peromyscus sp.) during daily torpor." Comp Biochem Physiol **33**(2): 441-457.

Morrison, S. F. (2016). "Central control of body temperature." F1000Res **5**.

Morrison, S. F. and C. J. Madden (2014). "Central nervous system regulation of brown adipose tissue." Compr Physiol **4**(4): 1677-1713.

Morrison, S. F. and K. Nakamura (2011). "Central neural pathways for thermoregulation." Front Biosci (Landmark Ed) **16**: 74-104.

Morrison, S. F., A. F. Sved, et al. (1999). "GABA-mediated inhibition of raphe pallidus neurons regulates sympathetic outflow to brown adipose tissue." Am J Physiol **276**(2 Pt 2): R290-297.

Muroya, S., K. Uramura, et al. (2001). "Lowering glucose concentrations increases cytosolic Ca2+ in orexin neurons of the rat lateral hypothalamus." Neurosci Lett **309**(3): 165-168.

Musacchia, X. J. and D. R. Deavers (1981). The regulation of carbohydrate metabolism in hibernators. Survival in the Cold. X. J. M. a. L. Jansky. Amsterdam, Elsevier North Holland**:** 55-75.

Nakagawa, T., Y. Ogawa, et al. (2003). "Anti-obesity and anti-diabetic effects of brain-derived neurotrophic factor in rodent models of leptin resistance." Int J Obes Relat Metab Disord **27**(5): 557-565.

Nakamura, K., K. Matsumura, et al. (2004). "Identification of sympathetic premotor neurons in medullary raphe regions mediating fever and other thermoregulatory functions." J Neurosci **24**(23): 5370-5380.

Nakamura, K. and S. F. Morrison (2007). "Central efferent pathways mediating skin cooling-evoked sympathetic thermogenesis in brown adipose tissue." Am J Physiol Regul Integr Comp Physiol **292**(1): R127-136.

Nakamura, K. and S. F. Morrison (2010). "A thermosensory pathway mediating heat-defense responses." Proc Natl Acad Sci U S A **107**(19): 8848-8853.

Nambu, T., T. Sakurai, et al. (1999). "Distribution of orexin neurons in the adult rat brain." Brain Res **827**(1-2): 243-260.

Nedergaard, J., T. Bengtsson, et al. (2007). "Unexpected evidence for active brown adipose tissue in adult humans." Am J Physiol Endocrinol Metab **293**(2): E444-452.

Nestler, J. R. (1990). "Relationships between respiratory quotient and metabolic rate during entry to and arousal from daily torpor in deer mice (Peromyscus maniculatus)." Physiol Zool **63**: 504-515.

Nestler, J. R. (1991). "Metabolic substrate change during daily torpor in deer mice." Can. J. Zool. **69**: 322-327.

Nowak, K. W., P. Mackowiak, et al. (2000). "Acute orexin effects on insulin secretion in the rat: in vivo and in vitro studies." Life Sci **66**(5): 449-454.

Nowakowski, S. G., S. J. Swoap, et al. (2009). "A single bout of torpor in mice protects memory processes." Physiol Behav **97**(1): 115-120.

Obal, F., Jr., G. Rubicsek, et al. (1985). "Changes in the brain and core temperatures in relation to the various arousal states in rats in the light and dark periods of the day." Pflugers Arch **404**(1): 73-79.

Oelkrug, R., G. Heldmaier, et al. (2011). "Torpor patterns, arousal rates, and temporal organization of torpor entry in wildtype and UCP1-ablated mice." J Comp Physiol B **181**(1): 137-145.

Ohno, K. and T. Sakurai (2008). "Orexin neuronal circuitry: role in the regulation of sleep and wakefulness." Front Neuroendocrinol **29**(1): 70-87.

Ortmann, S. and G. Heldmaier (2000). "Regulation of body temperature and energy requirements of hibernating alpine marmots (Marmota marmota)." Am J Physiol Regul Integr Comp Physiol **278**(3): R698-704.

Otlivanchik, O., C. Le Foll, et al. (2015). "Perifornical hypothalamic orexin and serotonin modulate the counterregulatory response to hypoglycemic and glucoprivic stimuli." Diabetes **64**(1): 226-235.

Ouedraogo, R., E. Naslund, et al. (2003). "Glucose regulates the release of orexin-a from the endocrine pancreas." <u>Diabetes</u> **52**(1): 111-117.

Palchykova, S., T. Deboer, et al. (2002). "Selective sleep deprivation after daily torpor in the Djungarian hamster." <u>J Sleep Res</u> **11**(4): 313-319.

Park, J. H., H. M. Shim, et al. (2015). "Orexin A regulates plasma insulin and leptin levels in a time-dependent manner following a glucose load in mice." <u>Diabetologia</u> **58**(7): 1542-1550.

Parmeggiani, P. L. (2003). "Thermoregulation and sleep." <u>Front Biosci</u> **8**: s557-567.

Parsons, M. P., N. Belanger-Willoughby, et al. (2012). "ATP-sensitive potassium channels mediate the thermosensory response of orexin neurons." <u>J Physiol</u> **590**(19): 4707-4715.

Paul, M. J., D. A. Freeman, et al. (2005). "Neuropeptide Y induces torpor-like hypothermia in Siberian hamsters." <u>Brain Res</u> **1055**(1-2): 83-92.

Peier, A. M., A. Moqrich, et al. (2002). "A TRP channel that senses cold stimuli and menthol." <u>Cell</u> **108**(5): 705-715.

Penicaud, L., D. A. Thompson, et al. (1986). "Effects of 2-deoxy-D-glucose on food and water intake and body temperature in rats." <u>Physiol Behav</u> **36**(3): 431-435.

Peyron, C., J. Faraco, et al. (2000). "A mutation in a case of early onset narcolepsy and a generalized absence of hypocretin peptides in human narcoleptic brains." <u>Nat Med</u> **6**(9): 991-997.

Peyron, C., D. K. Tighe, et al. (1998). "Neurons containing hypocretin (orexin) project to multiple neuronal systems." <u>J Neurosci</u> **18**(23): 9996-10015.

Plazzi, G., K. K. Moghadam, et al. (2011). "Autonomic disturbances in narcolepsy." <u>Sleep Med Rev</u> **15**(3): 187-196.

Polderman, K. H. (2009). "Mechanisms of action, physiological effects, and complications of hypothermia." <u>Crit Care Med</u> **37**(7 Suppl): S186-202.

Postic, C., R. Dentin, et al. (2007). "ChREBP, a transcriptional regulator of glucose and lipid metabolism." <u>Annu Rev Nutr</u> **27**: 179-192.

Prendergast, B. J., D. A. Freeman, et al. (2002). "Periodic arousal from hibernation is necessary for initiation of immune responses in ground squirrels." <u>Am J Physiol Regul Integr Comp Physiol</u> **282**(4): R1054-1062.

Ramsey, K. M., J. Yoshino, et al. (2009). "Circadian clock feedback cycle through NAMPT-mediated NAD+ biosynthesis." <u>Science</u> **324**(5927): 651-654.

Rani, M., R. Kumar, et al. (2018). "Role of orexins in the central and peripheral regulation of glucose homeostasis: Evidences & mechanisms." <u>Neuropeptides</u> **68**: 1-6.

Rayner, D. V. (2001). "The sympathetic nervous system in white adipose tissue regulation." <u>Proc Nutr Soc</u> **60**(3): 357-364.

Rechtschaffen, A. (1968, repr. 1973.). <u>A manual of standardized terminology: Techniques and Scoring system for sleep stages of human subjects.</u>

. Los Angeles, Calif. , Brain Information Service/Brain Research Institute, University of California.

REINERTSEN, R. E. (1983). "Nocturnal hypothermia and its energetic significance for small birds living in the arctic and subarctic regions. A review." <u>Polar Research</u> **1**(3): 269-284.

Revel, F. G., A. Herwig, et al. (2007). "The circadian clock stops ticking during deep hibernation in the European hamster." Proc Natl Acad Sci U S A **104**(34): 13816-13820.

Rodgers, J. T., C. Lerin, et al. (2005). "Nutrient control of glucose homeostasis through a complex of PGC-1alpha and SIRT1." Nature **434**(7029): 113-118.

Romanovsky, A. A. (2007). "Thermoregulation: some concepts have changed. Functional architecture of the thermoregulatory system." Am J Physiol Regul Integr Comp Physiol **292**(1): R37-46.

Ruby, N. F., M. T. Barakat, et al. (2004). "Phenotypic differences in reentrainment behavior and sensitivity to nighttime light pulses in siberian hamsters." Journal of biological rhythms **19**(6): 530-541.

Ruf, T. and F. Geiser (2015). "Daily torpor and hibernation in birds and mammals." Biol Rev Camb Philos Soc **90**(3): 891-926.

Rusyniak, D. E., D. V. Zaretsky, et al. (2011). "The role of orexin-1 receptors in physiologic responses evoked by microinjection of PgE2 or muscimol into the medial preoptic area." Neurosci Lett **498**(2): 162-166.

Sakurai, T. (2007). "The neural circuit of orexin (hypocretin): maintaining sleep and wakefulness." Nat Rev Neurosci **8**(3): 171-181.

Sakurai, T., A. Amemiya, et al. (1998). "Orexins and orexin receptors: a family of hypothalamic neuropeptides and G protein-coupled receptors that regulate feeding behavior." Cell **92**(5): 1 page following 696.

Sakurai, T., T. Moriguchi, et al. (1999). "Structure and function of human prepro-orexin gene." J Biol Chem **274**(25): 17771-17776.

Saper, C. B., T. E. Scammell, et al. (2005). "Hypothalamic regulation of sleep and circadian rhythms." Nature **437**(7063): 1257-1263.

Sarajas HSS (1967). Blood glucose studies in permanently cannulated hedgehogs during a bout of hibernation. Helsinki, Suomalainen tiedeakatemia.

Satoh, S., H. Matsumura, et al. (2004). "FOS expression in orexin neurons following muscimol perfusion of preoptic area." Neuroreport **15**(7): 1127-1131.

Scheen, A. J., M. M. Byrne, et al. (1996). "Relationships between sleep quality and glucose regulation in normal humans." Am J Physiol **271**(2 Pt 1): E261-270.

Schmieg, G., J. B. Mercer, et al. (1980). "Thermosensitivity of the extrahypothalamic brain stem in conscious goats." Brain Res **188**(2): 383-397.

Sessler, D. I. (2009). "Defeating normal thermoregulatory defenses: induction of therapeutic hypothermia." Stroke **40**(11): e614-621.

Shiraishi, T., Y. Oomura, et al. (2000). "Effects of leptin and orexin-A on food intake and feeding related hypothalamic neurons." Physiol Behav **71**(3-4): 251-261.

Shiuchi, T., M. S. Haque, et al. (2009). "Hypothalamic orexin stimulates feeding-associated glucose utilization in skeletal muscle via sympathetic nervous system." Cell Metab **10**(6): 466-480.

Sieminski, M., J. Szypenbejl, et al. (2018). "Orexins, Sleep, and Blood Pressure." Curr Hypertens Rep **20**(9): 79.

Silvani, A., S. Bastianini, et al. (2014). "Sleep and cardiovascular phenotype in middle-aged hypocretin-deficient narcoleptic mice." J Sleep Res **23**(1): 98-106.

Silvani, A., S. Bastianini, et al. (2009). "Sleep modulates hypertension in leptin-deficient obese mice." Hypertension **53**(2): 251-255.

Silvani, A., M. Cerri, et al. (2018). "Is Adenosine Action Common Ground for NREM Sleep, Torpor, and Other Hypometabolic States?" Physiology (Bethesda) **33**(3): 182-196.

Smith, G. D., M. J. Gunthorpe, et al. (2002). "TRPV3 is a temperature-sensitive vanilloid receptor-like protein." Nature **418**(6894): 186-190.

Snapp, B. D. and H. C. Heller (1981). "Suppression of Metabolism during Hibernation in Ground Squirrels (Citellus lateralis)." Physiological Zoology **54**(3): 297-307.

Somers, V. K., M. E. Dyken, et al. (1993). "Sympathetic-nerve activity during sleep in normal subjects." N Engl J Med **328**(5): 303-307.

Stamper, J. L. and J. Dark (1996). "Metabolic Fuel Availability Influences Thermoregulation in Deer Mice." Physiology & Behavior **61**(4): 521-524.

Stanley, S., S. Pinto, et al. (2010). "Identification of neuronal subpopulations that project from hypothalamus to both liver and adipose tissue polysynaptically." Proc Natl Acad Sci U S A **107**(15): 7024-7029.

Staples, J. F. (2014). "Metabolic suppression in mammalian hibernation: the role of mitochondria." J Exp Biol **217**(Pt 12): 2032-2036.

Storey, K. B. and J. M. Storey (1990). "Metabolic rate depression and biochemical adaptation in anaerobiosis, hibernation and estivation." Q Rev Biol **65**(2): 145-174.

Storey, K. B. and J. M. Storey (2010). "Metabolic rate depression: the biochemistry of mammalian hibernation." Adv Clin Chem **52**: 77-108.

Strijkstra, A. M. and S. Daan (1998). "Dissimilarity of slow-wave activity enhancement by torpor and sleep deprivation in a hibernator." Am J Physiol **275**(4 Pt 2): R1110-1117.

Sudo, M., Y. Minokoshi, et al. (1991). "Ventromedial hypothalamic stimulation enhances peripheral glucose uptake in anesthetized rats." Am J Physiol **261**(3 Pt 1): E298-303.

Sunagawa, G. A. and M. Takahashi (2016). "Hypometabolism during Daily Torpor in Mice is Dominated by Reduction in the Sensitivity of the Thermoregulatory System." Sci Rep **6**: 37011.

Suzuki, K., C. N. Jayasena, et al. (2012). "Obesity and appetite control." Exp Diabetes Res **2012**: 824305.

Switonska, M. M., P. Kaczmarek, et al. (2002). "Orexins and adipoinsular axis function in the rat." Regul Pept **104**(1-3): 69-73.

Swoap, S. J. (2001). "Altered leptin signaling is sufficient, but not required, for hypotension associated with caloric restriction." Am J Physiol Heart Circ Physiol **281**(6): H2473-2479.

Swoap, S. J. and M. J. Gutilla (2009). "Cardiovascular changes during daily torpor in the laboratory mouse." Am J Physiol Regul Integr Comp Physiol **297**(3): R769-774.

Swoap, S. J., M. J. Gutilla, et al. (2006). "The full expression of fasting-induced torpor requires beta 3-adrenergic receptor signaling." J Neurosci **26**(1): 241-245.

Swoap, S. J., G. Kortner, et al. (2017). "Heart rate dynamics in a marsupial hibernator." J Exp Biol **220**(Pt 16): 2939-2946.

Swoap, S. J., M. Rathvon, et al. (2007). "AMP does not induce torpor." Am J Physiol Regul Integr Comp Physiol **293**(1): R468-473.

Swoap, S. J. and D. Weinshenker (2008). "Norepinephrine controls both torpor initiation and emergence via distinct mechanisms in the mouse." PLoS One **3**(12): e4038.

Szekely, M., E. Petervari, et al. (2002). "Effects of orexins on energy balance and thermoregulation." Regul Pept **104**(1-3): 47-53.

Takahashi, J. S., H. K. Hong, et al. (2008). "The genetics of mammalian circadian order and disorder: implications for physiology and disease." Nat Rev Genet **9**(10): 764-775.

Takahashi, Y., W. Zhang, et al. (2013). "Orexin neurons are indispensable for prostaglandin E2-induced fever and defence against environmental cooling in mice." J Physiol **591**(22): 5623-5643.

Takeuchi, S., S. Iwase, et al. (1994). "Sleep-related changes in human muscle and skin sympathetic nerve activities." J Auton Nerv Syst **47**(1-2): 121-129.

Tansey, E. A. and C. D. Johnson (2015). "Recent advances in thermoregulation." Advances in Physiology Education **39**(3): 139-148.

Tashima, L. S., S. J. Adelstein, et al. (1970). "Radioglucose utilization by active, hibernating, and arousing ground squirrels." Am J Physiol **218**(1): 303-309.

Tayefeh, F., O. Plattner, et al. (1998). "Circadian changes in the sweating-to-vasoconstriction interthreshold range." Pflugers Arch **435**(3): 402-406.

Ter Horst, G. J., P. de Boer, et al. (1989). "Ascending projections from the solitary tract nucleus to the hypothalamus. A Phaseolus vulgaris lectin tracing study in the rat." Neuroscience **31**(3): 785-797.

Tian, L., Y. Y. Zhao, et al. (2011). "[Expression of orexin receptor 1 in rat pancreatic tissue with alimentary obesity]." Zhonghua Yi Xue Za Zhi **91**(6): 409-411.

Trachsel, L., D. M. Edgar, et al. (1991). "Are ground squirrels sleep deprived during hibernation?" Am J Physiol **260**(6 Pt 2): R1123-1129.

Tseng, Y. H., A. M. Cypess, et al. (2010). "Cellular bioenergetics as a target for obesity therapy." Nat Rev Drug Discov **9**(6): 465-482.

Tsiouris, J. A. (2005). "Metabolic depression in hibernation and major depression: an explanatory theory and an animal model of depression." Med Hypotheses **65**(5): 829-840.

Tsuneki, H., S. Murata, et al. (2008). "Age-related insulin resistance in hypothalamus and peripheral tissues of orexin knockout mice." Diabetologia **51**(4): 657-667.

Tsuneki, H., T. Nagata, et al. (2016). "Nighttime Administration of Nicotine Improves Hepatic Glucose Metabolism via the Hypothalamic Orexin System in Mice." Endocrinology **157**(1): 195-206.

Tupone, D., C. J. Madden, et al. (2011). "An orexinergic projection from perifornical hypothalamus to raphe pallidus increases rat brown adipose tissue thermogenesis." J Neurosci **31**(44): 15944-15955.

Van Cauter, E., D. Desir, et al. (1989). "Nocturnal Decrease in Glucose Tolerance During Constant Glucose Infusion." The Journal of Clinical Endocrinology & Metabolism **69**(3): 604-611.

Van Cauter, E., K. S. Polonsky, et al. (1997). "Roles of circadian rhythmicity and sleep in human glucose regulation. ." Endocr Rev **18**: 716-738.

van der Lans, A. A., J. Hoeks, et al. (2013). "Cold acclimation recruits human brown fat and increases nonshivering thermogenesis." J Clin Invest **123**(8): 3395-3403.

van der Vinne, V., J. A. Gorter, et al. (2015). "Diurnality as an energy-saving strategy: energetic consequences of temporal niche switching in small mammals." The Journal of Experimental Biology **218**(16): 2585-2593.

Venner, A., M. M. Karnani, et al. (2011). "Orexin neurons as conditional glucosensors: paradoxical regulation of sugar sensing by intracellular fuels." J Physiol **589**(Pt 23): 5701-5708.

Vicent, M. A., E. D. Borre, et al. (2017). "Central activation of the A1 adenosine receptor in fed mice recapitulates only some of the attributes of daily torpor." J Comp Physiol B **187**(5-6): 835-845.

Walker, J. M., A. Garber, et al. (1979). "Sleep and estivation (shallow torpor): continuous processes of energy conservation." Science **204**(4397): 1098-1100.

Walker, J. M., S. F. Glotzbach, et al. (1977). "Sleep and hibernation in ground squirrels (Citellus spp): electrophysiological observations." Am J Physiol **233**(5): R213-221.

Wang, H. and J. Siemens (2015). "TRP ion channels in thermosensation, thermoregulation and metabolism." Temperature (Austin) **2**(2): 178-187.

Wang, L. (2011). Time patterns and metabolic rates of natural torpor in the Richardson's ground squirrel.

Wang, L. and M. W. Wolowyk (2011). Torpor in mammals and birds.

Wechselberger, M., C. L. Wright, et al. (2006). "Ionic channels and conductance-based models for hypothalamic neuronal thermosensitivity." American Journal of Physiology-Regulatory, Integrative and Comparative Physiology **291**(3): R518-R529.

Westman, W. and F. Geiser (2004). "The effect of metabolic fuel availability on thermoregulation and torpor in a marsupial hibernator." J Comp Physiol B **174**(1): 49-57.

Wick, A. N., D. R. Drury, et al. (1957). "Localization of the primary metabolic block produced by 2-deoxyglucose." J Biol Chem **224**(2): 963-969.

Willie, J. T., R. M. Chemelli, et al. (2003). "Distinct narcolepsy syndromes in Orexin receptor-2 and Orexin null mice: molecular genetic dissection of Non-REM and REM sleep regulatory processes." Neuron **38**(5): 715-730.

Willie, J. T., R. M. Chemelli, et al. (2001). "To eat or to sleep? Orexin in the regulation of feeding and wakefulness." Annu Rev Neurosci **24**: 429-458.

Withers, P. C. (1977). "Metabolic, respiratory and haematological adjustments of the little pocket mouse to circadian torpor cycles." Respir Physiol **31**(3): 295-307.

Xue, Y., Y. Yang, et al. (2016). "In vitro thermosensitivity of rat lateral parabrachial neurons." Neurosci Lett **619**: 15-20.

Yamanaka, A., C. T. Beuckmann, et al. (2003). "Hypothalamic orexin neurons regulate arousal according to energy balance in mice." Neuron **38**(5): 701-713.

Yamanaka, A., N. Tsujino, et al. (2002). "Orexins activate histaminergic neurons via the orexin 2 receptor." Biochem Biophys Res Commun **290**(4): 1237-1245.

Yi, C. X., M. J. Serlie, et al. (2009). "A major role for perifornical orexin neurons in the control of glucose metabolism in rats." Diabetes **58**(9): 1998-2005.

Yoshimoto, M., T. Sakagami, et al. (2004). "Relationship between renal sympathetic nerve activity and renal blood flow during natural behavior in rats." Am J Physiol Regul Integr Comp Physiol **286**(5): R881-887.

Young, J. B. and L. Landsberg (1979). "Sympathoadrenal activity in fasting pregnant rats. Dissociation of adrenal medullary and sympathetic nervous system responses." J Clin Invest **64**(1): 109-116.

Zervanos, S. M., C. R. Maher, et al. (2014). "Effect of Body Mass on Hibernation Strategies of Woodchucks (Marmota monax)." Integrative and Comparative Biology **54**(3): 443-451.

Zhang, S., J. M. Zeitzer, et al. (2007). "Sleep/wake fragmentation disrupts metabolism in a mouse model of narcolepsy." J Physiol **581**(Pt 2): 649-663.

Zhang, W., J. Sunanaga, et al. (2010). "Orexin neurons are indispensable for stress-induced thermogenesis in mice." J Physiol **588**(Pt 21): 4117-4129.

Zhao, Y. and J. A. Boulant (2005). "Temperature effects on neuronal membrane potentials and inward currents in rat hypothalamic tissue slices." J Physiol **564**(Pt 1): 245-257.

Zheng, H., L. M. Patterson, et al. (2005). "Orexin-A projections to the caudal medulla and orexin-induced c-Fos expression, food intake, and autonomic function." J Comp Neurol **485**(2): 127-142.

Zhu, Y., Y. Miwa, et al. (2003). "Orexin receptor type-1 couples exclusively to pertussis toxin-insensitive G-proteins, while orexin receptor type-2 couples to both pertussis toxin-sensitive and -insensitive G-proteins." J Pharmacol Sci **92**(3): 259-266.

Zimmerman, M. L. (1982). "Carbohydrate and torpor duration in hibernating golden-mantled ground squirrels (Citellus lateralis)." J. Comp. Physiol. **147**(B): 129-135.

Zimmermann-Belsing, T., G. Brabant, et al. (2003). "Circulating leptin and thyroid dysfunction." Eur J Endocrinol **149**(4): 257-271.

Zosky, G. R. (2002). "The parasympathetic nervous system: its role during torpor in the fat-tailed dunnart (Sminthopsis crassicaudata)." J Comp Physiol B **172**(8): 677-684.

Zosky, G. R. and A. N. Larcombe (2003). "The parasympathetic nervous system and its influence on heart rate in torpid western pygmy possums, Cercatetus concinnus (Marsupialia: Burramyidae)." Zoology (Jena) **106**(2): 143-150.

Abstract

Introduction: Spontaneous torpor is a physiological phenomenon which occurs in many species, from birds to mammals. Torpor is an extreme energy saving method adopted in conditions of scarcity of food and adverse environmental conditions, characterized by a controlled lowering of body temperature, basal metabolic rate, breath, and heart rate. The mechanisms ruling the torpor bouts are still unknown. Orexins (ORXS) are neuropeptides released by neurons in the lateral hypothalamus and are involved in the control of food behavior, in thermoregulation and sleep-wake cycle regulation. They promote wakefulness, feeding and the increase of the body temperature (Tb). The involvement of ORXS in the control of these physiological functions, suggests that these neuropeptides could have a role in inducing torpor and/or in the arousal from torpor. The signals that relay the lack of fuel to initiate a bout of torpor are not known. The mouse will only enter a torpid state when calorically challenged, one of the inputs for initiation into a bout of torpor might be the lack of the primary fuel (glucose) used to power brain metabolism.

Aims: To investigate whether 1) the lack of ORXs has a role in the modifications of physiological parameters during the entrance and/or exiting from torpor; 2) the level of circulating glucose at the onset of torpor differs from both glucose during arousal from torpor and from feeding conditions that do not lead to torpor.

Material and methods: In order to evaluate the role of orexins, 8 KO-HCRT and 8 WT mice, were implanted with a telemetric blood pressure (Data Sciences International, DSI) transducer for cardiovascular parameters recordings, two cranial electrodes for the discrimination of the wake-sleep state and a thermistor in the brain cortex. Tb, activity (ACT), heart period (HP) systolic blood pressure (SBP) and the sleep pattern (percentage of time spent in NREM, REM and indeterminate states, slow wave activity, SWA) were studies during the different phases of torpor (entry, deep torpor, and arousal). To induce torpor, mice were calorically restricted and exposed to an ambient temperature of 20°C.

For the study of changes in glycemia related to torpor, 6 mice were implanted intraperitoneally with glucose telemeter (DSI) with a glucose sensor positioned in the arch. Blood glucose levels (GLC), Tb, and ACT were recorded continuously, with minimal animal handling, during entry and arousal from torpor. Torpor inducing protocol was the same of the one described above.

Results and Discussion: The lack of ORXS does not cause significative differences in the physiological parameters during the different torpor phases. The sleep pattern is smoothly conditioned by ORXs, showing during the cooling phase an increased REM sleep propensity in mice lacking ORXs. An increased percentage of NREM sleep during entrance into torpor was evident in both groups. During deep torpor, in both the experimental groups, electroencephalogram (EEG) trace is similar to that described during active wakefulness while electromyogram (EMG) is almost flat, similarly to NREM sleep. This unusual sleep tracings can be observed when the minimum Tb is recorded.

We found a strong positive and linear correlation between circulating glucose and Tb during ad libitum feeding at thermoneutrality. Furthermore, mice that were calorically restricted entered torpor bouts readily. Circulating blood glucose was low during torpor entry but did not drop precipitously as Tb did at the onset of a torpor bout. Blood glucose significantly increased during arousal from torpor. Finally, while low blood glucose itself was not predictive of a bout of torpor, the onset of torpor was associated with the combination of low blood glucose and hyperactivity

Conclusion: These results suggest that ORXS do not play a central role in the control of fasting-induced daily torpor in mice. The onset of torpor is associated with the combination of low glycemia and hyperactivity a decreased propensity for sleep, but low glycemia its self is not sufficient to induce the torpor bout. In conclusion, torpor can be considered a multifactorial and complex mechanism involving both metabolism and central nervous system control.